UCRL-10687

University of California

Ernest O. Lawrence Radiation Laboratory

FORMATION OF ENERGETIC FRAGMENT IONS BY BOMBARDMENT OF ORGANIC MOLECULES WITH SLOW ELECTRONS

TWO-WEEK LOAN COPY

This is a Library Circulating Copy which may be borrowed for two weeks. For a personal retention copy, call Tech. Info. Division, Ext. 5545

DISCLAIMER

This document was prepared as an account of work sponsored by the United States Government. While this document is believed to contain correct information, neither the United States Government nor any agency thereof, nor the Regents of the University of California, nor any of their employees, makes any warranty, express or implied, or assumes any legal responsibility for the accuracy, completeness, or usefulness of any information, apparatus, product, or process disclosed, or represents that its use would not infringe privately owned rights. Reference herein to any specific commercial product, process, or service by its trade name, trademark, manufacturer, or otherwise, does not necessarily constitute or imply its endorsement, recommendation, or favoring by the United States Government or any agency thereof, or the Regents of the University of California. The views and opinions of authors expressed herein do not necessarily state or reflect those of the United States Government or any agency thereof or the Regents of the University of California.

Research and Development

UCRL-10687
UC-4 Chemistry
TID-4500 (19th Ed.)

UNIVERSITY OF CALIFORNIA
Lawrence Radiation Laboratory
Berkeley, California

Contract No. W-7405-eng-48

FORMATION OF ENERGETIC FRAGMENT IONS BY BOMBARDMENT OF ORGANIC MOLECULES WITH SLOW ELECTRONS

John A. Olmsted

(Ph.D. Thesis)

February 18, 1963

Printed in USA. Price $2.50. Available from the
Office of Technical Services
U. S. Department of Commerce
Washington 25, D.C.

FORMATION OF ENERGETIC FRAGMENT IONS BY BOMBARDMENT OF ORGANIC MOLECULES WITH SLOW ELECTRONS

Contents

Abstract v

Introduction 1

The Mass Spectrometer

The Basic Instrument 4

Modifications 6

Accelerating Voltage 7

Metastable Suppressor and Repellers 7

Ionizing Voltage 10

Magnetic Field 11

Characteristics of Excess-Kinetic-Energy Peaks

Measurement of Energy 12

Effect of Metastable Suppressor 17

Effect of Accelerating Voltage 18

Effect of Repellers 21

Data 24

Excess Kinetic Energies 24

Abundances of Excess-Kinetic-Energy Ions 38

Appearance Potentials 44

Other Data

Duplication of Kandel's Experiments 57

Negative-Repeller Mass Spectra 57

Discussion and Conclusions

Mechanism of Formation of Excess-Kinetic-Energy Ions . . . 61

Experimental Evidence

Deuterium 65

Polyatomic Molecules 68

Appearance Potentials
Threshold Law 74
Magnitudes 79
Kandel's Values 80
Abundances
Extent of Occurrence 81
Calculation of Collection Efficiencies 82
Absolute Abundances 87
Fragmentation Patterns 87
Implications for the Quasi-Equilibrium Theory of Mass Spectra 92
Appendices
Appendix I: Excess Kinetic Energies 98
Appendix II: Excess-Kinetic-Energy-Ion Peak Heights . . . 105
Acknowledgments 124
References 125

FORMATION OF ENERGETIC FRAGMENT IONS BY BOMBARDMENT OF ORGANIC MOLECULES WITH SLOW ELECTRONS

John A. Olmsted

Lawrence Radiation Laboratory
University of California
Berkeley, California

February 18, 1963

ABSTRACT

Excess-kinetic-energy fragment ions resulting from the bombardment of organic molecules with 0- to 100-volt electrons have been studied by using the techniques of mass spectrometry. The effects on such ions of variations in the mass-spectrometer operating conditions have been determined. The excess kinetic energies possessed by both near-thermal and excess-kinetic-energy methyl ions have been measured for a large number of organic compounds, and it is found that most "thermal" methyl ions have about 0.3 eV excess kinetic energy. Energies measured for excess-kinetic-energy methyl ions are in agreement with those determined by other experimenters, if the latter values are corrected by the addition of the excess kinetic energies of the near-thermal methyl ions.

Relative abundances of thermal and excess-kinetic-energy methyl ions have been determined for several organic compounds, and it is found that under normal operating conditions, the M/q=15 ion peak observed in the mass spectrometer is made up, for most of the compounds studied, of 50 to 70% excess-kinetic-energy ions. Moreover, the absolute abundances of excess-kinetic-energy ions have been estimated from the measured peak heights, and it is found that for hydrocarbon molecules like propane and n-butane the excess-kinetic-energy methyl ions make up more than 10% of all ions formed from those molecules by impact of 70-V electrons.

Appearance-potential measurements have been made for the excess-kinetic-energy methyl ions from several organic compounds. In all cases,

the appearance-potential curves have a second-power dependence on excess electron energy in the threshold region. This behavior is explained by modifying slightly the theory for threshold behavior of appearance-potential curves. All the appearance potentials determined lie in the 25 to 30 V range.

The mechanism for formation of excess-kinetic-energy ions is discussed, and it is shown that the previously postulated mechanism involving the fragmentation of doubly charged ions is not consistent with the data. An alternative mechanism involving excited states of singly charged ions is presented.

Finally, the implications of the existence and abundances of excess-kinetic-energy ions for the quasi-equilibrium theory of mass spectra are examined. It is concluded that the assumption of randomization of excitation energy on which that theory is based is completely invalid. Furthermore, the complete failure of the theory to predict the existence of an abundant-methyl-ion peak in the propane mass spectrum is pointed out.

INTRODUCTION

Among the many processes that can lead to the fragmentation of a molecule under electron impact to form ions, there are some that lead to products possessing an amount of kinetic energy significantly greater than that of thermal motion. Such kinetic-energy ions were first observed by Bleakney, who studied the H^+ ions arising from electron bombardment of H_2 in a mass spectrometer.[1] Bleakney found H^+ ions of kinetic energy equal to about 4.5 electron volts, which ions he proposed resulted when the H_2^+ ion was formed in the repulsive $^2\Sigma_u^+$ state and subsequently fragmented. Lozier built a special apparatus to study excess-kinetic-energy ions and with it studied the high-energy H^+ ions from H_2 in greater detail.[2] Lozier,[3-5] Tate and Lozier,[6] and Hanson[7] extended work with the Lozier apparatus to include the diatomic molecules N_2, CO, O_2, NO, and HCl and found for each of these molecules that ionic fragments possessing excess kinetic energy were formed.

The Lozier apparatus, although well suited to the study of ions with excess kinetic energy, is not capable of distinguishing ions of different M/q ratios.* Hagstrum and Tate[8] and Hagstrum[9] returned to the tool that Bleakney had used initially with H_2, the mass spectrometer, to eliminate this shortcoming. They extended and improved the work done on CO, NO, N_2, and O_2. All the above investigators studied the energy of the bombarding electrons at which high-kinetic-energy fragments first appear (the appearance potential) and the distribution in kinetic energy of the ions formed.

With the extension of mass-spectrographic work to organic molecules came the discovery that ions of excess kinetic energy could also result from the electron bombardment of polyatomic molecules. Hustrulid, Kusch,

---

*It is standard practice in mass spectrometry to denote the mass-to-charge ratio of an ion by the symbol m/e. This symbol is rather loosely defined, with both m and e taking on different meanings at different times. It shall be the practice in this report to denote by the symbol "m" a mass in grams, by "M" a mass in atomic-mass units, by "e" the charge of the electron in esu or emu, and by "q" the number of electronic charges an ion possesses.

and Tate in 1938 found that the mass spectrum for benzene showed double peaks for M/q values 12 to 15 (C^+- CH_3^+) and 25 to 27 (C_2H^+-$C_2H_3^+$).[10] They attributed these doublets to ions of two distinct kinetic energies, one of which was thermal. They also advanced the hypothesis, based on the high appearance potentials of the excess-kinetic-energy ions, that the high-energy ions were the result of doubly charged ions fragmenting into singly charged parts. Hustrulid and co-workers also found doublet peaks occurring in the mass spectrum of cyclohexane.

Hipple, Fox, and Condon, studying the occurrence of metastable ions in the mass spectra of hydrocarbons, found some peaks of apparently nonintegral M/q whose characteristics were such that they could best be explained as being due to ions of excess kinetic energy.[11] Such peaks were observed at M/q=14 (CH_2^+) for butadiene and at M/q=15 (CH_3^+) and several other M/q values for n-butane.

The first extensive work on such excess-kinetic-energy peaks was carried out by Mohler, Dibeler, and Reese on a series of 13 hydrocarbons and CH_3CF_3.[12] These investigators, using a mass spectrometer, measured the most probable kinetic energy of the high-energy ions and in some cases estimated their appearance potentials. They felt their data to be in good agreement with what would be expected if the doubly-charged-ion mechanism suggested by Hustrulid et al.[10] were correct, with the single exception of CH_3CF_3, whose high-kinetic-energy peak did not seem to arise from a doubly charged ion.

No further investigations were made into this phenomenon until some years later, when Stanton reopened the problem with a study of the mass spectrum of propane.[13] From his data on the high-kinetic-energy M/q=15 and the M/q=26 to M/q=29 peaks, he concluded that fragment ions possessing excess kinetic energy could not, in the case of propane, be adequately explained by the doubly-charged-ion hypothesis. On the other hand, Tsuchiya has recently published the results of mass-spectral work on propane[14] and various other hydrocarbons[15] wherein he explains the high-kinetic-energy fragments by means of the doubly-charged-ion hypothesis. Hall, working on CO_2, has also used that hypothesis to rationalize the high-kinetic-energy O^+ ions he observed.[16]

Working along a somewhat different line, Kandel studied the excess kinetic energy possessed by "thermal" ions near their appearance potentials.[17,18] His data indicated that some such ions, in particular the methyl ions from ethane and propane, are formed even at the appearance potentials with kinetic energies of up to 1 eV.

Aside from these empirical studies, there has also been some theoretical work carried out on the behavior of excess-kinetic-energy ions in the electric and magnetic fields of the mass spectrometer. Coggeshall considered the discrimination effects created by the various slits in the ion-accelerating region of the mass spectrometer.[19] Washburn and Berry applied Coggeshall's theory to mass-spectral data to obtain a measure of the excess kinetic energies of various higher-mass ions in the n-butane spectrum.[20] Berry later enlarged on both the theoretical and experimental aspects of the discrimination occurring in the mass spectrometer, at the same time investigating the kinetic-energy distributions of a number of fragment ions from various molecules.[21] Coggeshall has recently treated quite rigorously the discrimination effects in various mass-spectrometer ion sources.[22]

The question of the origin of high-kinetic-energy ions and their importance in mass spectra remains an open one despite the above-mentioned work. No previous investigator has been able to assess the relative abundance of high-kinetic-energy ions with respect to thermal ions of the same M/q, nor has it been determined how widespread is the occurrence of such high-energy ions. In addition, the various studies in the field have not been successful in presenting a conclusive argument for a mechanism explaining the formation of high-kinetic-energy ions. The excess-energy ions are also of interest for implications their existence holds for theories concerning mass spectra in general. It was in hopes of shedding light on some of these topics that this investigation of excess-kinetic-energy ions in mass spectra was undertaken.

THE MASS SPECTROMETER

The Basic Instrument

All data obtained in this research were taken on a Consolidated Electrodynamics Corporation model 21-103A mass spectrometer. This instrument is a 180°-magnetic-deflection spectrometer of the type first developed by Dempster.[23] The particular instrument used was modified in several ways described below.

In the Consolidated 21-103A instrument, the material to be analyzed is admitted to the ionization chamber, called the Isatron, through a gold leak (see Fig. 1). In the Isatron it is subjected to bombardment by a beam of reasonably monoenergetic electrons produced by a directly heated rhenium filament. Positive ions thus formed are subjected to a repelling electric field provided by the repellers, which field "pushes" the ions through an exit slit into the accelerating region. The energy of the bombarding electrons can be adjusted by adjusting the accelerating potential between the filament and the Isatron chamber, and a suitable potentiometer arrangement allows adjustment of the potentials applied to the repellers.

Upon passing into the accelerating region, the ions are subjected to an accelerating electric field provided by a potential difference between the exit slit of the Isatron and a second--so-called accelerating--slit. In the region between these slits, a further focusing field is provided by a pair of plates whose potential may be varied. After passing through the accelerating slit, the ions enter an electric field-free region wherein they are deflected by a constant magnetic field directed perpendicular to the direction of their motion. Under the proper conditions, some of the ions will pass through a final slit at the end of this region and strike a collector, whereby they give rise to an electrical signal and are detected. Just ahead of the collector slit is a pair of plates, called the metastable suppressor, to which a positive potential may be applied, thereby retarding the motion of the ions.

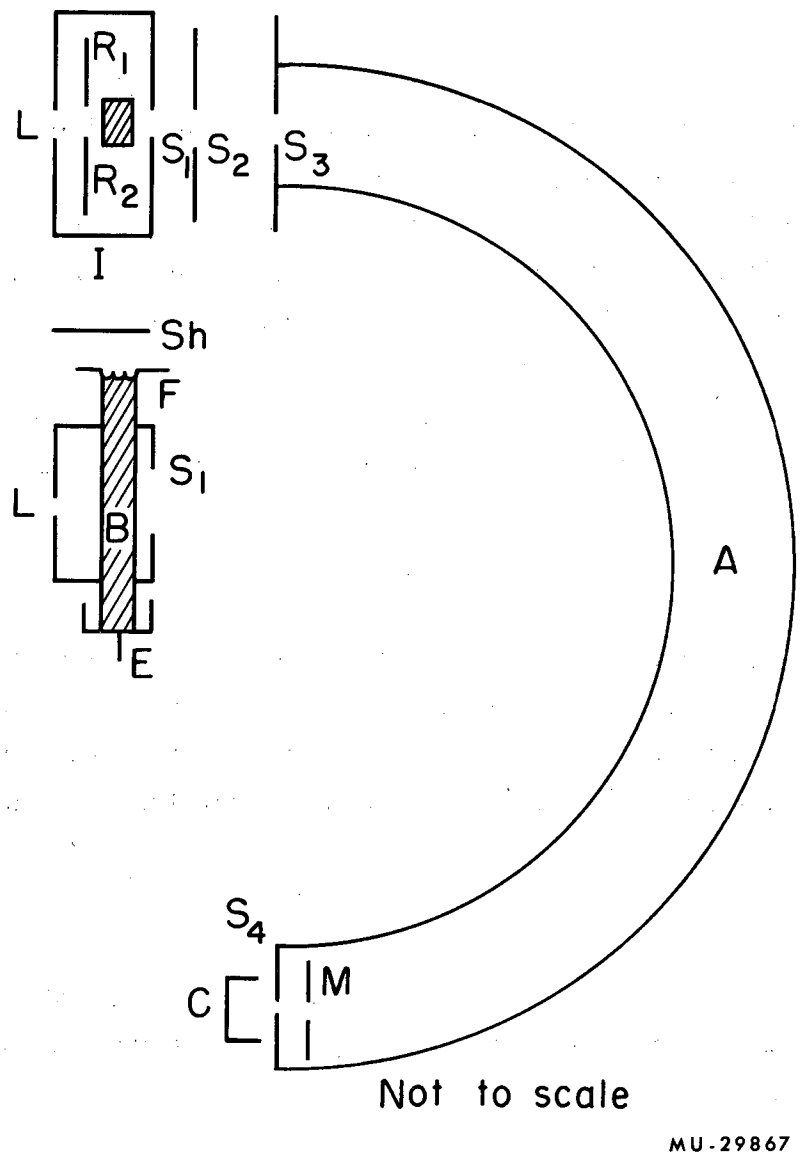

Fig. 1. Schematic diagram of mass spectrometer. I: Isatron; L: gold leak; R_1, R_2: repellers; S_1: exit slit; S_2: focus slits; S_3: accelerating slit; A: analyzer; M: metastable suppressor; S_4: collector slit; C: collector; Sh: shield; F: filament; B: electron beam; and E: electron collector (anode). The Isatron is shown in two views, one rotated by 90° from the other.

An ion that has entered the electric-field-free analyzer region will describe a circular path whose radius is given by the relation

$$R = \frac{mv}{qeB} , \qquad (1)$$

where R is the radius in cm, m is the mass of the ion in grams, e is the electronic charge in abcoulombs, q is the number of such charges resident on the ion, v is the ion velocity in cm/sec, and B is the magnetic-field strength in gauss. Thus for a constant R and a given magnetic field, ions of the same momentum will be collected provided also that their charges are the same.

The momentum of an ion in the analyzer region is determined by its velocity when it enters that region, which may be expressed as

$$v = (2Veq/m + v_i^2)^{1/2} , \qquad (2)$$

where V is the potential difference between the exit slit of the Isatron and the accelerating slit, expressed in abvolts, and v_i is the velocity the ion possessed when it entered the accelerating region. Combining Eqs. (1) and (2), one obtains for the path radius the expression

$$R = \frac{m}{qeB} (2Veq/m + v_i^2)^{1/2} , \qquad (3)$$

from which it is apparent that if either the magnetic field B or the electric field V is varied, the M/q ratio focused at the collector will vary also.

Modifications

On the particular mass spectrometer used for this research, five modifications were made on the basic Consolidated instrumentation affecting the circuits controlling the accelerating voltage, the metastable suppressor, the repellers, the electron beam, and the magnetic field.

Accelerating Voltage

The accelerating-voltage power-supply control circuit was modified to allow lower accelerating voltages to be attained, as shown in Fig. 2. The voltage applied between the Isatron and the accelerating slit is determined by the current flowing through a 400-kΩ resistor, which current is in turn set by the current flowing from filament to plate of a 100TH electronic tube. The latter current is controlled by regulating the voltage applied to the grid of the tube. Normally, this grid voltage may be varied from -135 V to 0 V, where the accelerating voltage reaches a lower limit of about 430 V, owing to residual output current flowing through the tube. However, by inserting a battery supplying a small (0 to 9 V) positive potential to the grid, the output current can be reduced to almost zero, and the accelerating voltage can be reduced to about 75 V.

The accelerating-voltage circuitry was further modified in two ways: (a) by inserting between the accelerating-voltage divider circuit and ground a 10-turn 100-Ω Helipot, and (b) by replacing the potentiometer supplied with the instrument with a Rubicon Type-B potentiometer and a Leeds and Northrup Model-2420D galvanometer. These changes permitted the accelerating voltage to be set and measured with a precision of better than 0.02 V.

Metastable suppressor and repellers

The control circuits for the metastable suppressor and repeller voltages were modified as shown in Fig. 3. The metastable-suppressor control was modified by replacing the 2.5-MΩ one-turn logarithmic potentiometer controlling the metastable-suppressor voltage with a 1.0-MΩ 15-turn linear Helipot in series with a 1.5-MΩ fixed resistor. This replacement limited the range of voltages through which the metastable suppressor could be varied but allowed the voltage to be controlled reproducibly to 0.01 V within that range.

The repeller-voltage control circuit was modified in two ways: firstly, by replacing the fixed 40-kΩ resistor with a pair of 50-kΩ

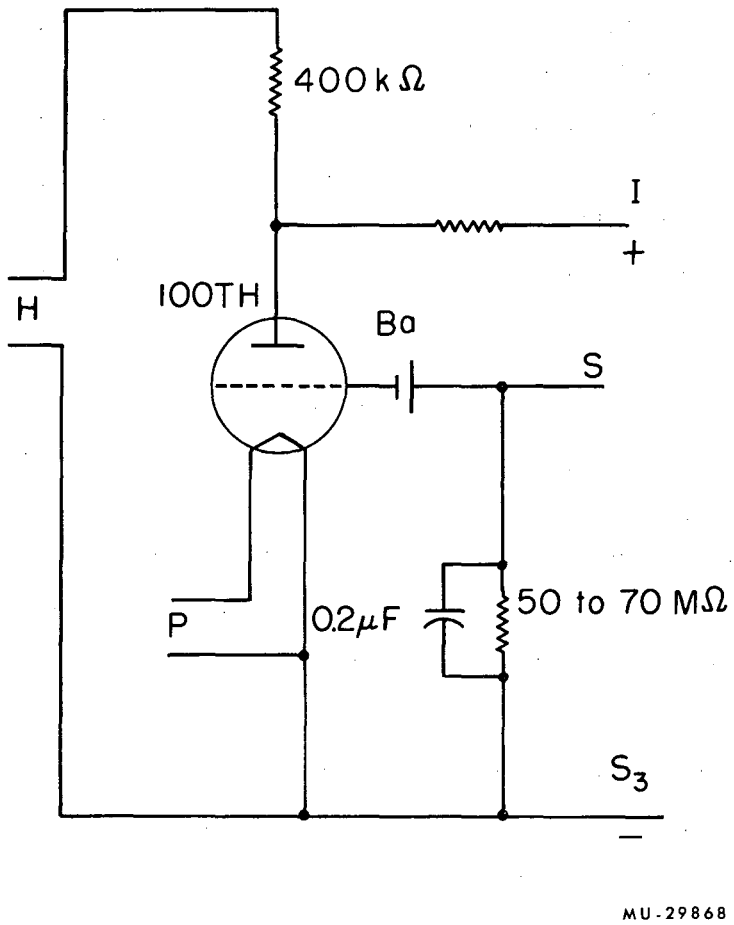

Fig. 2. Modified accelerating-voltage power supply. H: high voltage; P: filament power supply; Ba: 0 to 9-V battery; I: to Isatron; S_3: to accelerating slit; and S: to sweep switch and accelerating-voltage control circuit.

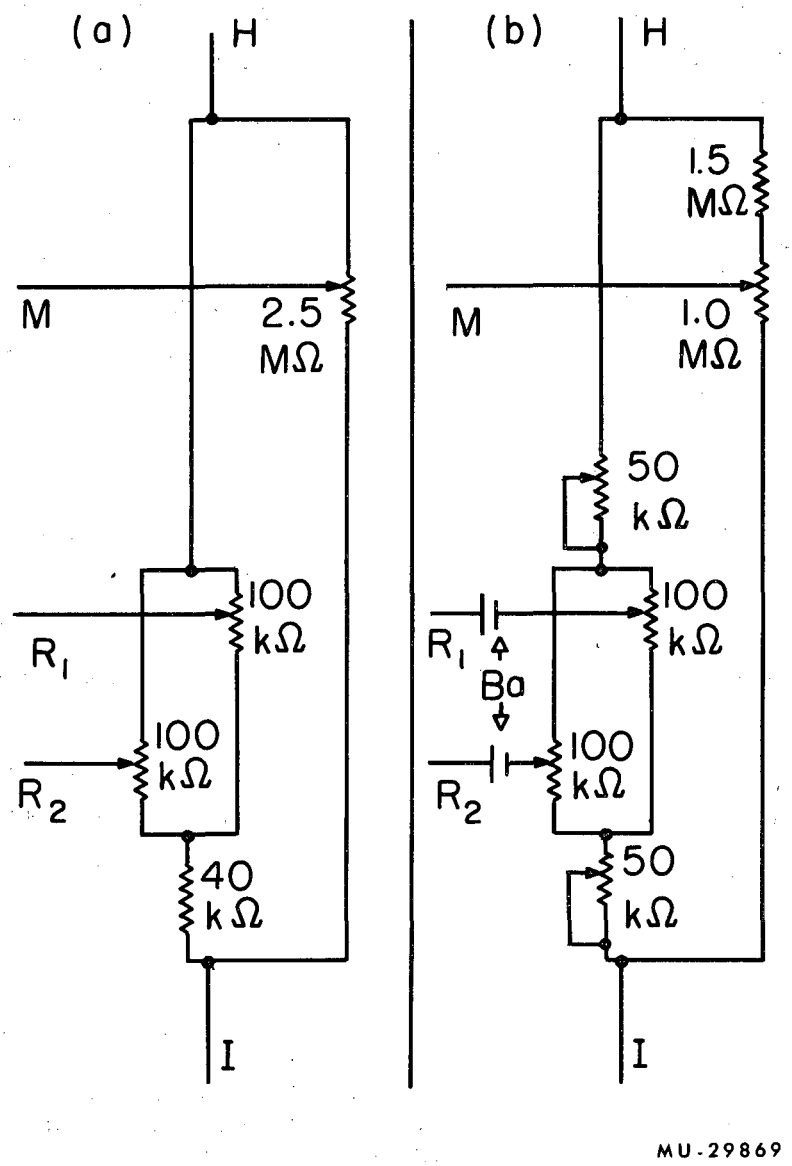

Fig. 3. Metastable-suppressor and repeller-voltages control circuit: (a) unmodified, (b) modified. H: high voltage; M: to metastable suppressor; R_1: to inner repeller; R_2: to outer repeller; I: to Isatron; and Ba: variable-voltage dry-cell batteries.

potentiometers, controlled in tandem, on either side of the divider circuit controlling the repeller voltages; and secondly, by inserting into the network supplying the voltage to each repeller a multi-terminal dry-cell battery capable of supplying either a bucking (negative) voltage or an additional positive voltage of up to 22.5 V. These alterations permitted the repeller voltages to be varied from -22.5 V to + 80 V. A Hexem Inc. battery-operated vacuum-tube voltmeter was installed in the circuit, with connections to each repeller and to the metastable suppressor, permitting measurement of the voltages applied to each of these components. This voltmeter was mounted so it could operate while floating at high voltage.

Ionizing Voltage

The electron-beam-control network was modified in two ways: firstly, by including in the ionizing voltage circuit a Leeds and Northrup Model 7655 potentiometer to permit measurement of the ionizing voltage to within 0.05 V; and secondly, by installing a bucking battery in the anode circuit to permit the voltage of the anode to be varied from its original setting of +220 V relative to the Isatron down to 0 V relative to the Isatron. Connections were also provided to the vacuum-tube voltmeter mentioned above to allow the anode-Isatron voltage to be monitored.*

---

*Operating the anode-Isatron voltage at a value below about 10 V has the advantage of eliminating from the mass spectra complicating factors due to charge-exchange processes, in which the initial ions were formed by electron impacts in the region between the Isatron and collector. Such processes become of considerable importance at the very high source pressures at which some of the appearance potentials determined in this work had to be measured. When the anode-Isatron voltage is high, ions leading to these processes will be formed at all ionizing voltages with fairly high probability, since the cross section for their formation will be determined essentially by the anode-Isatron potential difference. If that voltage is low, on the other hand, the probability of ion formation in the collector region will be sufficiently low that the contributions to the mass spectra arising from such charge-exchange processes will be negligible.

Magnetic field

A charging condenser and switch installed in the magnet-current control circuit allowed the magnetic field to be varied in a uniform manner for purposes of scanning a short range of M/q values magnetically.

During a series of experiments in which the accelerating voltage was varied, the magnetic field was held constant at a given value by maintaining constant flux--as measured by a bismuth wire fluxmeter[24]--through manual adjustment of the magnet-current control.

CHARACTERISTICS OF EXCESS-KINETIC-ENERGY PEAKS

Measurement of Energy

The behavior of an ion of excess kinetic energy in a mass spectrometer differs considerably from that of an ion of thermal energy. Of greatest significance, since it permits the high-energy ion to be measured separately from the thermal ion, is that an excess-kinetic-energy ion will is focused under conditions slightly different from those required to focus a thermal ion of the same M/q. Figure 4 shows the observed peak shapes when the accelerating voltage is scanned at constant magnetic field for ion peaks from n-butane. The M/q=14, M/q=15, M/q=16, and M/q=29 peaks have two components, the leading peak composed essentially of thermal ions whereas the trailing peak is made up of excess-kinetic-energy ions. If one writes Eq. (3) in terms of the initial kinetic energy T_i of the ions, one obtains

$$R = \frac{m}{qeB} (2Veq/m + 2T_i/m)^{1/2} . \qquad (4)$$

Rearranging this equation and changing the units to express B in gauss, e in esu, and V in statvolts, one obtains

$$R^2 = \frac{2mc^2}{qeB^2} (V + \frac{T_i}{qe}) , \qquad (5)$$

from which it is apparent that when the magnetic field is held constant, a change in the initial kinetic energy of the ion requires a change in the opposite direction of the accelerating voltage if the focus conditions are to be maintained.

Furthermore, if one converts the voltage from statvolts to volts absolute and expresses the kinetic energy in electron volts (eV), one obtains the expression

$$150eR^2/c^2 = \frac{m}{qB^2} (V + T_i/q). \qquad (6)$$

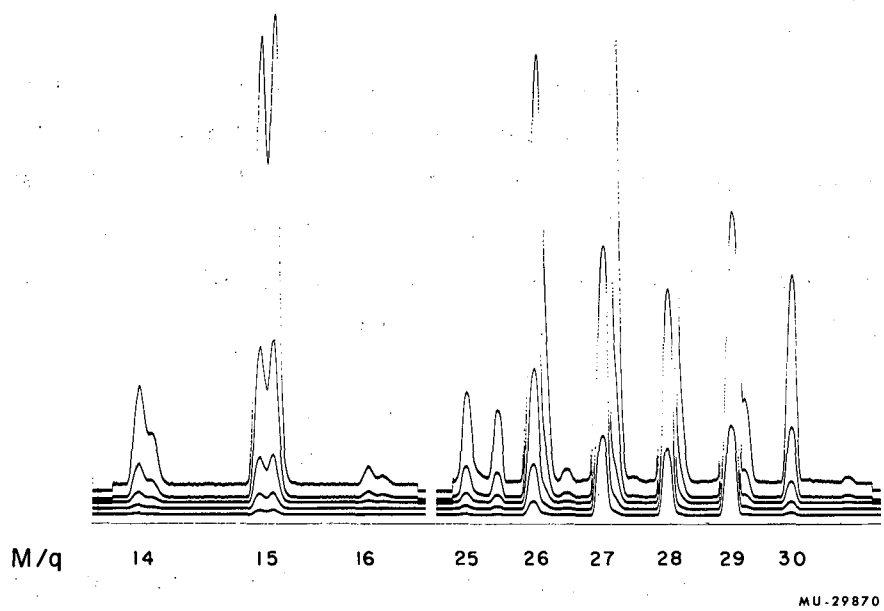

Fig. 4. Typical peak shapes obtained by scanning the mass-spectrometer accelerating voltage at constant magnetic field. Peaks shown are from the mass spectrum of n-butane: M/q=14 to 16 scanned at MV=4500 and M/q=25 to 31 at MV=6000, repeller voltage at 0 V, and amplifier at high sensitivity.

Hence it is seen that, for singly charged ions, the difference in voltage required to focus thermal ions and excess-kinetic-energy ions of the same M/q is just equal to the difference in kinetic energies in eV between the thermal and excess-kinetic-energy ions.

In many instances the so-called thermal ions are not truly thermal, but are themselves formed with some small increment of excess kinetic energy. When high-kinetic-energy ions are associated with such "thermal" ions, the total kinetic energy possessed by the high-kinetic-energy ions can be obtained only by adding to the excess kinetic energy as measured by the difference in focus voltage the kinetic energy possessed by the "thermal" ions.

Every mass spectrometer has a limit to its resolving power which is determined by the geometry of the analyzer and the widths of the slits. This limit in resolution sets a lower limit to the excess kinetic energy, below which the ions with excess kinetic energy will not be separated from those that are thermal. Considering only singly charged ions, from Eq. (6) one can obtain a ratio

$$\frac{R_B^{\,2}}{R_A^{\,2}} = \frac{m_B}{m_A} \; \frac{V_B + T_{iB}}{V_A + T_{iA}} \tag{7}$$

which can be used to calculate the resolving power of the mass spectrometer. The subscript A denotes an ion that strikes the near edge of the collector slit; the subscript B denotes an ion of different kinetic energy which, for resolution to be complete, must strike the far edge of the collector slit. If the two ions are of identical mass, but ion B possesses more kinetic energy than ion A, and if T_A is much smaller than V, then at a given accelerating voltage Eq. (7) becomes

$$\frac{R_B^{\,2}}{R_A^{\,2}} = 1 + \frac{T_i}{V} \; . \tag{8}$$

The radii of curvature, R_A and R_B, of the two ions may be determined from the slit widths and radius of curvature of the analyzer. Since the entrance slit to the analyzer (the accelerating slit) has a width of 0.006 in., the minimum beam width will be equal to that figure. The collector slit, on the other hand, has a width of 0.03 in. The conditions required for complete resolution, as illustrated in Fig. 5, are then

$$R_A = R - (0.006 + 0.03)/4$$

and

$$R_B = R + (0.006 + 0.03)/4$$

Since $R = 5$ in., $R_A = 4.991$ in. and $R_B = 5.009$ in. Substituting these values into Eq. (8) and solving, one obtains for the minimum completely resolvable kinetic energy the expression

$$T_i = 0.0072 \text{ V}. \tag{9}$$

The practical lower limit for resolution of peaks of different kinetic energies is somewhat lower than the value given by this expression, as it is not necessary to have complete separation of the peaks but only to have the maxima separated sufficiently for a valley to be between them. At the same time, however, the expression is somewhat unrealistic because the width of most ion peaks is greater than the lower limit set by the accelerating slit width. This additional width of the ion peaks is caused primarily by three factors: the spread of initial ion kinetic energies about the most probable value, rapid small variation (ripple) in the high-voltage supply, and variations in the accelerating potentials that different ions experience. The first factor is unavoidable; the second is minimized by proper tuning of the electronic circuits; and the third can be minimized by adjusting operating conditions.

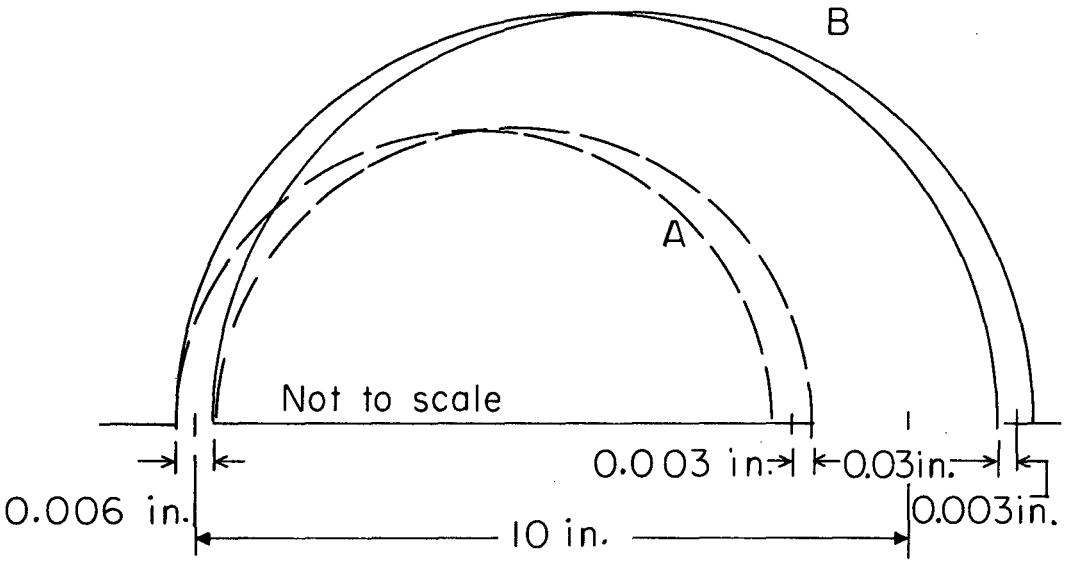

MU-29871

Fig. 5. Schematic diagram of ion paths in the analyzer, showing conditions for complete peak resolution. A and B represent envelopes of paths of ions of two distinct M/q ratios or initial kinetic energies.

A major source of small differences in accelerating potentials for different ions is the repeller voltage. Since ions may be formed at any point in the electron beam, an ion will experience a greater or lesser potential difference in moving from its point of formation to the exit slit of the Isatron, depending on whether it is formed relatively far from or near the exit slit. To minimize peak broadening then, it is desirable to operate with the repellers as near 0 V as is feasible.

From Eq. (9) it is clear that greater energy resolution may be obtained at lower accelerating voltages. Since another source of a difference in accelerating potentials for different ions is the penetration into the Isatron of the accelerating field, it is also advantageous from that point of view to operate at low accelerating voltages. The lower the accelerating voltage, then, the better; but at the very low magnetic field required to focus ions of low energy, the mass spectrometer loses its stability. Furthermore, the collection efficiency of the machine falls rapidly as the accelerating potential is reduced to low values. This fall in efficiency results from the discrimination of the mass-spectrometer slits against ions possessing kinetic energy. The extent of such discrimination depends on the ratio of kinetic energy to accelerrating voltage; hence, as low accelerating voltages are reached, even thermal kinetic energy is sufficient to cause considerable discrimination. Thus the apparatus itself sets a practical lower limit on the accelerating voltage that can be employed.

Effect of Metastable Suppressor

The behavior of an ion with excess kinetic energy is also different in other ways from that of a thermal ion. The simplest of these other differences is the behavior in response to the metastable suppressor, a retarding plate located in the analyzer tube near the collector. As one applies a greater and greater positive potential to this plate, ions traveling down the analyzer are retarded more and more, until at some

metastable-suppressor setting the ion beam is completely prevented from striking the collector. The potential required to stop the ion beam at a given accelerating voltage is about the same for all thermal peaks; however, a higher potential must be applied to stop ions that possess excess kinetic energy. This behavior is illustrated in Fig. 6, which shows a plot of ion current vs metastable-suppressor voltage for typical thermal and excess-kinetic-energy ion peaks.

The difference in metastable-suppressor voltages necessary to extinguish thermal and high-kinetic-energy ions may be taken as a measure of the difference in the amounts of excess kinetic energy possessed by those ions, if suitable corrections are applied to convert the metastable-suppressor voltage to the voltage actually experienced by the ions.[17] This technique is discussed further in another section.

Effect of Accelerating Voltage

The effect on an ion of a variation in the accelerating voltage of the mass spectrometer is strikingly different for excess-kinetic-energy ions than for thermal ions, as demonstrated in Fig. 7, which shows the variation of peak height with accelerating voltage for typical thermal and high-energy ions. The kinetic energies possessed by thermal ions is sufficient at low accelerating voltages to cause them to be discriminated against strongly by the various slits in the mass spectrometer. However, as the accelerating voltage is increased, the kinetic energies become insignificant compared with the accelerating voltage, and the discrimination lessens. Above about 500 V accelerating voltage, the thermal-ion peak reaches a constant height, thereby indicating that discrimination effects are no longer of importance. For excess-kinetic-energy peaks, on the other hand, even at the maximum accelerating voltage available in the mass spectrometer the ratio of excess kinetic energy to accelerating voltage is so great that there still are considerable discrimination effects. This is indicated by the continual increase in peak height of the excess-kinetic-energy ions with accelerating voltage.

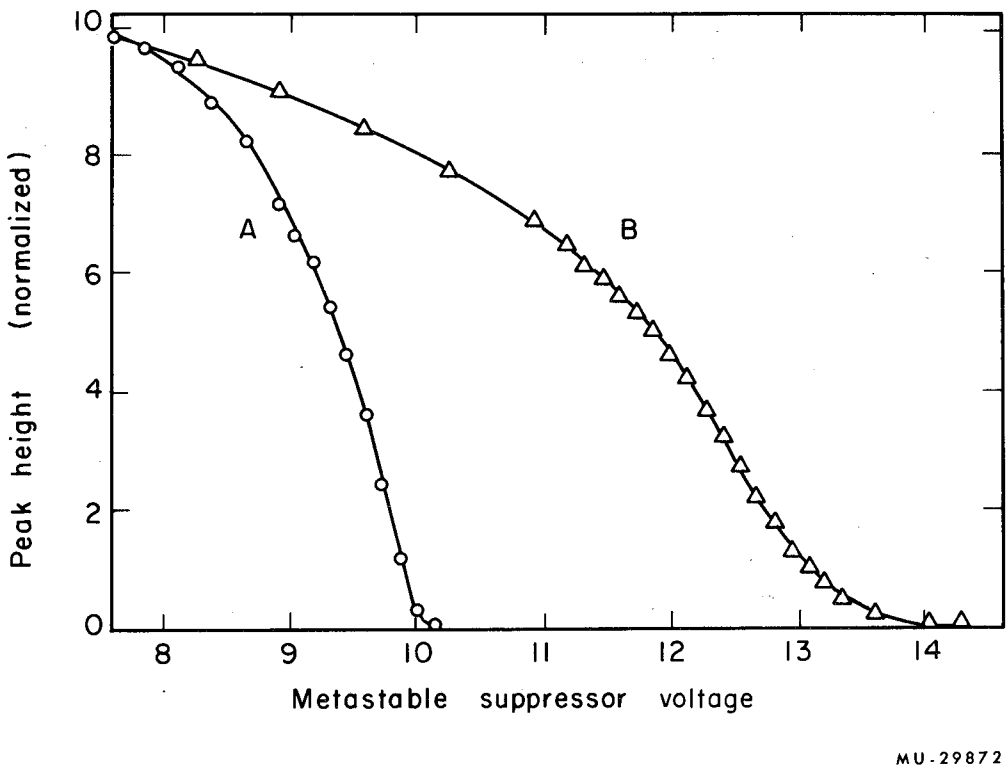

Fig. 6. Variation of peak heights with metastable-suppressor voltage. Data taken at 0-V repellers and 300-V accelerating voltage. A: Curve for thermal M/q=20 peak from neon; B: Curve for 2.66-eV excess-kinetic-energy M/q=15 peak from isobutane.

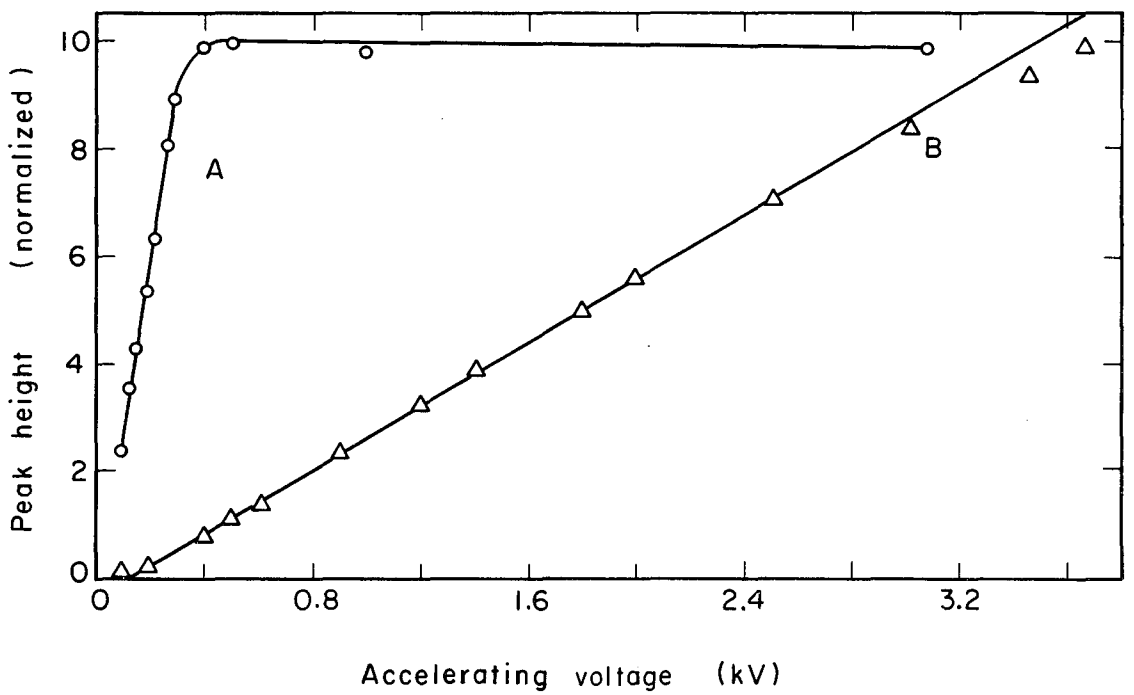

MU-29873

Fig. 7. Variation of peak heights with accelerating voltage. Data taken with repeller voltage at 1% of accelerating voltage. A: Curve for thermal M/q=15 peak from methane; B: Curve for 2.27-eV excess-kinetic-energy M/q=15 peak from benzene.

Effect of Repellers

If one varies the repeller voltage while holding the accelerating voltage constant, one observes different behavior for an excess-kinetic-energy ion than for a thermal ion. Figure 8 shows these behaviors for a typical thermal ion and a typical excess-energy ion. As was observed for the metastable suppressor, there is a difference in cutoff points for the two types of ions. Whereas the peak due to a thermal ion falls very rapidly in the vicinity of zero repeller voltage, reaching zero peak height at a few tenths of a volt negative repeller setting, the peak due to an excess-energy ion diminishes much more slowly and is not eliminated until moderate negative voltages are applied to the repellers.

The shape of the curve in the negative region roughly reflects the kinetic-energy distribution within the ion peak, the slope of the curve reaching a maximum value at the repeller voltage that results in a potential in the region of ion formation equal to the most probable kinetic energy of the ion. The voltage at which the peak height finally falls to zero, on the other hand, represents the setting at which the potential in the ionization region becomes equal to the highest kinetic energy attained by any ion of the appropriate mass.

The problem of determining the relationship between the voltage applied to the repellers and the potential resulting in the ionization region is seriously complicated by the perturbation of the repeller field by the penetration of the accelerating field and the space-charge effect of the electron beam. For this reason it is not feasible to use curves of peak height vs repeller as a quantitative measure of the energy of high-kinetic-energy ions.

For positive repeller settings, it is observed that peaks due to thermal ions increase very rapidly in height at low positive voltages and approach an asymptotic limit. Peaks due to high-kinetic-energy ions, on the other hand, increase in height very slowly, if at all, up to a voltage corresponding roughly to the energy of the ion, whereupon the peak-height curve breaks and the peak height begins to increase linearly with repealler

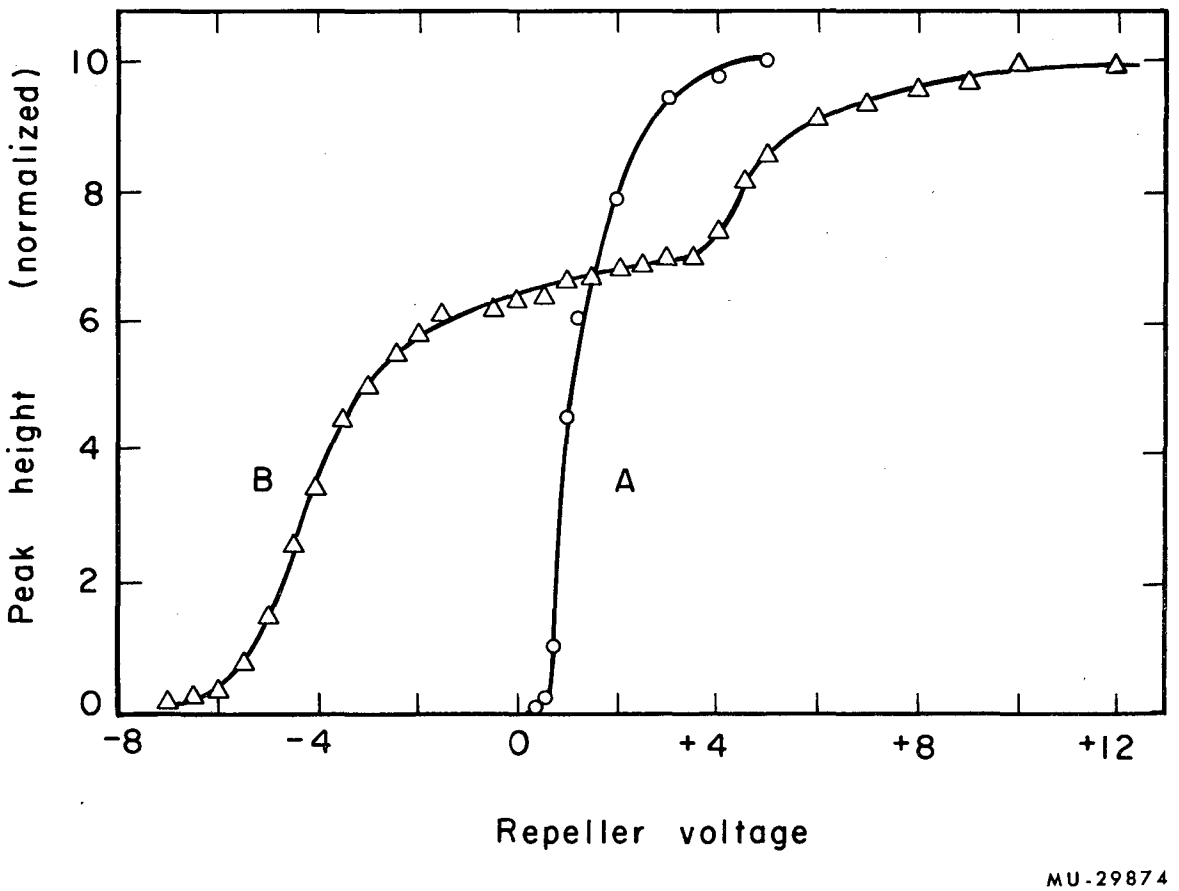

Fig. 8. Variation of peak heights with repeller voltage. Data taken with accelerating voltage constant at 300 V. A: Curve for thermal M/q=15 peak from methane; B: Curve for 2.27-eV excess-kinetic-energy M/q=15 peak from benzene.

voltage. At still higher repeller settings, the height increase deviates from linearity, with the peak height eventually approaching a limit. The break point in the curve corresponds qualitatively to the location of Coggeshall's boundary between conditions under which the orbits are partially collectible and those under which they are completely collectible.[22] One might then characterize the conditions at repeller voltages lower than the break point as such that an increase in repeller voltage serves to "turn around" more of the ions that had initial velocities pointing in the direction away from the exit slit, but does not improve significantly the angular distribution of velocities of those ions passing through the exit slit. Thus, the discrimination effects at the accelerating slit remain about the same. At repeller voltages above the break point, on the other hand, all the orbits are "turned around," and as the repeller voltage is increased the focus conditions become increasingly better. This picture is of course only qualitative; the actual potential distribution within the ion source is undoubtedly very complex in nature, owing to contributions from several sources, and therefore the effect of varying any one of the sources, e.g. the repeller voltages, is in general not quantitatively predictable.

DATA

All the data obtained in this research were taken with the modified Consolidated 21-103A mass spectrometer described previously. The settings of this instrument at which mass spectra are normally recorded are as follows: MV = 45,000;* repeller voltages approximately 1% of accelerating voltage (inner repeller slightly higher in potential than outer, set to optimize focus conditions); metastable suppressor grounded to analyzer; ionizing voltage = 70 V; ionizing current = 37.5 μA; amplifier set on low sensitivity; gas pressure in the source variable, usually in the neighborhood of 50 μ. For much of the data taken in this research these conditions were altered to permit study of the excess-kinetic-energy-ion peaks, as follows: MV = 6000; repellers at Isatron potential; amplifier set on high sensitivity (gain 11.38 times gain at low sensitivity).

Excess Kinetic Energies

Excess kinetic energies have been measured for the M/q=15 ion peaks of a large number of organic compounds. As is evident from the focus equation of the mass spectrometer,

$$150eR^2/c^2 = \frac{m}{qB^2} (V + T_i/q), \qquad (6)$$

the difference in kinetic energy between an excess-kinetic-energy ion peak and a thermal-ion peak of the same M/q can be obtained directly by

---

*MV, the product of the molecular weight of the focused ion and the accelerating voltage at which it is focused, is commonly used as a designation of the magnetic field at which the mass spectrum is measured. It is apparent from Eq. (6) that at constant magnetic field for thermal ions bearing a single charge the product MV will be constant. This is to be expected for a momentum-analyzing machine like the 180° mass spectrometer since $MV = p^2/2eq$.

measuring the difference in accelerating voltage between the focus conditions for the two peaks. In order to know the actual kinetic energy of the excess-energy ions, however, one must determine the kinetic energy possessed by the thermal ions and add it to the measured difference in accelerating voltage.

In principle, the kinetic energy of a thermal ion may be determined by comparing the accelerating voltage at which it is focused with the voltage required to focus an ion of the same M/q ratio which is known to be thermal. The M/q=15 ion formed from methane is thermal or nearly so (comparison of the voltages required to focus the M/q=16 ion and the M/q=15 ion at constant magnetic field indicates that the average excess kinetic energy of the latter ion is less than 0.02 eV, the limits of accuracy of the measurement). It is, however, not possible to compare directly the focus voltage for the M/q=15 ion from methane and that for the M/q=15 ion from some other organic compound because of the presence of contact potentials within the ion source. Such potentials, whose magnitudes may in general vary with the compound present in the source, the pressure in the source, and even the previous history of the source, influence the focus voltages. This is demonstrated in Table I, wherein are listed focus voltages for a series of hydrocarbon—rare-gas mixtures run in sequence. It is seen that the introduction of neon along with methane does not shift the focus voltages for the M/q=15 or M/q=16 ion peaks, but upon addition of n-heptane to the methane—neon mixture both of the above peaks, as well as the M/q=20 peak from neon, shift by a constant increment, owing to the contact potential created by the presence of n-heptane in the ion source.

The following procedure was used to determine contact potentials, excess energies of thermal peaks, and excess kinetic energies of high-energy ion peaks. Initially, a reference mixture of methane and neon was admitted to the ion source and, with the magnetic field held constant, the accelerating voltages required to focus the M/q=15 and M/q=20 ion peaks were measured. Then, after pumpout of the system, an organic compound of interest was admitted to the ion source, again in the presence of neon, and the focus voltages for the M/q=15, M/q=15* (excess-

Table I. Sample data: Determination of contact potential and excess energy of thermal ion peak.

Components of mixture				Measured voltages			Derived values	
component 1	P_1	component 2	P_2	M/q=15 focus voltage	M/q=16 focus voltage	M/q=20 focus voltage	contact potential	KE of thermal peak
methane	10.7	---	----	216.84	203.13	------	0.00(ref.)	-----
methane	10.7	neon	27.8	216.83	203.13	162.81	0.00	-----
methane-neon	35.2	n-heptane	45.0	216.62	202.95	162.61	0.20	-----
n-heptane	41.5	neon	31.2	216.44	-----	162.61	0.20	0.19

kinetic-energy component), and M/q=20 peaks were measured. Under such conditions, the shift observed in the M/q=20 focus voltage (ΔV_{20}) represents the influence of the contact potential; the shift in focus voltage (ΔV_{15}) for the M/q=15 peak represents the excess kinetic energy of the thermal peak plus the influence of the contact potential; and the actual kinetic energy of the excess-kinetic energy ion is given by the expression

$$T_1 = V_{15} - V_{15}^{*} + \Delta V_{15} - \Delta V_{20} \quad . \qquad (10)$$

Table II lists the measured focus voltages and resultant values for the contact potential, kinetic energy of the thermal peak, and kinetic energy of the high-energy peak for a few hydrocarbons run in sequence. It will be noted that between the initial and final measurements, the focus voltages for the methane—neon reference mixture shifted by 0.03 V. Shifts in focus voltage of comparable magnitude, attributed to slight variations in the magnetic field of the mass spectrometer, occurred occassionally during the experiments to determine kinetic energies. Such shifts, although they influenced the values obtained for the contact potentials, did not change the values for the kinetic energies, since all the measured voltages shifted uniformly.

For these measurements, the mass spectrometer was operated at conditions that permitted maximum resolution of the thermal and excess-kinetic-energy peaks and greatest precision of measurement of the focus voltages, those conditions being different from the normal operating conditions in that the MV was reduced to 3220 and the repellers were operated at 0 V. At MV's below 3220, the stabilization of the magnetic field became difficult and reasonable peak heights could not, in general, be obtained at moderate source pressures. At MV = 3220, the accuracy with which the focus voltages could be determined was dependent on the precision with which the voltage giving the maximum ion current could be located. This is estimated to be ± 0.02 V, and since each determination of the kinetic energy of a high-energy ion involved three such measurements, the limits of error of the kinetic energies are ± 0.06 V.

In Table III the values obtained in this research for the energy separation between thermal and high-energy peaks are compared with the results of Mohler, Dibeler, and Reese (MDR)[12] and those of Tsuchiya.[15]

Table II. Sample data: Measurement of kinetic energy of excess-kinetic energy peaks.

Components of mixture				Measured voltages			Derived values		
component 1	P_1	component 2	P_2	M/q=15 focus voltage	M/q=15* focus voltage	M/q=20 focus voltage	contact potential	KE of thermal peak	KE of high-energy peak
methane	13.7	neon	25.7	213.69	-----	160.45	0.0 (ref.)	0.0(ref.)	-----
propane	68.2	neon	26.5	213.41	210.91	160.32	0.13	0.15	2.65
n-butane	94.3	neon	33.5	213.26	210.98	160.22	0.23	0.20	2.48
isobutane	65.1	neon	30.5	213.16	210.62	160.08	0.33	0.20	2.66
methane	21.7	neon	30.1	213.72	-----	160.48	-0.03	0.0	-----

Table III. Comparison of kinetic-energy data with data of previous workers.[a]

Compound	Energy difference between thermal and high-energy peaks (in eV) as measured by		
	MDR[12]	Tsuchiya[15]	This research
ethane	2.3	2.5	2.39
propane	2.2	2.4	2.40
n-butane	2.2	2.3	2.28
n-pentane	2.0	---	2.07
n-hexane	1.8	---	1.72
n-heptane	1.7	---	1.66
isobutane	2.6	2.5	2.46
neopentane	2.4	---	2.51
propylene	---	2.6	2.67
1-butene	2.2	---	2.44
1,3-butadiene	---	2.5	2.47
cyclohexane	2.0	---	2.14
benzene	1.8	---	2.13

[a]Excess energy of thermal peak not included in values listed in this table.

Since the effect of excess kinetic energy present in the thermal ion was not taken into account in those studies, one cannot compare the actual kinetic energies obtained in this work, but only the measured energy difference between thermal and high-energy peaks. The agreement between values obtained in this work and those of Tsuchiya is quite good, while agreement with the measurements of MDR is satisfactory except in the case of benzene. The lack of agreement for that compound probably arises because of the very low peak height of the thermal peak, which makes determination of its focus voltage difficult. The quality of agreement of the results shown in Table III indicates that the conditions under which the kinetic energies were measured did not appreciably affect the values obtained.

In Table IV the measured values for kinetic energies of thermal peaks and excess-kinetic-energy peaks are given for the M/q=15 (CH_3^+) ion originating from a large number of organic compounds. In addition, the total kinetic energy released in the fragmentation that gives rise to the CH_3^+ ion is listed for both thermal and excess-energy ions. This total kinetic energy is easily calculated if it is assumed that the immediate products of the fragmentation are only two. Then, the law of conservation of momentum requires that the total kinetic energy be related to the kinetic energy of the mass-15 fragment by the relation

$$KE_{tot} = KE_{15}(M_{tot}/M_{tot} - 15) , \qquad (11)$$

where M_{tot} is the molecular weight of the parent molecule.

A few kinetic energies were accurately measured for ions of M/q ratios different from 15. The values measured for these ions are given in Sec. J of Table IV. Values listed in that part of the table that are less than 1.5 V were measured by determining the metastable-suppressor-cutoff curve for the peak in question. Since the energy of interest is not the maximum kinetic energy of the ions but the most probable energy, the actual disappearance voltage for the peak may not be used. Rather, an average disappearance voltage must be determined.

Table IV. Kinetic energies of M/q=15 fragment ions.

Compound	Thermal ion		Excess-KE ion	
	KE of M/q=15 ion	Total KE fragmentation	KE of M/q=15 ion	Total KE fragmentation
	A. Paraffins			
ethane	0.06	0.12	2.45	4.90
propane	0.15	0.28	2.65	4.02
n-butane	0.20	0.27	2.48	3.35
isobutane	0.20	0.27	2.66	3.59
n-pentane	0.17	0.21	2.24	2.83
neopentane	0.20	0.25	2.71	3.42
n-hexane	0.23	0.28	1.95	2.36
di-isopropyl	0.17	0.21	2.50	3.03
n-heptane	0.17	0.20	1.83	2.15
2,4-dimethyl pentane	0.23	0.27	2.08	2.45
2,5-dimethyl hexane	0.19	0.22	2.06	2.37
	B. Olefins			
propylene	0.08	0.12	2.75	4.28
butene-1	0.15	0.20	2.59	3.54
cis-butene-2	0.15	0.20	2.65	3.62
isobutylene	0.12	0.16	2.76	3.77
pentene-1	0.13	0.17	2.30	2.93
3-methyl butene-1	0.17	0.22	2.52	3.21
hexene-1	0.11	0.13	2.02	2.46
4-methyl pentene-1	0.16	0.19	2.21	2.69
heptene-1	0.16	0.19	1.85[a]	2.2

Table IV. (cont.)

Compound	Thermal ion		Excess-KE ion	
	KE of M/q=15 ion	Total KE fragmentation	KE of M/q=15 ion	Total KE fragmentation
	C. Dienes			
1,2-butadiene	0.14	0.19	2.61	3.61
1,3-butadiene	0.12	0.17	2.59	3.59
2-methyl butadiene-1,3	0.20	0.26	2.60	3.34
2,3-dimethyl butadiene-1,3	0.09	0.11	2.48	3.04
1,5-hexadiene	0.16	0.20	2.20	2.69
2,5-dimethyl hexadiene-1,5	0.17	0.20	2.09	2.42
	D. Alcohols			
ethanol	0.12	0.18	2.96	4.39
n-propanol	0.16	0.21	2.71	3.61
isopropyl alcohol	0.16	0.21	2.83	3.77
n-butyl alcohol	0.13	0.16	2.28	2.86
isobutyl alcohol	0.16	0.20	2.76	3.46
t-butyl alcohol	0.18	0.23	2.82	3.54
n-amyl alcohol	0.25	0.30	1.75[a]	2.1[a]
isoamyl alcohol	0.22	0.27	2.40	2.89
neopentyl alcohol	0.24	0.29	2.80	3.38
1,2-propane diol	0.04	0.05	2.7[a]	3.35[a]
	E. Aromatic compounds			
benzene	0.14	0.17	2.27	2.81
chlorobenzene	b	b	2.35	2.71
aniline	0.06	0.07	2.01	2.40

Table IV. (cont.)

Compound	Thermal ion		Excess-KE ion	
	KE of M/q=15 ion	Total KE fragmentation	KE of M/q=15 ion	Total KE fragmentation
toluene	0.20	0.24	2.32	2.77
ethyl benzene	0.23	0.27	2.26	2.63
n-propyl benzene	0.28	0.32	2.11	2.41
F. Halides				
methyl chloride	0.27	0.39	4.15	5.93
ethyl chloride	0.21	0.27	3.02	3.94
n-propyl chloride	0.20	0.25	2.85	3.53
isopropyl chloride	0.22	0.27	2.95	3.65
n-butyl chloride	0.21	0.25	2.50	2.99
isobutyl chloride	0.21	0.25	2.78	3.32
t-butyl chloride	0.26	0.31	2.89	3.45
n-amyl chloride	0.16	0.19	2.26	2.63
isoamyl chloride	0.17	0.20	2.54	2.96
n-heptyl chloride	0.22	0.25	1.79	2.02
ethyl bromide	0.21	0.24	3.31	3.84
n-propyl bromide	0.21	0.24	2.94	3.35
n-butyl bromide	0.21	0.24	2.48	2.78
n-butyl iodide	0.23	0.25	2.27	2.47
1,1-dichloroethane	0.27	0.32	3.51	4.14
1,1-dichloropropane	0.21	0.24	2.90	3.35
1,2-dichloropropane	0.21	0.24	3.08	3.56
2,2-dichloropropane	0.20	0.24	3.23	3.73
1,1-dichlorobutane	0.26	0.29	2.54	2.88
1,1,1-trichloroethane	0.24	0.27	3.25	3.67

Table IV. (cont.)

Compound	Thermal ion		Excess KE ion	
	KE of M/q=15 ion	Total KE fragmentation	KE of M/q=15 ion	Total Ke fragmentation
1,1,1,2-tetra chloropropane	0.23	0.25	3.10	3.38
1-chloropropene-1	0.16	0.20	2.8[a]	3.5[a]
3-chloro-2-methyl propene-1	0.12	0.14	2.76	3.31
1,1-dichloro propene-1	0.21	0.24	3.11	3.60
G. Cyclic compounds				
methyl cyclopropane	0.20	0.27	2.65	3.62
cyclopentane	0.15	0.19	2.53	3.22
cyclopentene	0.25	0.32	2.54	3.26
cyclopentanone	0.20	0.24	2.49	3.03
cyclopentanol	0.25	0.30	2.23	2.70
cyclopentyl chloride	0.13	0.15	2.35	2.75
methyl cyclopentane	0.22	0.27	2.30	2.80
cyclohexane	0.12	0.15	2.26	2.75
cyclohexene	0.17	0.21	2.37	2.90
cyclohexyl bromide	0.20	0.22	2.23	2.46
methyl cyclohexane	0.12	0.14	2.16	2.55
cyclooctatetraene	b	b	2.21	2.58
H. Miscellaneous compounds				
methyl acetylene	0.02	0.03	2.47	3.95
acetone	0.12	0.16	3.41	4.60
di-n-propyl ketone	0.18	0.25	c	c
propionaldehyde	0.11	0.13	2.97	4.01
n-butyraldehyde	0.15	0.19	2.35[a]	2.95[a]

Table IV. (cont.)

Compound	Thermal ion		Excess KE ion	
	KE of M/q=15 ion	Total KE fragmentation	KE of M/q=15 ion	Total KE fragmentation
propionic acid	0.10	0.13	2.95	3.70
n-butyric acid	0.16	0.19	2.48	2.99
n-propyl formate	0.23	0.28	2.25[a]	2.71[a]
di-n-propyl ether	0.18	0.21	c	c
n-propyl carbonate	0.25	0.28	c	c
methyl amine	0.09	0.17	2.86	5.54
ethyl amine	0.01	0.02	2.67	4.01
n-propyl amine	0.10	0.13	2.39	3.20
di-n-propyl amine	0.20	0.23	2.26	2.65
tri-n-propyl amine	0.19	0.21	2.10	2.35
n-butyronitrile	0.17	0.22	2.65	3.39
n-propyl mercaptan	0.16	0.20	2.49	3.10
J. Other M/q ratios				
methyl chloride (35)[d]	e	e	1.48	4.93
methyl amine (16)	e	e	2.37	4.90
propane (27)	e	e	1.2	3.5
propane (28)	e	e	1.2	3.5

[a]Resolution of excess-KE peak was poor; value imprecise.

[b]Height of thermal peak insufficient to permit determination of KE.

[c]Excess-KE peak present but not sufficiently resolved to permit determination of KE.

[d]M/q value shown in parentheses.

[e]Thermal peak energies not measured for these compounds.

Good agreement was found with the values obtained by measuring accelerating voltages if the midpoint of the region of linear decrease of the peak height with metastable-suppressor voltage was taken to be the average disappearance voltage. (See, for example, Fig. 6, in which the difference in voltage between the midpoints of the regions of linear decrease for the Ne^+ peak and the CH_3^+ peak from isobutane is 2.7 V, in agreement with the measured value of 2.66 V.) All voltages measured in this way were multiplied by 0.971 to take into account the difference between applied voltage and voltage actually experienced by the ions.*

In addition to those experiments for which the results are given in Table IV, some experiments were run in which neon was not used as a reference gas; rather, the focus voltages of the thermal M/q=15 peaks were compared with the focus voltage for the M/q=15 peak of methane run separately from the compounds of interest. Under these conditions, it is not possible to determine the contribution of contact potentials to the shift in voltage of the thermal M/q=15 peaks. Hence, the actual kinetic energies of thermal and high-energy peaks cannot be determined exactly. However, the difference in voltage between thermal and excess-kinetic-energy peaks can be determined, along with the sum of the contact potential and the kinetic energy of the thermal peak. These values are given in Table V for compounds for which kinetic energies do not appear in Table IV. Results for those compounds run under both sets of conditions are omitted from Table V because the quantities determined under the first set include all quantities determined under the second set, and because the results were in agreement, within the limits of error, for all such compounds. The mass-spectrometer operating conditions were the same for these experiments as for the previously described ones.

---

*This value was determined by measuring the metastable-suppressor voltage required to cut off a thermal peak. It is in agreement with the value 0.969 computed by Berry for the CEC 21-103 instrument (see reference 17).

Table V. Energy differences between thermal and high-energy M/q=15 peaks

Compound	E_1 [a]	E_2 [b]	Compound	E_1 [a]	E_2 [b]
isopropyl bromide	2.85	0.39	nitromethane	3.86	0.15
isobutyl bromide	2.56	0.36	nitroethane	2.98	0.24
t-butyl bromide	2.82	0.30	1-nitropropane	2.35	0.23
methyl iodide	4.21	0.33	2-nitropropane	2.76	0.26
1,1-dibromoethane	3.24	0.36	propionitrile	3.08	0.25
1,2-dibromopropane	2.55	0.33	isobutyl nitrile	2.82	0.30
1,3-dibromobutane	2.41	0.40	ethyl thiocyanate	3.13	0.26
1,3-dichloro-2-butylene	2.41	0.34	anisole	1.80	0.44
o-chlorotoluene	2.33	0.31	ethyl cyclohexane	2.02	0.42
p-chlorotoluene	2.23	0.32	isobutyraldehyde	2.85	0.24
isopropyl benzene	1.99	0.52	isobutyric acid	2.59	0.41
n-butyl benzene	1.53	0.61	n-butyl formate	1.92	0.38
t-butyl benzene	2.05	0.49	isobutyl formate	2.39	0.38
diethyl ketone	2.44	0.25	n-capronitrile	2.35	0.39
di-isopropyl ketone	2.06	0.44	isocapronitrile	2.36	0.46

[a] Difference between focus voltages for thermal peak and excess-kinetic-energy peak.

[b] Difference between focus voltages for thermal peak and thermal peak of methane.

The measurement of kinetic energies of ions of M/q different from 15 is in most instances complicated by one or more of three factors: low intensity of the excess-kinetic-energy ion, very high intensity of the thermal ion, and small difference in energy between the thermal and excess-kinetic-energy ions. For most compounds the first of these factors prevents accurate determination of the kinetic energy of the M/q=12, M/q=13, and M/q=14 fragments, whereas the second two factors prevent even approximate determinations for higher-mass fragments. In addition, for many M/q values it is not certain whether there exists any compound giving rise to ions that are truly thermal. For these reasons it was not feasible to determine kinetic energies of ions of different M/q values accurately as was done for ions of M/q=15. However, a number of semiquantitative results were obtained in conjunction with experiments concerned primarily with abundances of excess-kinetic-energy ions. These results are tabulated in Appendix I.

Abundances of Excess-Kinetic-Energy Ions

The measurement of excess-kinetic-energy-ion abundances involves considerably more difficulty than does the measurement of excess kinetic energy. The abundance property of intrinsic interest, namely the absolute cross section for formation of a given type of ion per electron per molecule, cannot at present be measured with the instrument used in this research because the number of molecules present in the ion source at any given time is an unknown quantity. Furthermore, the absolute collection efficiency of the mass spectrometer is not known accurately even for thermal ions, much less for excess-kinetic-energy ions.

Most investigators of the phenomenological aspects of mass spectrometry have been faced with this problem. The solution generally has been to measure not absolute cross section but instead fragmentation patterns; that is, the percentage of the total ions observed by the mass spectrometer that are of a given type. If the assumption is made that the collection efficiency of the instrument is the same for all ions formed,

then the observed fragmentation corresponds to the actual fragmentation pattern for the molecule. If any of the ions formed in the fragmentation of the molecule possess excess kinetic energy, however, even this method is not applicable, since it is known that the collection efficiency of the instrument is grossly different for excess-kinetic-energy ions than for thermal ions.

In the course of this research it was found that, although the absolute abundances of excess-kinetic-energy ions cannot easily be measured, it is possible to determine the abundances of excess-kinetic-energy ions relative to thermal ions of the same M/q, as observed with the mass spectrometer under normal operating conditions. Knowledge of these relative abundances permits improved interpretation of the mass-spectral patterns obtained under normal conditions. In addition, it is possible to estimate from the relative abundances the absolute abundances of excess-kinetic-energy ions in a manner described in the discussion section of this report.

The method of determination of relative abundances of excess-kinetic-energy and thermal ions of a given M/q depends on the following characteristics of ion peaks: firstly, the additive character of peak heights when two or more types of ions appear in a single peak; secondly, a similarity in the dependence of collection efficiency on accelerating voltage for ions of the same M/q and initial kinetic energy, regardless of the molecule from which they are formed; and thirdly, the complete resolution of thermal and excess-kinetic-energy ion peaks at low accelerating voltages. These have been utilized in the manner described below.

First of all, the variation of peak height with accelerating voltage was measured for several M/q=15 ion peaks known to consist only of ions of thermal or near-thermal energy. These variations are plotted in Fig. 9 for the M/q=15 peaks from methane (thermal), methanol (0.15 eV kinetic energy), and methyl chloride (0.25 eV kinetic energy). The methyl ion peaks from the latter two compounds have small excess-kinetic-energy components, as evidenced from the fact that the kinetic energies of excess-kinetic-energy ions have been measured for them. However, the relative abundance of thermal ions compared with excess-kinetic-energy ions is so great for these compounds (at least 200 to 1) that the variation of peak height with accelerating voltage for them can be considered to be that of near-thermal ions.

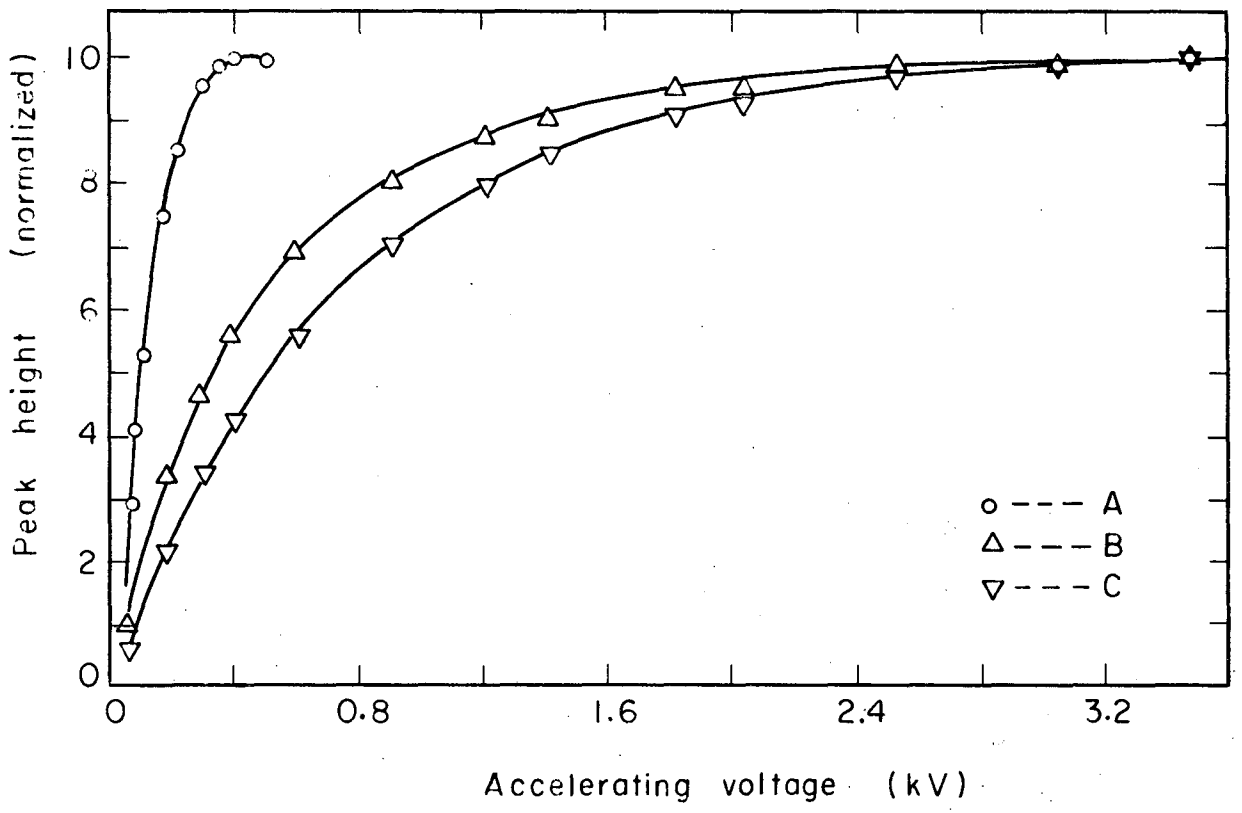

Fig. 9. Variation with accelerating voltage of peak heights for near-thermal ions of M/q=15. Data taken with repeller voltage at 1% of accelerating voltage. A: Curve for thermal ions (methane); B: Curve for 0.15-eV ions (methanol); C: Curve for 0.25-eV ions (methyl chloride).

Secondly, the variation of peak height with accelerating voltage was determined for some compound whose M/q=15 peak was composed of both thermal and excess-kinetic-energy ions. Included in this determination was measurement of the thermal and excess-kinetic-energy peak heights individually at low accelerating voltages for which resolution of the two peaks was complete. Table VI gives the results of such a determination for the propane M/q=15 peak. Note that below 500 V accelerating voltage the resolution of the thermal and excess-energy peaks is sufficient to permit separate measurement of peak heights, but that above 500 V accelerating voltage only the sum peak height can be measured.

Finally, the curve from Fig. 9 corresponding to a near-thermal ion of the same kinetic energy as the near-thermal ion of the compound possessing both thermal and excess-kinetic-energy ions was normalized to give agreement of thermal peak heights in the low-accelerating-voltage region. The contribution of thermal ions to the total peak height at higher accelerating voltages was then considered to be given by the normalized values from the Fig. 9 curve. The excess-kinetic-energy-ion contribution was determined by subtraction of these normalized values from the total measured peak heights. This process is illustrated for propane in Table VI, where the normalized thermal peak heights obtained from the methanol M/q=15 curve are tabulated. When these values are subtracted from the total peak heights, the values for the excess-kinetic-energy peak heights given in Table VI result.

In Fig. 10, the excess-kinetic-energy peak height is plotted as a function of accelerating voltage for the propane M/q=15 ion. In that figure the measured peak heights are used for accelerating voltages below 500 V, and the computed peak heights are used for accelerating voltages above 500 V. These two sets of values all fall on the same straight line, with the exception of two points in the intermediate accelerating-voltage region. The lack of agreement of those two points is due to incomplete addition of ion peaks and consequent erroneously low sums of peak heights in the intermediate region. With the exception of that explainable discrepancy, the curve obtained agrees quite well with the Fig. 7 curve for

Table VI. Breakdown of total peak into its components for propane M/q=15 ion peak.

I Accelerating voltage	II Peak height thermal (meas.)	III Sum peak height (meas.)	IV Excess KE peak height (meas.)	V Computed thermal peak height[a]	VI Computed excess KE peak height[b]
78	77.7	--[c]	4.4	79.1	--
115	142.8	--	10.5	149.7	--
145	193.2	--	16.8	195.7	--
195	264	--	29.9	264[d]	--
300	396	--	67.4	375.7	--
400	470[e]	--	111.6[f]	452	--
500	546[e]	--	157.8[f]	516	--
600	---[g]	684[h]	---[g]	565	119[h]
900	---	976[h]	---	656	320[h]
1210	---	1182	---	708	474
1410	---	1314	---	734	580
1810	---	1533	---	769	764
2010	---	1632	---	777	855
2515	---	1872	---	793	1079
3035	---	2103	---	803	1300
3480	---	2280	---	809	1471
3615	---	2316	---	809	1507

[a]Obtained from measured variation of peak height with accelerating voltage for methanol M/q=15 ion (0.15-eV KE) by normalization.

[b]Obtained by subtraction of column V from column III.

[c]Sum of peak heights not measured when thermal and excess-energy peaks were resolved.

[d]Methanol peak-height variation curve normalized to propane thermal peak height at this accelerating voltage.

[e]Measured peak height somewhat too high because of partial addition of the excess KE peak.

[f]Measured peak height somewhat too high because of partial addition of the thermal peak.

[g]Individual peak heights not measurable because two peaks were merged.

[h]Somewhat too low because of incomplete addition of peak heights.

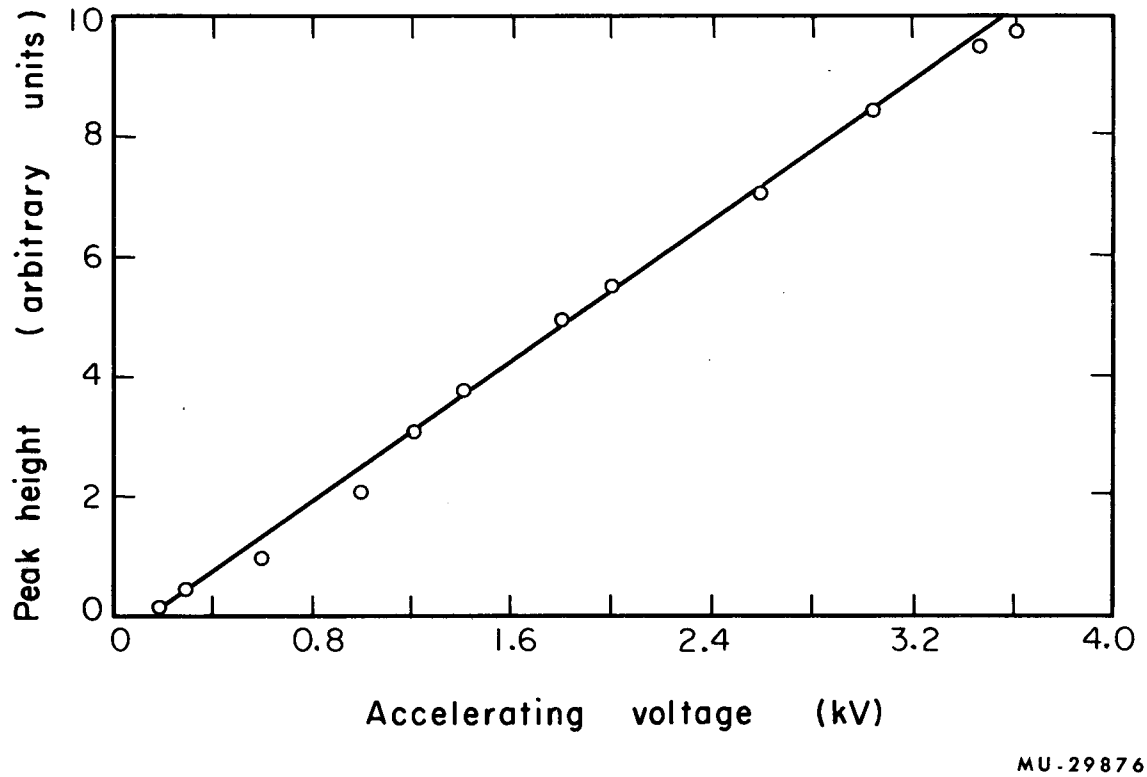

Fig. 10. Variation with accelerating voltage of peak height of excess-kinetic-energy M/q=15 peak from propane. Data obtained by subtraction method outlined in text (see Table VI).

the excess-kinetic-energy M/q=15 ions from benzene. It should be emphasized that this agreement of the computed excess-kinetic-energy curve with a similar curve measured experimentally was not forced by the method of computation; the agreement thus is a strong indication that the method accurately partitions the total peak heights into near-thermal and excess-kinetic-energy fractions.

That the method is not unique for M/q=15 ions is demonstrated in Fig. 11, which shows a curve obtained in a similar manner for the M/q=29 peak of n-heptane. The normalized thermal ion curve used to compute the values for Fig. 11 was obtained from the thermal M/q=29 peak from ethyl chloride.

In Table VII are listed the relative abundances of thermal and excess-kinetic-energy ions observed under normal operating conditions, as derived in the manner described above. In addition, percentage figures are given that show what percent of all the ions observed in the mass spectrometer under normal conditions is comprised of ions of that particular M/q and initial kinetic energy.

In addition to the abundances given in Table VII, a survey of excess-kinetic-energy peak heights was carried out for a large number of different organic compounds under operating conditions that allowed good resolution of the thermal-energy and excess-kinetic-energy peaks. The results of this survey are tabulated in Appendix II.

Appearance Potentials

All appearance potentials measured in this research were determined by a linear extrapolation method, by comparing the extrapolated energy-axis intercept of the ionization-efficiency curve for the ion being investigated with the energy-axis intercept for a reference ion whose appearance potential was known. The accuracy of this method has been criticized by a number of workers,[25,26] but the character of the data obtained in this work was such that other methods did not seem applicable; furthermore, because of the difficulty of obtaining full separation of

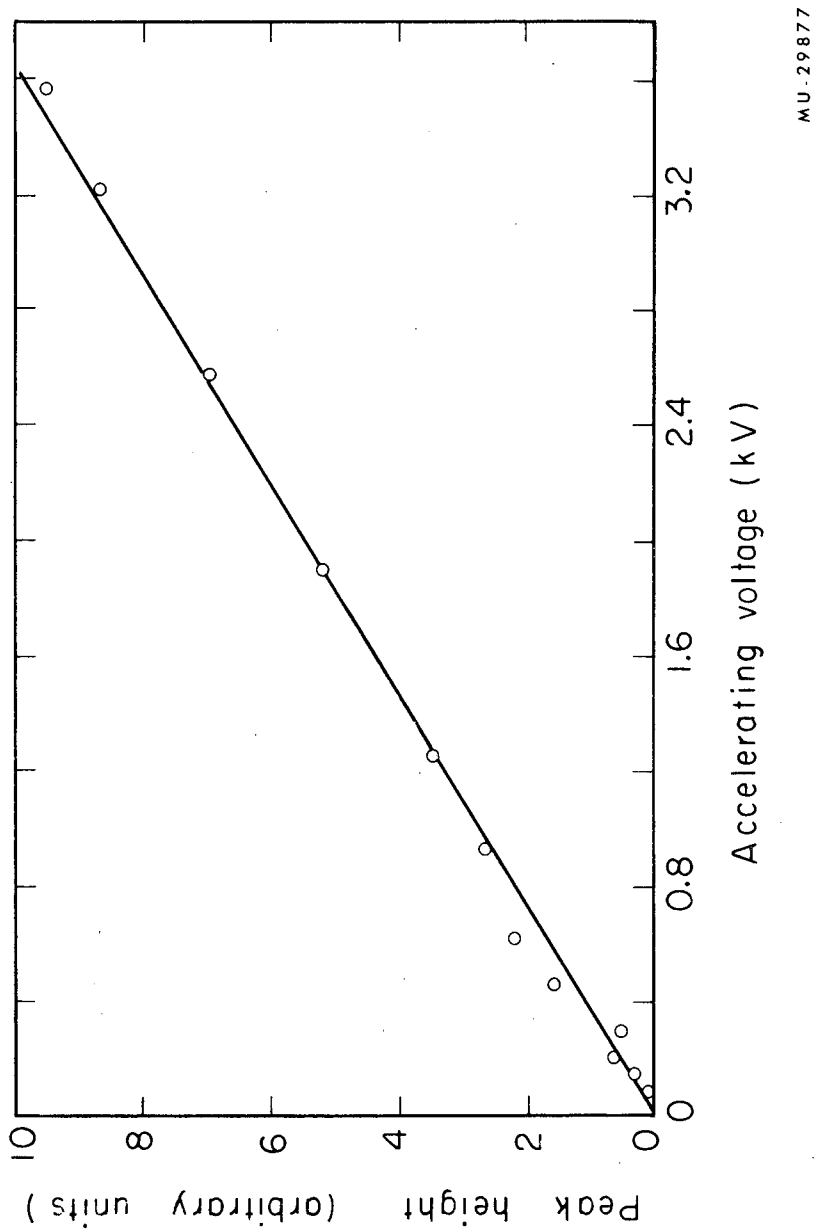

Fig. 11. Variation with accelerating voltage of peak height of excess-kinetic-energy M/q=29 peak from n-heptane. Data obtained by subtraction method outlined in text.

Table VII. Measured abundances of excess-kinetic-energy ions.[a]

Compound	M/q	Abundances			
		Thermal ion		Excess KE ion	
		peak height	portion of total ions (%)	peak height	portion of total ions (%)
ethane	15	635	1.54	468	1.13
propane	15	608	1.10	986	1.79
n-butane	15	674	0.95	1333	1.88
isobutane	15	972	1.41	1652	2.39
n-pentane	15	719	0.77	1217	1.30
neopentane	15	801	0.97	2613	3.17
n-heptane	15	554	0.51	805	0.74
2,4-dimethyl pentane	15	661	0.63	2087	1.95
n-decane	15	345	0.22[b]	564	0.36[b]
benzene	15	--[c]	--[c]	485	0.65
p-xylene	15	103	0.11	1232	1.36
ethyl benzene	15	228	0.25	1620	1.76
isopropyl chloride	15	713	1.30	820	1.50
isopropyl alcohol	15	1965	3.66	1254	2.34
n-heptane	29	8234	8.25	1077	1.08

[a]All peak heights given for normal operating conditions, corrected to source pressure of 50 μ and high amplifier sensitivity. Peak height of M/q=58 peak of n-butane equals 2590 divisions under these conditions.

[b]Estimated. Accurate figure for total ion-peak height not available.

[c]Thermal peak of negligible height.

excess-kinetic-energy and thermal-energy peaks, the quality of the data probably is not sufficient to justify their treatment by other, perhaps more sophisticated, techniques.

All the excess-kinetic-energy ion peaks whose appearance potentials were measured had ionization efficiency curves that increased linearly with the square of the excess energy above threshold. For this reason it was considered expedient to use a doubly charged ion of a rare gas as a standard, since such ions exhibit the same type of cross-section behavior near threshold. The doubly charged krypton ion was chosen as a standard because it is the lowest-M/q rare-gas ion of this type having an appearance potential relatively close to the appearance potentials being determined. The ionization efficiency curves for the excess-kinetic-energy M/q=15 ion from benzene and the Kr^{++} ion are plotted in Fig. 12. The second-power dependence of both curves is evident.

Unfortunately, the Kr^{++} ion proved unsuitable as a standard for the determination of the appearance potentials of other excess-kinetic-energy ions, owing to interference with the Kr^{++}-ion peak by M/q=40 and M/q=41 ion peaks from the compounds being studied. Therefore, for the determination of other appearance potentials the singly charged neon ion was chosen as a standard, that being one of the few possible reference ions having an ion peak that was not interfered with and an appearance potential close to those being determined. A comparison of the ionization efficiency curves for the two standard ions and for He^{+} is shown in Fig. 13. It can be seen that the Ne^{+} curve, in addition to displaying curvature at the foot caused by the energy spread in the ionizing electrons, has two linear portions. The extrapolation of the first (lowest) linear portion gives the correct appearance potential for Ne^{+} relative to He^{+} and Kr^{++}; the second portion extrapolates to a value some 0.7 V higher.

A comparison of the uncorrected appearance potentials of the three rare-gas ions shown in Fig. 13 reveals that the difference in potentials is 105% of the spectroscopic difference for both the He^{+}-Ne^{+} pair and the He^{+}-Kr^{++} pair. This factor is exactly that which would be predicted as the effect of the shield mounted behind the filament. This shield provides a potential between it and the Isatron, which the

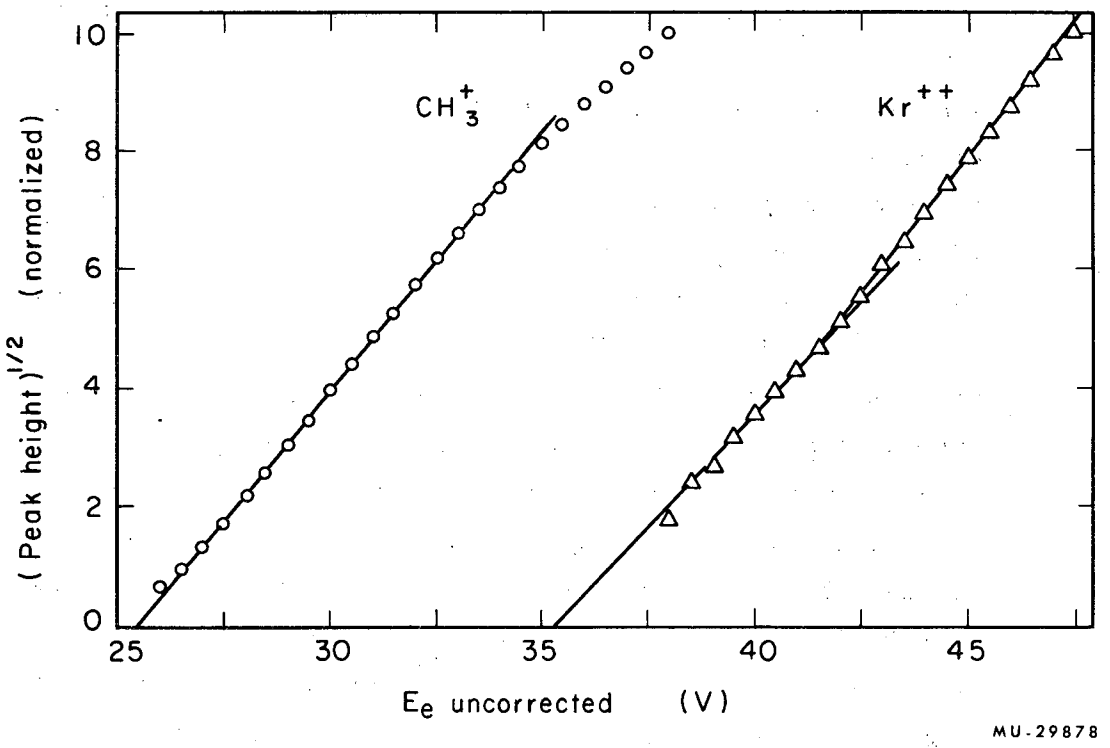

Fig. 12. Ionization efficiency curves for Kr^{++} and CH_3^+ ions from a krypton—benzene mixture.

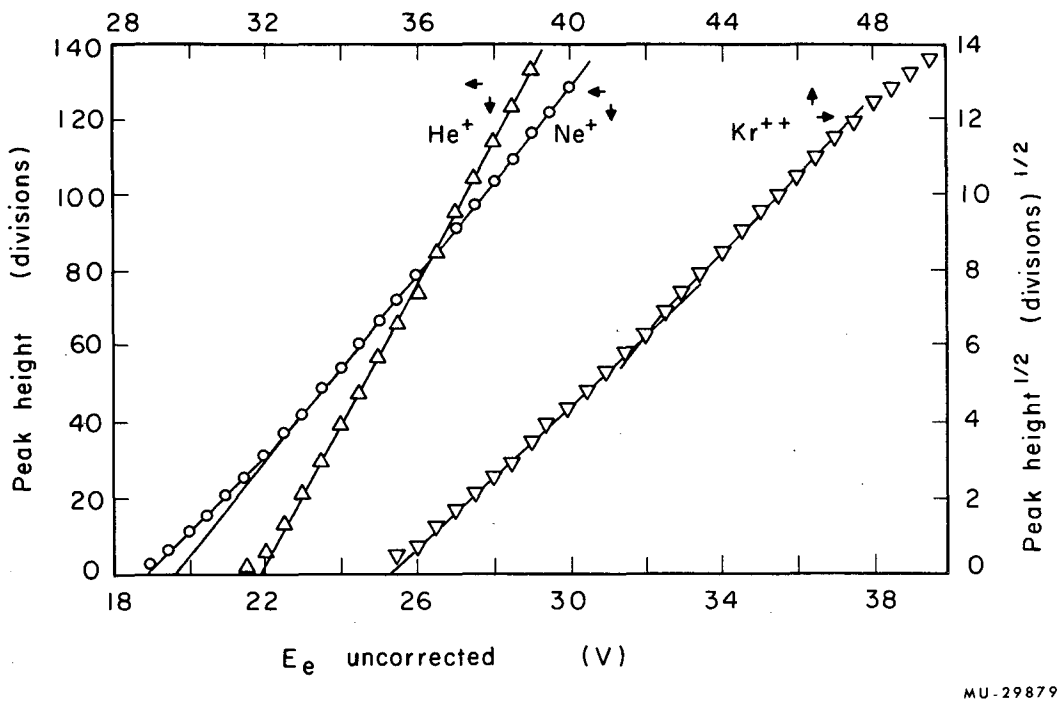

Fig. 13. Ionization efficiency curves for He^+, Kr^{++}, and Ne^+ ions from a rare-gas mixture. Partial pressures of the gases adjusted to give equal peak heights at 70-V ionizing voltage.

electrons leaving the filament experience and which acts to focus them in the direction of the slit into the Isatron. The negative potential applied to the shield relative to the Isatron was measured and found to be 6% of the ionizing voltage, under the conditions for which appearance potentials were measured. Since the filament lies roughly 1/5 of the distance from the shield to the Isatron slit, it is expected that the electrons experience about 80% of the measured potential applied to the shield; hence, the actual electron energy is 105% of the measured electron energy--exactly what is observed. (In addition, of course, correction must be made to the measured electron voltages for the effect of the magnetic field and repellers. This is accomplished by the usual device of normalizing the electron-energy scale to make the measured appearance potential of the reference ion agree with the spectroscopic appearance potential.)

Figure 14 shows ionization efficiency curves for the M/q=15 (CH_3^+) ion peak from benzene and the Ne^+ peak. The two linear portions of the Ne^+ curve are again evident, and the first linear segment extrapolates to a value which, if chosen as the actual appearance potential for Ne^+, gives a value for the appearance potential of the CH_3^+ ion that is in agreement with that determined by using Kr^{++} as a standard. However, if one chooses to assign to the intercept of the extrapolation of the second linear segment of the curve a voltage value 0.7 V above the appearance potential, one also obtains agreement with the previously determined appearance potential for the benzene CH_3^+ ion. Because it was considerably easier to determine the slope of the second linear segment of the ionization efficiency curve for neon than the slope of the first linear segment, the former was used as a standard in subsequent determinations of appearance potentials of excess-kinetic-energy ions. In every case it could be estimated that the difference in intercepts for the two linear portions of the neon curve was 0.7 V; thus the appearance potentials determined by using this standard are not significantly different from those which would have been obtained had the intercept of the first linear segment of the neon curve been used.

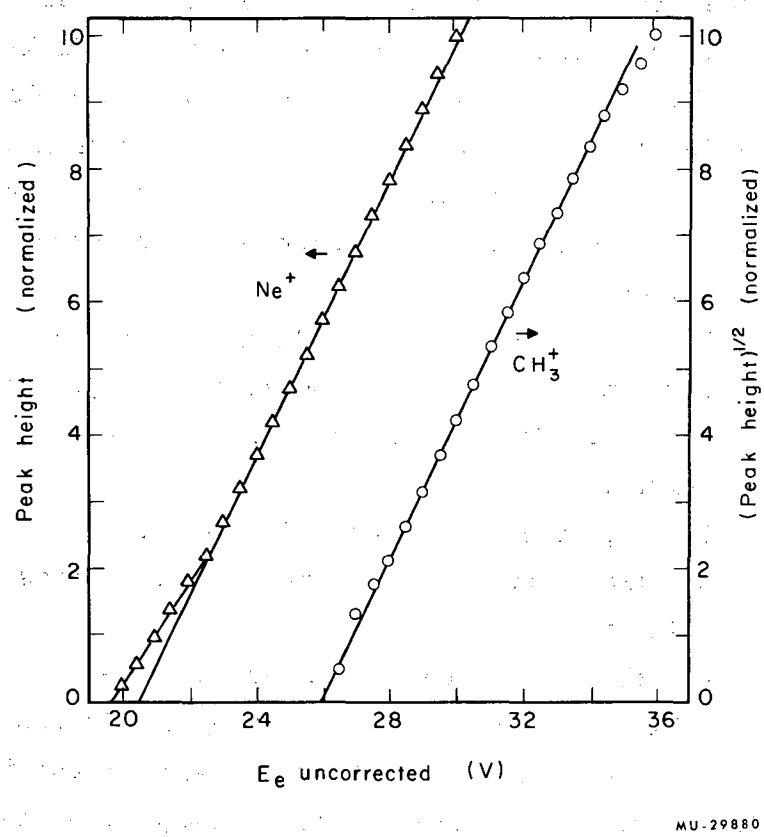

Fig. 14. Ionization efficiency curves for Ne^+ and CH_3^+ ions from a neon—benzene mixture.

It has been shown, by comparisons with accurately measured photoionization potentials, that the appearance potentials determined by using the linear-extrapolation method generally are reliable only to about ± 0.3 V.[25] This is attributed to inadequacies in the method itself. The data obtained in this study indicate that the appearance-potential measurements could be reproduced to ± 0.2 V. To the extent, then, that the linear extrapolation method is valid, the appearance potentials measured in this work and listed in Table VIII are accurate to ± 0.2 V. For ions for which the linear extrapolation method is not applicable, the accuracy may be somewhat less than this. On the basis of the excellent linearity of the square-root curves used to determine the appearance potentials, the extrapolation method is probably valid for these ions.

Table VIII contains, in addition to the appearance potentials of excess-kinetic-energy ions, the appearance potential of the $C_2H_5^{++}$ ion from ethane. The ionization efficiency curve for the latter ion is shown in Fig. 15.

The appearance potentials for the CH_3^+ and $C_2H_3^+$ excess-kinetic-energy ions from propane were compared. The curves for these two ions are shown in Fig. 16.

All the appearance potentials for excess-kinetic-energy ions given in Table VIII were measured at operating conditions of the mass spectrometer yielding maximum resolution of the high-energy and thermal peaks. These conditions were: 300 V accelerating voltage, 0 V repellers, and metastable-suppressor-voltage setting 310.5 V. Standard ion appearance potentials were measured under the same conditions except that the metastable suppressor was grounded to the analyzer. Appearance-potential measurements for the benzene CH_3^+ excess-energy ion at both settings of the metastable suppressor indicated that it had no effect on the observed appearance potentials.

One other ionization efficiency curve was obtained, that for the thermal M/q=15 peak from propane. This curve, shown in Fig. 17, was too complicated to permit an unambiguous appearance-potential value to be extracted from it, although Kandel must have obtained a value from a curve similar to this.[17]

Table VIII. Appearance potentials of excess-kinetic-energy ions.

Compound	Ion	Appearance potential	Reference ion
benzene	CH_3^+	28.2	[a]
ethane	CH_3^+	30.3	Ne^+
propane	CH_3^+	30.8	Ne^+
propane	$C_2H_3^+$	29.9	[b]
n-butane	CH_3^+	29.7	Ne^+
isobutane	CH_3^+	29.4	Ne^+
n-pentane	$C_2H_5^+$	28.1	Ne^+
neopentane	CH_3^+	29.5	Ne^+
n-heptane	CH_3^+	27.9	Ne^+
n-heptane	$C_2H_5^+$	24.3	Ne^+
isopropyl chloride	CH_3^+	29.7	Ne^+
isopropyl alcohol	CH_3^+	30.2	Ne^+
benzene	$C_2H_3^+$	31.1	Ne^+
benzene	$C_2H_2^+$	32.6	Ne^+
deuterium	D^+	25.3	[c]
methyl amine	CH_3^+	28.0	[d]
methyl amine	NH_2^+	28.4	[e]
ethane[f]	$C_2H_5^{++}$	33.5	Kr^{++}

[a] Value represents the average of four separate determinations by using both Ne^+ and Kr^{++} as reference ions.

[b] Excess-kinetic-energy CH_3^+ ion from propane used as a reference.

[c] Measured at negative repeller voltage. Excess-kinetic-energy CH_3^+ ion from benzene used as a reference.

[d] No reference. Correction on an absolute basis estimated to be less than ± 1 V.

[e] Measured relative to excess-kinetic-energy CH_3^+ ion from methyl amine.

[f] Not an excess-kinetic-energy ion. Literature value for this ion is 32.2 ± 1.5 V.[37]

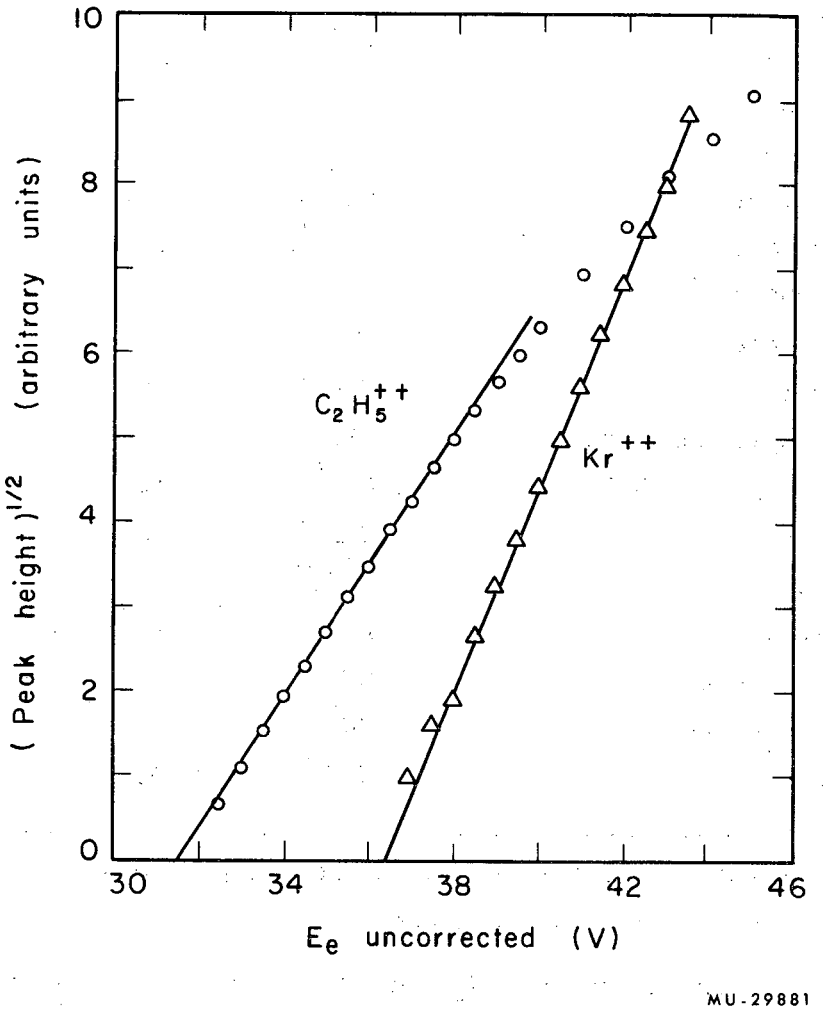

Fig. 15. Ionization efficiency curves for $C_2H_5^{++}$ and Kr^{++} ions from an ethane—krypton mixture.

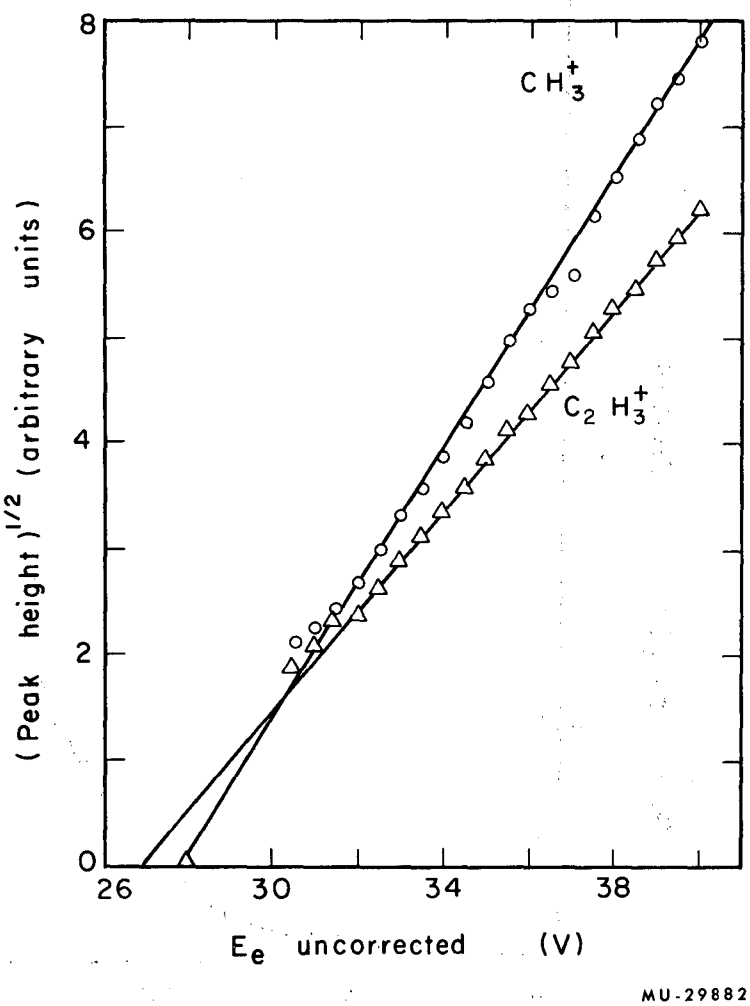

Fig. 16. Ionization efficiency curves for CH_3^+ and $C_2H_3^+$ excess-kinetic-energy ions from propane.

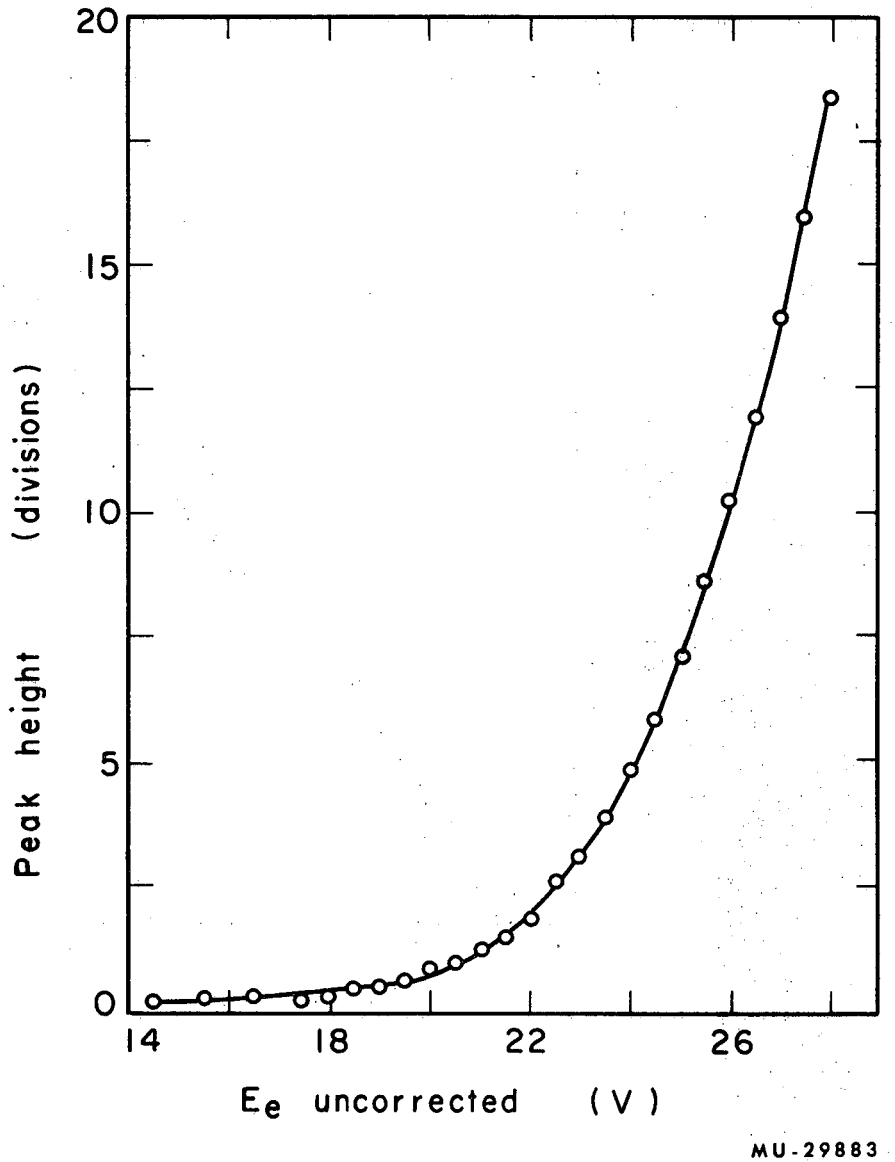

Fig. 17. Ionization efficiency curve for CH_3^+ thermal ions from propane.

Other Data

Duplication of Kandel's Experiments

Inasmuch as the excess kinetic energy of the thermal M/q=15 peaks of ethane and propane measured in this work were not in agreement with values obtained by Kandel,[17] we attempted to duplicate that worker's results. The variation with metastable-suppressor setting of the height of the CH_3^+ peak was determined at various ionizing voltages. A curve demonstrating the type of behavior obtained is shown in Fig. 18. At the same time, similar data were taken for an ion peak known to be thermal, in this case the M/q=20 ion peak from neon run simultaneously with the hydrocarbon. The cutoff points were determined by extrapolating the linearly decreasing portions of the curves to zero peak height, as demonstrated in Fig. 18. The difference in cutoff voltage, after correction by multiplication by the 0.971 factor mentioned earlier, was then assumed to be the difference in ion kinetic energies.

It was found for both propane and ethane that at ionizing voltages 10 V or more above the appearance potential the M/q=15 ion possessed excess kinetic energy approximately equal to the excess kinetic energies of thermal peaks given for those compounds in Table IV. However, at lower ionizing voltages (20 V for propane, 17.5 V for ethane) the metastable-suppressor cutoff voltages were the same, within experimental error, for the M/q=15 and M/q=20 peaks. Thus the evidence, in definite disagreement with Kandel's observations, is that the M/q=15 ions in both propane and ethane are formed at the appearance potential without any excess kinetic energy.

Negative-Repeller Mass Spectra

To demonstrate the existence of excess-kinetic-energy ions over a wide range of M/q values, the mass spectrum of benzene was measured at a series of negative-repeller voltages. The spectra obtained are presented in Table IX. In this experiment all peaks were scanned magnetically at 300-V acceleration. The pressure in the source was approximately 125μ.

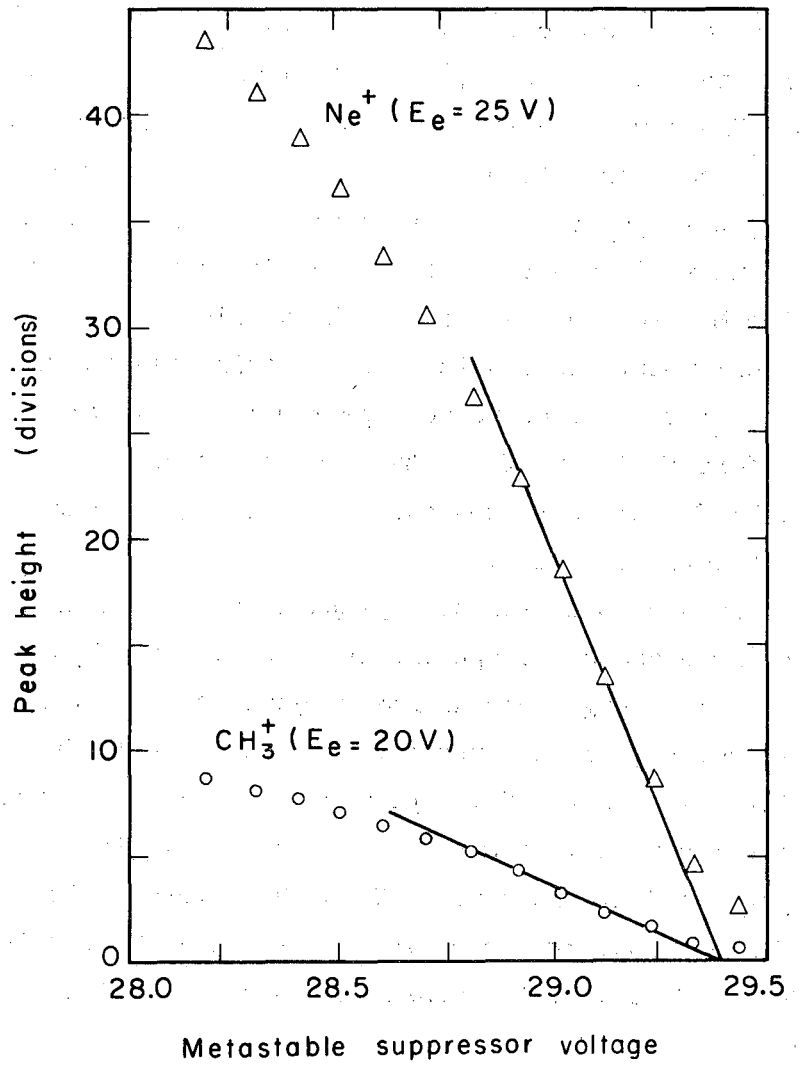

Fig. 18. Metastable-suppressor cutoff curves for thermal CH_3^+ and Ne^+ ions from a propane—neon mixture. Data taken at 1000-V accelerating voltage and 0.2-V repellers.

Table IX. Benzene mass spectra at negative repeller voltages.[a]

M/q	Repeller voltage								
	-2.5	-2.75	-3.0	-3.5	-4.0	-4.5	-5.0	-5.5	-6.0
14	4.5	4.1	4.0	3.4	2.8	2.1	1.4	1.0	0.6
15	75.6	68.8	62.2	46.7	31.6	19.0	9.8	4.9	2.3
24	0.9	0.8	0.8	0.5	0.3	--	--	--	--
25	9.2	8.2	7.2	5.3	3.9	2.9	1.9	1.1	0.8
26	84.5	76.2	67.9	49.2	34.4	23.2	14.9	9.1	5.7
27	41.7	38.7	35.0	25.8	18.0	11.6	6.7	3.9	2.2
28	1.9	1.8	1.5	1.0	0.7	0.3	0.1	--	--
36	3.1	2.3	1.8	1.0	0.6	0.3	0.1	--	--
37	39.2	29.1	21.2	11.1	6.1	3.6	2.1	1.1	0.5
38	72.3	53.8	39.4	19.4	10.2	5.7	3.0	1.5	0.7
39	62.3	48.2	35.7	16.7	8.0	4.1	2.0	1.0	0.4
40	3.3	2.4	1.7	0.6	0.2	0.1	--	--	--
48	0.6	0.3	0.1	--	--	--	--	--	--
49	5.0	3.0	1.6	0.5	--	--	--	--	--
50	19.7	10.4	5.2	1.4	0.4	--	--	--	--
51	13.3	6.2	2.7	0.4	0.1	--	--	--	--
52	2.4	1.0	0.2	--	--	--	--	--	--

[a]Mass-spectrometer conditions: magnetic scan of peaks at constant accelerating voltage=300 V; metastable suppressor grounded to analyzer; amplifier on high sensitivity; and pressure in source about 125 μ.

It can be seen that the C_4 fragments, masses 48 to 52, possess some excess-kinetic-energy components. The earlier disappearance of these fragments relative to lighter mass fragments is a consequence of their possessing less kinetic energy than the lighter fragments. There are indications that the C_5 fragments also can possess some kinetic energy. Similar data taken for n-heptane showed that for that compound also all fragments of mass less than the parent ion had components possessing excess kinetic energy.

DISCUSSION AND CONCLUSIONS

Mechanism of Formation of Excess-Kinetic Energy Ions

The formation of excess-kinetic-energy fragment ions in a relatively collision-free region such as the ion source of a mass spectrometer can be described in terms of potential-energy surfaces for the molecular states involved. Such surfaces for polyatomic molecules are (N + 1) dimensional, where N is the number of oscillators in the molecule. This makes pictorial representation of such surfaces difficult if not impossible; however, one can depict examples of the various types of processes leading to molecular fragmentation for the two-dimensional surfaces representing states of diatomic molecules. Although the surfaces for polyatomic molecules are considerably more complex and the number of possible modes of fragmentation correspondingly greater, the types of processes that may occur are alike for diatomic and polyatomic species.

In Fig. 19 is shown a set of potential energy curves for the ground state and various ionic states of a hypothetical diatomic molecule AB. The system AB is represented as a point moving about the plane of the paper but constrained to move in certain specified ways. In the absence of any external stimulus adding energy to the system (e.g., intermolecular collisions, electron or photon impact), the point is constrained to move along a line of constant energy (Law of Conservation of Energy). In addition, it is constrained to remain always above the curve describing the potential energy of the state in which it exists; that is, to maintain at all times a positive kinetic energy. (Quantum-mechanical considerations modify this restriction to permit slight penetration into negative-kinetic-energy regions.) Thus, in the absence of external stimuli, the point representing the system will oscillate along the line representing the ground-state energy of the molecule, between the limits imposed by the potential-energy curve.

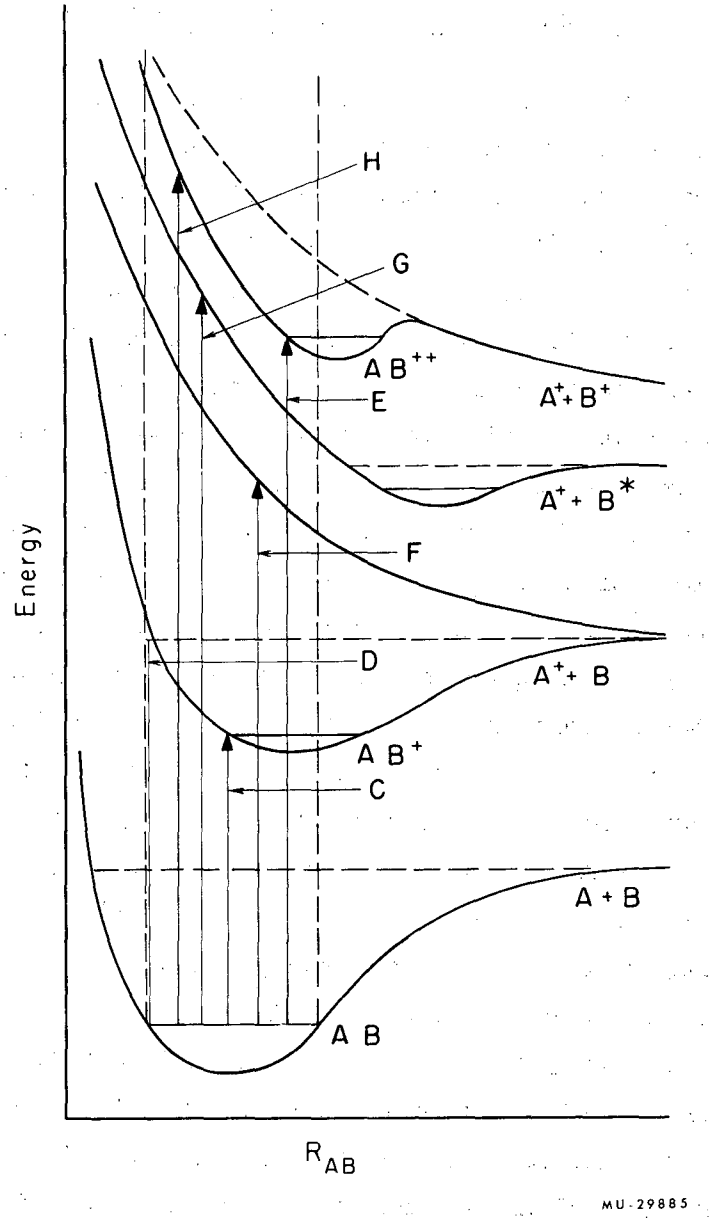

Fig. 19. Potential-energy curves for the ground state and some ionized states of the hypothetical diatomic molecule AB. The vertical dotted lines show the classical limits of the Franck-Condon transition region. C through H are typical transitions.

If now an electron impinges upon the system, the constant-energy constraint is modified to the extent that the electron can transfer some or all of its energy into the AB system, thereby moving the point to some other energy level. There are severe restrictions on such transfers. Firstly, since the transfer of energy takes place in a short time increment, the internuclear distance cannot change significantly during the transition; in terms of the diagram, all energy transfers by electron or photon impact are required to be vertical (Franck-Condon principle). Secondly, the probability of transition occurring between any two points is dependent on the overlap integral of the wave functions describing the system at those points. Hence, there is a large transition probability only between those points for which there is a higher probability of finding the system. The character of the wave functions is generally such that the transitions between points near the edges of the potential-energy curves (i.e., points at which the kinetic energy of the system is small) are the only probable ones. (The ground vibrational level of a bound state is an exception because the probability function is greatest in the center of the potential well, where the kinetic energy is also greatest.)*

The general types of transitions satisfying these constraining conditions are shown as vertical lines in Fig. 19. Transitions C, D, and E are typical of processes leading to ions of thermal (or very nearly thermal) kinetic energies: process C leading to the production of the molecular ion AB^+; process D leading to the production of a fragment ion A^+ and a neutral atom B; and process E leading to the doubly charged ion AB^{++}. The transitions typified by F, G, and H, on the other hand, produce ions possessing excess kinetic energy, the amount of such kinetic energy given by the vertical separation at $R_{A-B} = \infty$ between the dotted line denoting the total energy of the system and the solid line giving the potential energy. This total kinetic energy must be partitioned between the two fragments inversely as the ratio of their masses. Process F

*The author is indebted to Professor John Rasmussen for an enlightening discussion on the subject of transition probabilities.

represents excitation to a bound-state energy curve at an energy well above the dissociation limit for the products A^+ and B; process G, excitation to a repulsive-state curve leading to the same products; and process H, excitation to a potential-energy curve for the doubly charged ion AB^{++} at an energy equal to or greater than the dissociation energy.

It will be noted that there is no way in which the parent ions, AB^+ and AB^{++}, can be formed with excess kinetic energy, although there are many possible excitation processes that lead to the formation of these ions with varying amounts of excess vibrational energy.

It should be remarked that the energy curves shown in Fig. 19 in no way represent all the processes that can lead to production of fragments. Two types of processes in particular have been omitted from the diagram. One of these is excitation not involving ionization, which can lead to excited states of the parent molecule, thermal neutral atoms, or excess-kinetic-energy neutral atoms. This type of process has not been indicated, since the interest here is focused on ions rather than on neutral species. The second type of neglected process is one that involves level transfer either through emission of radiation or through level crossing and the possibility of the system's transferring from one level to another at the crossing point. Although such processes have the effect of permitting products to be formed with a wider variety of energy distributions, the general types of products formed are the same as those arising from processes shown in Fig. 19. Chupka has considered such processes.[27]

When the above treatment is extended to polyatomic molecules the major difference is the proliferation of available energy states and possible modes of fragmentation. With this proliferation, the occurrence of energy-level crossings becomes more widespread, and many of the rates of formation of fragment ions are affected by competition among the various fragmentations that can occur.

The vast majority of ions observed in the mass spectrometer is the result of processes of types C, D, and E or of a process involving energy-level transfers. Fragment ions produced from these processes are expected in general to be formed with small amounts of excess kinetic

energy. That such is indeed the case is demonstrated by the data given in the second and third columns of Table IV. Investigations carried out by Taubert[28] and by Monahan and Stanton[29] indicate that a very large number of the fragment ions formed from hydrocarbons have kinetic energies in slight excess of thermal ion energy. Processes of type D almost always impart to the fragments some excess kinetic energy, since it is rather unlikely that the limit of the region of allowable excitation processes will intersect the potential-energy curve at precisely the energy of dissociation of that curve.

The question raised regarding the ions formed with large amounts of excess kinetic energy is: Which one of the three types of processes F, G, or H is the dominant process leading to formation of these ions? Processes F and G are indistinguishable unless detailed knowledge concerning the shapes of the potential energy curves is available, but the type H process--giving rise as it does to a pair of ions--may be experimentally distinguished from the others.

Experimental Evidence

Deuterium

For hydrogen, the potential-energy curves are sufficiently well known to allow unambiguous assignment of processes leading to high-energy H^+ ions. Excitation to the repulsive $^2\Sigma_u^+$ potential-energy curve is expected to produce ions with kinetic energy of about 7 V and an appearance potential in the neighborhood of 30 V, while excitation to the doubly charged ionic state will produce ions with kinetic energies in excess of 9 V and an appearance potential of about 45 V. The experimental data unquestionably indicate type-G excitation to the repulsive - $^2\Sigma_u^+$ state. Bleakney measured the appearance potential of the excess-kinetic-energy fragments to be 26 ± 1 V,[1] and Lozier determined the most probable kinetic energy of the fragments to be about 5.5 V.[2] The results of this work on deuterium give 25.3 ± 0.4 V for the appearance potential and about the same most probable energy as Lozier found. From the known dissociation energy for the hydrogen molecule (4.6 eV) and the ionization potential of the hydrogen atom (13.6 V) it follows that the appearance potential of of an H^+ ion of 5.5 V kinetic energy should be $4.6 \pm 13.6 \pm 2(5.5) = 29.2$ V.

The measured value of 25.3 V corresponds to the appearance potential of an ion of 3.6 eV kinetic energy. If this energy is assigned to the lowest-energy process accessible within the Franck-Condon region, two points determined by the minimum and most probable kinetic energies can be determined on an experimental potential-energy curve. The justification of the assignment of the minimum-accessible kinetic energy to the 3.6 V value corresponding to the measured appearance potential is based on the observation that the appearance-potential curve does not show any evidence of tailing toward lower electron energies near its foot. This lack of tailing is what is expected if the determined appearance potential corresponds to the minimum-accessible kinetic energy.

The two points on the experimental potential-energy curve determined in this way are shown in Fig. 20 along with the potential-energy curve for the ground state of the H_2 molecule[30] and theoretical potential-energy curves for the $^2\Sigma_g^+$ and $^2\Sigma_u^+$ states of the H_2^+ ion.[31] The lack of agreement between the experimental points and the theoretical curve is startling inasmuch as the theoretical curve is thought to be quite accurate because it was calculated from wave functions derived by ignoring only the finiteness of the mass of the protons.[31] The discrepancy may be explainable in terms of the limitations of the Franck-Condon principle. Coolidge, James, and Present found for the ultraviolet continuum of hydrogen that strict application of the principle is not valid.[32] They pointed out that the assumptions on which the principle is based are most likely to be in error for the low vibrational levels of light molecules.

Stevenson has recently considered for the hydrogen molecule experimental data not in agreement with predictions based on the Franck-Condon principle.[33] He suggested the existence of a transient complex (H_2^-) with a lifetime of the order of 10^{-13} sec to explain the discrepancies. Such a complex would have to be formed by the reaction

$$H_2 + e^- \longrightarrow (H_2^-) \longrightarrow H + H^+ + 2e^- , \qquad (12)$$

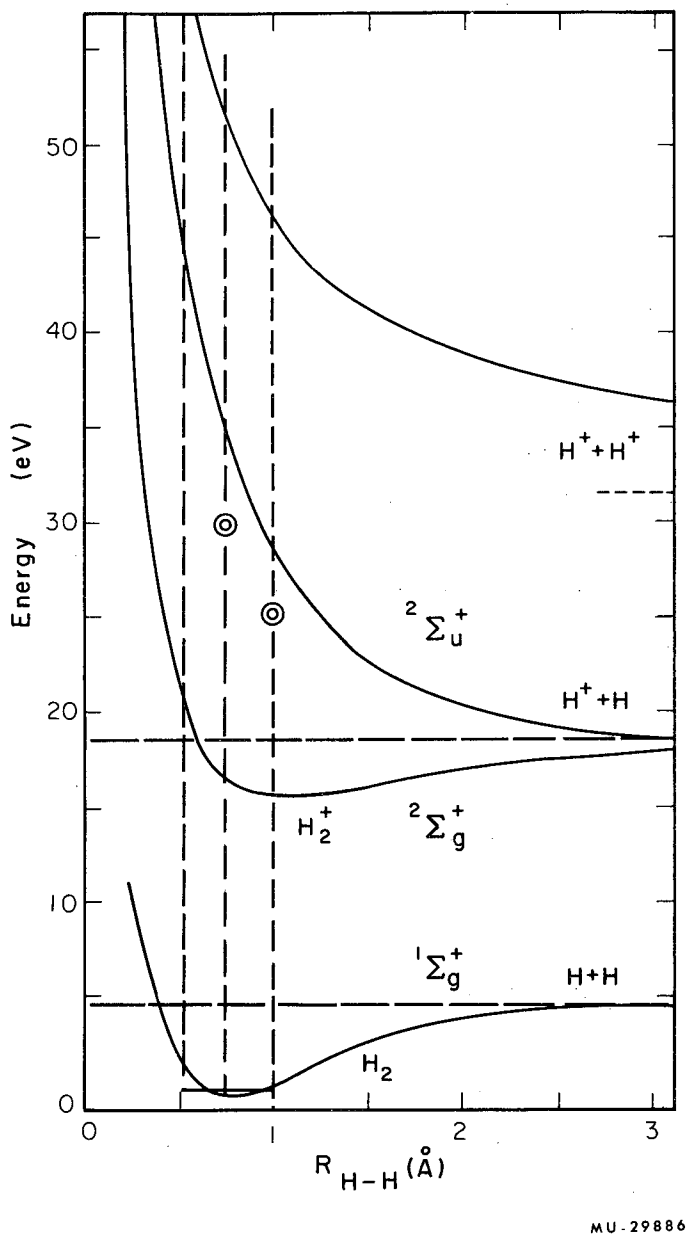

Fig. 20. Potential-energy curves for the ground state and ionized states of the hydrogen molecule. The ground-state curve was constructed from data given in reference 30 and the two states of the H_2^+ ion from data given in reference 31. Two experimentally determined points on the $^2\Sigma_u^+$ potential-energy curve are also shown.

which is a resonance-capture process for which the probability curve for attachment is expected to be spike-shaped, just as the probability curve for the process

$$CCl_4 + e^- \longrightarrow CCl_4^- \longrightarrow CCl_3^- + Cl \qquad (13)$$

is spike-shaped.[34] That there is a probability for formation of H^+ at bombarding energies of 100 V comparable to--if not higher than--the probability for formation at low energies therefore rules out the (H_2^-)-complex mechanism.

In the absence of a detailed quantum-mechanical treatment of the excitation process leading to the formation of excess-kinetic-energy protons, all that can be said is that since the situation is similar to that studied by Coolidge, James, and Present, one is not surprised to find some deviation from the predictions of the Franck-Condon principle.

Investigations carried out on diatomic molecules other than H_2, notably the work of Hagstrum and Tate on CO, NO, N_2, and O_2,[8] have shown that, in general, excess-kinetic-energy fragments from such molecules are the results of types F and G processes. For N_2, two processes could be distinguished, one clearly of type F or G, the other of type H.

Polyatomic Molecules

Excess-kinetic-energy ions formed from polyatomic molecules have been interpreted in previous studies to arise from type-H processes.[10,12,15] Mohler, Dibeler, and Reese supported this interpretation by comparing the total kinetic energies of fragmentation that they observed with Coulomb repulsion energies calculated for doubly charged ions of the molecules in question.[12] The value of such a comparison is highly questionable, in view of two uncertainties involved in the comparison. In the first place, the calculated repulsion energy depends on the initial distance of separation between the two charges, which must be estimated. Mohler, Dibeler, and Reese based their calculations on the greatest possible charge separation, associating the charges with the protons attached to the end carbons.

This is somewhat unrealistic because, for such a charge distribution, the C-H bonds would be considerably weakened; hence, one would expect such a configuration to give rise to fragmentation of a C-H bond rather than one of the C-C bonds.

A more realistic charge-separation distance would result from associating the net charges with the end-carbon nuclei. Even then, the Coulomb energy could not be directly associated with the kinetic energy of the fragments, as can be seen from the upper potential-energy curves in Fig. 19. The Coulomb repulsion curve is shown as a dotted line and the actual potential-energy curve as a solid line. As the figure indicates, in general the potential-energy curve for the doubly charged ion will deviate from the Coulomb repulsion curve, owing to the binding force exerted by the electrons remaining in the molecule. The extent of this binding will vary from molecule to molecule and from configuration to configuration. Hurley and Maslen have carried out calculations of potential curves for doubly charged diatomic ions which indicate that the extent of binding for such ions as O_2^{++} and N_2^{++} is between 3 and 6 eV.[35] For polyatomic molecules the variation in binding may be considerably greater, particularly if excited states of the doubly charged ions are considered.

A much more conclusive test of the doubly-charged-ion hypothesis involves the necessity that a pair of charged fragments be formed in any mechanism that results in the appearance of a singly charged ion. Thus, for example, if a doubly charged ion is the source of the excess-kinetic-energy CH_3^+ ion from methyl chloride, the reaction leading to formation of that ion must be

$$CH_3Cl^{++} \longrightarrow CH_3^+ + Cl^+ ; \qquad (14)$$

moreover, the law of conservation of momentum requires that the total kinetic energy be partitioned among the fragments inversely in proportion to their masses. Both the CH_3^+ and the Cl^+ ions are observed to possess excess-kinetic-energy components; however, the total kinetic energies of

fragmentation for the two ions are not in agreement, as indicated by the data in Table IV. In fact, they differ by 1 eV (4.93 eV for Cl^{++} ion, 5.93 eV for CH_3^+ ion). Reaction (14) is thereby ruled out as a mechanism of formation, and it is concluded that processes of type F or G are responsible for the high-kinetic-energy fragments observed in methyl chloride.

A second compound for which the above test was made is methyl amine. For this compound the total kinetic energies for the fragments CH_3^+ and NH_2^+ are also in disagreement, in this case by 0.6 eV (4.90 eV for NH_2^+ ion, 5.54 eV for CH_3^+ ion). Whereas this disagreement rules out the mechanism

$$CH_3NH_2^{++} \longrightarrow CH_3^+ + NH_2^+ , \qquad (15)$$

an alternative two-reaction mechanism may be postulated:

$$CH_3NH_2^{++} \longrightarrow H + CH_3NH^{++} \longrightarrow CH_3^+ + NH^+ \qquad (16)$$

and

$$CH_3NH_2^{++} \longrightarrow H + CH_2NH_2^{++} \longrightarrow CH_2^+ + NH_2^+ . \qquad (17)$$

Since in this mechanism the products CH_3^+ and NH_2^+ arise from different reactions, they could be formed with different total kinetic energies of fragmentation. However, a further check can be performed on this mechanism.

By using known dissociation energies and appearance potentials tabulated by Reed[36] and Field and Franklin,[37] the appearance potentials for the CH_3^+ and NH_2^+ ions arising from these reactions can be calculated. The values obtained are 35.7 eV for the NH_2^+ ion and 40.0 eV for the CH_3^+ ion. Measurements of the appearance potentials of these ions show

definite lack of agreement, not only of the values obtained but also of the difference between the two values (28.0 eV for the CH_3^+ ion, 28.4 eV for the NH_2^+ ion). Therefore, it must be concluded that doubly charged ions are not responsible for the bulk of the excess-kinetic-energy ions of methyl amine, and that types F or G processes must be the dominant mechanisms.

As one considers larger organic molecules, the type of analysis carried out for methyl chloride and methyl amine becomes very much more difficult because of the increasing complexities of the possible fragmentation processes. However, an analysis has been carried out for the propane molecule. Stanton concluded from his study of excess-kinetic-energy ions from propane that the reaction

$$C_3H_8^{++} \longrightarrow CH_3^+ + C_2H_5^+ \qquad (18)$$

must be ruled out because of the complete absence of excess-kinetic-energy $C_2H_5^+$ ions in the mass spectrum,[13] an observation with which this research is in agreement. He postulated three possible secondary reactions leading to decomposition of the ethyl ion, any one of which, in conjunction with Eq. (18), might satisfactorily account for the excess-kinetic-energy methyl ions:

$$C_2H_5^+ \longrightarrow C_2H_3^+ + H_2 \ ; \qquad (19)$$

$$C_2H_5^+ \longrightarrow C_2H_4^+ + H \ ; \qquad (20)$$

and

$$C_2H_5^+ \longrightarrow CH_3^+ + CH_2 \ . \qquad (21)$$

The conservation-of-momentum conditions for these reactions are somewhat more complex, since there are two fragmentations involved. However, for Reactions (19) and (20) the heavier fragment ions must retain virtually all the momentum with which the ethyl ion was formed, since, to change the momentum significantly, the H species would have to possess

a large amount of kinetic energy. The addition of such a quantity of energy to the calculated appearance potentials for these processes would put them well above the observed appearance potential of 30.6 eV for the excess-kinetic-energy methyl ion. The observed kinetic energies of the M/q=27 and M/q=28 fragments as given in Table IV do not give the same total kinetic energy of fragmentation as is observed for the CH_3^+ ion (3.5 eV compared with 4.02 for the methyl ion). Furthermore, measurement of the appearance potentials of the CH_3^+ and $C_2H_3^+$ ions gives values differing by at least 1 eV (see Fig. 16). Therefore, processes (19) and (20) must be ruled out as the dominant mechanism leading to formation of the excess-kinetic-energy methyl ions.

Process (21) may be ruled out in a similar manner. The calculated appearance potential for this process is in agreement with the measured value only if the fragmentation of the ethyl ion is assumed to impart no additional kinetic energy to the two fragments. From momentum considerations the ethyl ion must possess 1.37 eV kinetic energy, divided roughly equally between the CH_3^+ and the CH_2 fragments formed in Reaction (21). Hence, if reactions (18) and (21) represented the correct mechanism for formation of excess-kinetic-energy fragments the methyl ion peak would be expected to be made up of three components: the thermal peak, a peak due to ions of 0.67-eV kinetic energy, and a peak due to ions of 2.65-eV kinetic energy. Neither the peak shape nor the metastable-suppressor and negative-repeller cutoff curves for the M/q=15 peak of propane show any evidence of such triple character. Therefore Reaction (21) must be rejected, and it is concluded that for propane as well as for the methyl derivatives discussed above, processes of type F or G must be the dominant mechanisms giving rise to the excess-kinetic-energy ions.

The type-H process has been ruled out as the primary mechanism for excess-kinetic-energy-ion formation for each of the four compounds possessing excess-kinetic-energy ions for which a definitive study could be carried out: H_2, CH_3Cl, CH_3NH_2, and C_3H_8. It would be unreasonable to assume that these four compounds, in which breakage of four different bond types results in the excess-kinetic-energy ion, are unique. Rather, the dominant processes leading to excess-kinetic-energy ions in these compounds must be considered to be representative of processes giving rise

to such ions from all compounds studied in this research. Particular strength is lent to this consideration because most of the excess-kinetic-energy ions observed in this research arise out of breakage of a C-C bond, as is the case for propane.

This is not to say that type-H processes do not occur, however. Lozier observed H^+ ions whose properties definitely characterized them as resulting from a type-H process leading to the purely Coulombic repulsive state H_2^{++}.[2] It would certainly be surprising if there were no such processes occurring for organic molecules. The conclusion reached, however, is that at bombarding electron energies of about 70 V and less, the type-H processes are not nearly such important sources of excess-kinetic-energy ions as are types F and G processes.

The existence of small but measureable excess-kinetic-energy peaks at M/q=16 (CH_4^+) and the rather large M/q=15 and M/q=27 excess-kinetic-energy peaks arising from benzene are of considerable significance with respect to the mechanisms of formation of excess-kinetic-energy ions. The M/q=16 ions must be formed in a process involving the rearrangement of a proton, while the excess-kinetic-energy CH_3^+ and $C_2H_3^+$ ions from benzene must involve not only hydrogen migration but also the breakage of two C-C bonds. The lifetimes of the states that lead to these ions must therefore be somewhat greater than one vibrational cycle. The mechanism of formation of the CH_3^+ ion from benzene, in particular, must be quite complex because it involves ring opening, transfer of two H atoms (one of which probably occurs during ring opening), and breakage of an additional C-C bond. By the principle of microscopic reversibility one can rule out simultaneous occurrence of these steps; one is therefore forced to conclude that the lifetime of the excited state giving rise to excess-kinetic-energy methyl ions is fairly long, perhaps 10^{-12} to 10^{-13} sec.

It is of further interest that the appearance-potential curve for the methyl ion from benzene is identical in shape to those of excess-kinetic-energy methyl ions from other organic compounds, which indicates that the processes of formation of methyl ions are, at least initially, similar. These facts indicate that the processes leading to excess-kinetic-energy ions involve lifetimes longer than one vibrational cycle.

In fact, Franck, Sponer, and Teller have pointed out that, in general, a polyatomic molecule in an excited state will vibrate through a complex Lissajous figure before reaching an unstable configuration resulting in dissociation.[38] Therefore, the lifetime of an excited state of a polyatomic molecule can vary from one vibration to as long as 10^{-10} sec., depending on how long a path the system travels, within the confines of the potential-energy surface describing it, before reaching a configuration leading directly to fragmentation.

Appearance Potentials

Threshold Law

That the probability for formation of excess-kinetic-energy-ions rises as the second power of the excess energy of the impacting electrons seems at first sight at variance with the theory for ionization behavior near threshold. Wannier, proceeding from a treatment of two-particle interactions by Wigner,[39] calculated that for the three-body interaction represented by single ionization the threshold law should be nearly linear, or linear if interaction between the outgoing electrons is neglected.[40] Wannier also considered semiquantitively multiple-ionization processes, and deduced that n-fold ionization should have an nth-power threshold law.[41] Morrison later extended the reasoning to apply to certain molecular-fragmentation processes (e.g., $CO + e \rightarrow CO^{*} + e$, $CO^{*} \rightarrow C^{+} + O^{-}$) on the logical basis that the act wherein the cross section is determined, namely the interaction of electron and molecule, occurs in a time of the order of 10^{-15} sec., whereas the fragmentation of the molecule takes considerably longer.[34] Thus, the threshold law should be independent of whether or not the molecule eventually fragments. On the basis of this theory, the appearance-potential curves obtained in this work should be linear near threshold, rather than second power in energy, as is actually observed.

This discrepancy between theory and experiment is bolstered by the observation that the probability for formation of D^+ with excess kinetic energy rises as the second power of the excess energy above threshold, as shown in Fig. 21. Furthermore, the excitation function for N^+ thermal ions from the molecule NO was measured and was found also to obey a second-power threshold law, as demonstrated by Fig. 22. Thus, not only excess-kinetic-energy ions, including those arising from the simplest diatomic molecule, but also some near-thermal ions apparently obey second-power threshold laws.

The discrepancy may be resolved within the framework of the theory with the application of one additional assumption. Wannier's model for single ionization postulates that each of the two electrons leaving the complex must have sufficient kinetic energy to overcome the Coulomb energy e^2/b supplied by the ion where b is the unspecified radius of a sphere beyond which the electron is considered to be free. One can then plot the energies T_1 and T_2 of the two electrons as abscissa and ordinate of a graph, as in Fig. 23. The constant excess energy ΔE, which is the difference between the energy of the bombarding electron and the ionization potential, is represented by a straight line of slope -1, and the energy e^2/b that each electron must possess to escape the ion defines a limited region within which ionization can occur. From the diagram it is clear that the length of the segment of the ΔE = const line lying within the ionization region is directly proportional to the energy excess and so, also, must be the ionization probability. For double ionization, Wannier pointed out, the plane representing the energies of the two ejected electrons must be generalized to three dimensions, and the line of constant energy excess becomes a triangle whose area, varying as the square of the energy excess, determines the probability of ionization.

The observations made in this work may be brought into agreement with this theory if it is assumed that the electron that is excited to give the dissociative excited state of the singly charged ion is effectively a third free electron which can receive any amount of the excess energy, and that the Coulombic energy limit e^2/b is replaced for the excited electron by the energy of the transition it undergoes. When the excitation in question is to a dissociative state, the electron being

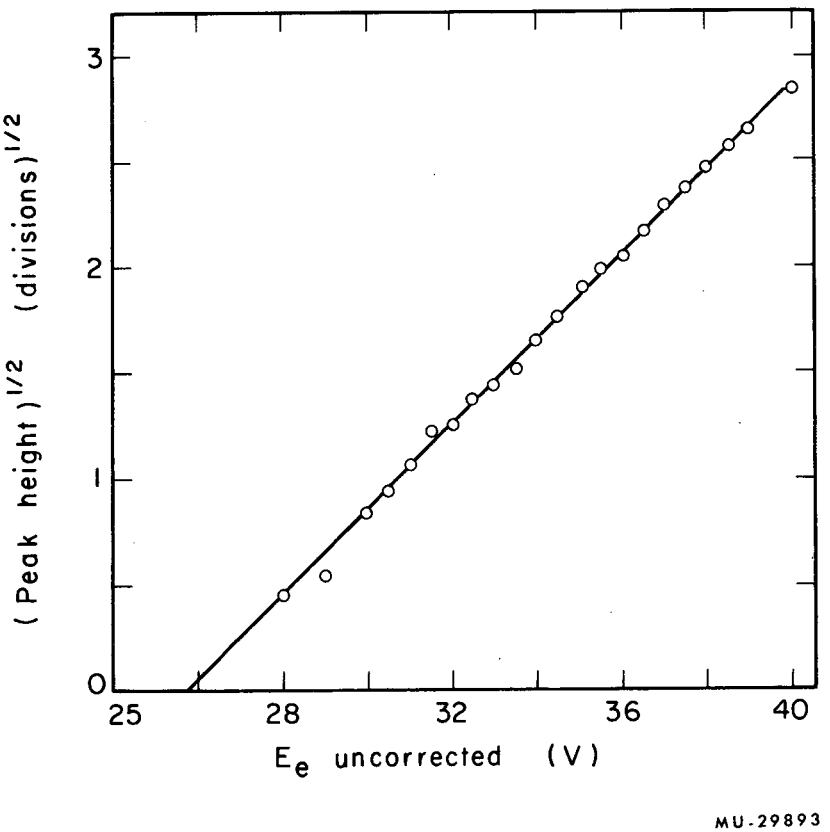

Fig. 21. Ionization efficiency curve for D^+ excess-kinetic-energy ions from deuterium.

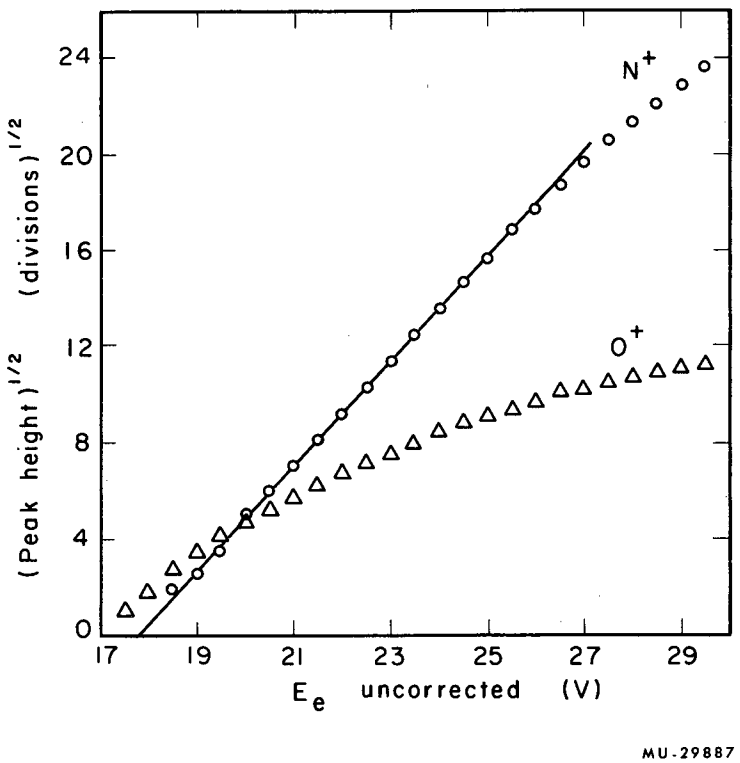

Fig. 22. Ionization efficiency curves for N^+ and O^+ ions from nitric oxide.

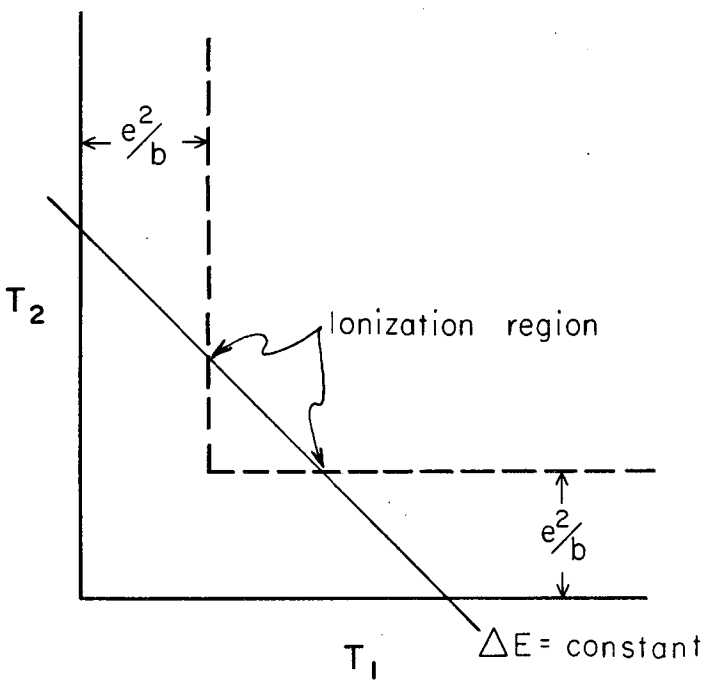

MU-29888

Fig. 23. Graphical model for single ionization. T_1 and T_2 are the kinetic energies of the two emerging electrons, and E is the excess energy of the bombarding electron above threshold (after Wannier).[41]

excited moves to a region of the potential-energy curve describing that state wherein the distribution of eigenfunctions is continuous in energy; hence, it appears that within the limits imposed by the transition probabilities to different points in that continuum, the assumption is a reasonable one. For each of the ions whose excitation functions were observed to follow second-power behavior with energy excess above threshold, the kinetic-energy distribution was rather broad, indicating a finite probability of transition over a fairly extended range of the continuum of dissociative states. Further experimental work needs to be done before it can be stated definitely whether the above assumption is tenable.

Magnitudes

A comparison of the appearance potentials measured for the excess-kinetic-energy ions and thermal ions of the same M/q for the same compounds[37] shows that in every case the amount of kinetic energy associated with the fragmentation leading to the excess-kinetic-energy process cannot account for all the additional energy of excitation associated with that fragmentation. From this it is concluded that the fragments are formed with excess vibrational and rotational energy, and perhaps also in excited electronic states, as well as with the observed excess kinetic energy. For ethane in particular, the appearance potential of the excess-kinetic-energy M/q=15 ions is some 16 V greater than the appearance potential of the thermal M/q=15 ions. Only 5 V of this energy appears as kinetic energy of the fragments, leaving 11 V of excitation still to be accounted for. As this is more than double the carbon-hydrogen bond dissociation energy, it is rather unlikely that all the excitation could be in vibrational and rotational modes without the occurrence of further fragmentation of the methyl ion. Therefore, it is probable that one or both of the products is formed in an excited electronic state.

The general usefulness of an energy analysis as given above is diminished considerably for methyl ions because reliable values are not

available for the appearance potentials of thermal methyl ions from many of the compounds under consideration. An examination of the typical appearance-potential curve that one obtains for a methyl ion from paraffins, illustrated by the propane curve shown in Fig. 17, indicates why this is so. From a curve like that given in Fig. 17 it is impossible to obtain an unambiguous value for the appearance potential by any of the methods of analysis that have been applied to such curves. The complexity of the appearance-potential curves obtained for methyl ions may be related to the fact that the difference in ionization potentials between methyl radicals and other paraffin radicals makes the fragmentation leading to a methyl radical and a heavier-mass ion energetically more favorable than the fragmentation leading to a methyl ion and a heavier-mass radical.

It is interesting to note that the appearance potentials for the thermal methyl ions from several hydrocarbons measured by Koffel and Lad by an extrapolation method,[42] although not compatible with other measured values for thermal methyl ions,[43] agree reasonably well with the appearance potentials measured in this work for excess-kinetic-energy methyl ions. Apparently the conditions under which Koffel and Lad operated their mass spectrometer were such that collection of excess-kinetic-energy ions was maximized. In that case it is not surprising that their extrapolations, which ignored a rather extensive tail on the appearance-potential curves, gave appearance potentials in rough agreement with those for excess-kinetic-energy ions.

Kandel's values

The failure of this research to obtain agreement with the values measured by Kandel for excess kinetic energy possessed by the thermal methyl ions from propane and ethane at the threshold casts considerable doubt on the validity of his corrected appearance potentials for those ions.[17] Both the attempts to duplicate Kandel's experiments and measurement of the excess kinetic energy possessed by the thermal M/q=15 peaks by the comparison of accelerating voltages indicate that, even at voltages well above threshold, the kinetic energies involved in fragmentations leading to thermal methyl ions from propane and ethane are 0.28 and 0.12 eV, respectively, rather than the 1.99- and 0.70-eV values

reported by Kandel. Furthermore, there is no evidence from this research of any excess kinetic energy present in the ions formed at the threshold energy.

The discrepancies may be explained by the fact that Kandel made rather long extrapolations to obtain the threshold kinetic energies he quoted. It is conceivable that at the ionizing energies considerably above threshold at which he apparently made his final kinetic-energy measurements, some excess-kinetic-energy ions were still present in the ion peaks. This would account for his measured kinetic-energy values lying intermediate between the values measured in this work for thermal ions and for excess-kinetic-energy ions.

Abundances

Extent of Occurrence

Excess-kinetic-energy ions are from all indications extremely widespread in occurrence. Virtually every organic compound studied in this research showed evidence of excess-kinetic-energy CH_3^+ fragments in its mass spectrum, and most, in addition, possessed excess-kinetic-energy M/q=16, M/q=14, M/q=13, and even M/q=12 fragments. All hydrocarbons from n-butane up exhibited excess-kinetic-energy peaks at M/q ratios 26 to 29, and even propane showed excess-kinetic-energy ions at M/q=27 and M/q=28. Negative-repeller spectra of benzene and n-heptane indicated that C_3, C_4, and C_5 fragment ions formed from those compounds may also possess kinetic energy. Nor does the phenomenon appear to be restricted to processes involving breakage of a C-C bond, as evidenced by the existence of excess-kinetic-energy M/q=15 ions from such methyl derivatives as methyl chloride and methyl amine. In addition to excess-kinetic-energy ions observed at masses corresponding to hydrocarbon fragment ions, excess-kinetic-energy ions were observed for Cl^+, NH_2^+, $COOH^+$, OH^+, CH_2OH^+, NO^+, and NO_2^+ when these groups were constituents of the molecule being studied. The processes by which excess-kinetic-energy ion fragments may arise are also not limited to simple bond breakage, as evidenced by the existence of excess-kinetic-energy CH_4^+ ions from

many compounds and the excess-kinetic-energy CH_3^+ and $C_2H_3^+$ ions observed in the mass spectra of benzene and cyclic hydrocarbons. Indeed, excess-kinetic-energy ions seem to be almost as widespread in occurrence as are thermal ions.

Calculation of Collection Efficiencies

Assessment of the absolute abundances of excess-kinetic-energy ions is made difficult by the severe discrimination of the mass-spectrometer slit system against high-kinetic-energy ions. It is not possible, unfortunately, to run the mass spectrometer under conditions for which the collection efficiencies for excess-kinetic-energy ions are comparable to those for thermal ions; however, the discrimination effects of the mass spectrometer have been examined theoretically in some detail, and the theory can be applied to estimate excess-kinetic-energy-ion collection efficiencies.

The most rigorous treatment of discrimination effects within the ion source is that by Coggeshall, who considered ion trajectories in an ion source in the presence of crossed electric and magnetic fields that varied with one and the same variable.[22,44] Coggeshall had previously shown that in the presence of an electric field only, the exit slit of the ion source does not discriminate against ions of excess kinetic energy.[19] In his more recent work it is shown that in the presence of a magnetic field there is discrimination at the exit slit if the electric field is sufficiently small.[22]

On the other hand, if the repeller field is sufficiently large, there are no discrimination effects at the exit slit of the Isatron--even in the presence of a magnetic field. In that case the derivation given by Berry for discrimination effects caused by the accelerating slit and the collector slit is applicable.[21] The repeller field necessary to eliminate discrimination at the exit slit of the Isatron is not easily determined; however, on the basis of some data presented by Coggeshall it is evident that repeller voltages greater than the kinetic energies (in eV) of the ions are certainly sufficient.*

*See Fig. 2 of reference 22.

One can calculate, using the derivation given by Berry, the variation of the collection efficiency of the mass spectrometer with accelerating voltage and repeller voltage. Berry gives for the collection efficiency N the equation

$$N = 1/2(k + 1)\mathrm{erf}[(k + 1)\sigma] - 1/2|k - 1|\ \mathrm{erf}[(k - 1)\sigma]$$
$$+ (2\pi^{1/2}\sigma)^{-1}\{\exp[-(k + 1)^2\sigma^2] - \exp[-(k - 1)^2\sigma^2]\} . \tag{22}$$

If one derives the equation by using commonly tabulated error functions,[45] one obtains the slightly different expression

$$N = (k + 1)\mathrm{erf}[\sqrt{2}\ (k + 1)\sigma] - |k - 1|\ \mathrm{erf}[\sqrt{2}\ (k - 1)\sigma]$$
$$+ (2\pi^{1/2}\sigma)^{-1}\{\exp[-(k + 1)^2\sigma^2] - \exp[-(k - 1)^2\sigma^2]\} , \tag{23}$$

where the error function is in integral form. The symbols used in the above equations are defined for two different regions: region 1, the accelerating region between the exit slit of the Isatron and the accelerating slit; and region 2, the analyzer region between the accelerating slit and the collector slit. N_1 is defined as the ratio of the number of ions of a given mass that pass through the accelerating slit to the number of ions of the same mass that are formed in an area of the electron beam equal to the area of the exit slit of the Isatron. N_2 is defined as the ratio of the number of ions of a given mass that pass through the collector slit to the number of ions of the same mass that pass through the accelerating slit. The k's are given by the expressions

$$k_1 = w_e/w_1; \qquad k_2 = \ell_2/\ell_1 , \tag{24}$$

where w_e is the half-width of the exit slit, w_1 and ℓ_1 the half-width and half-length of the accelerating slit, and ℓ_2 the half-length of the collector slit. The parameter σ is given by the expressions

$$\sigma_1 = 1/2(V/T_i)^{1/2} w_1/L_1 \; ; \quad \sigma_2 = (V/T_i)^{1/2} \ell_1/L_2 \; , \tag{25}$$

where L_1 and L_2 are the distances traveled by the ions in the regions 1 and 2, respectively; V is the accelerating voltage; and T_i is the initial kinetic energy of the ions. When the appropriate values are substituted for these parameters, as shown in Table X, the overall collection efficiency of the mass spectrometer, N_1N_2 , can be computed. Calculated collection-efficiency curves for a typical thermal ion and for an ion of 2.27-eV excess kinetic energy (the excess energy of the CH_3^+ fragment from benzene) are shown in Fig. 24.

Table X. Numerical values of parameters appearing in Eqs. (24) and (25).

parameter	ℓ_1	ℓ_2	w_1	w_e	L_1	L_2
value (in.)	0.125	0.250	0.003	0.003	0.273	5π

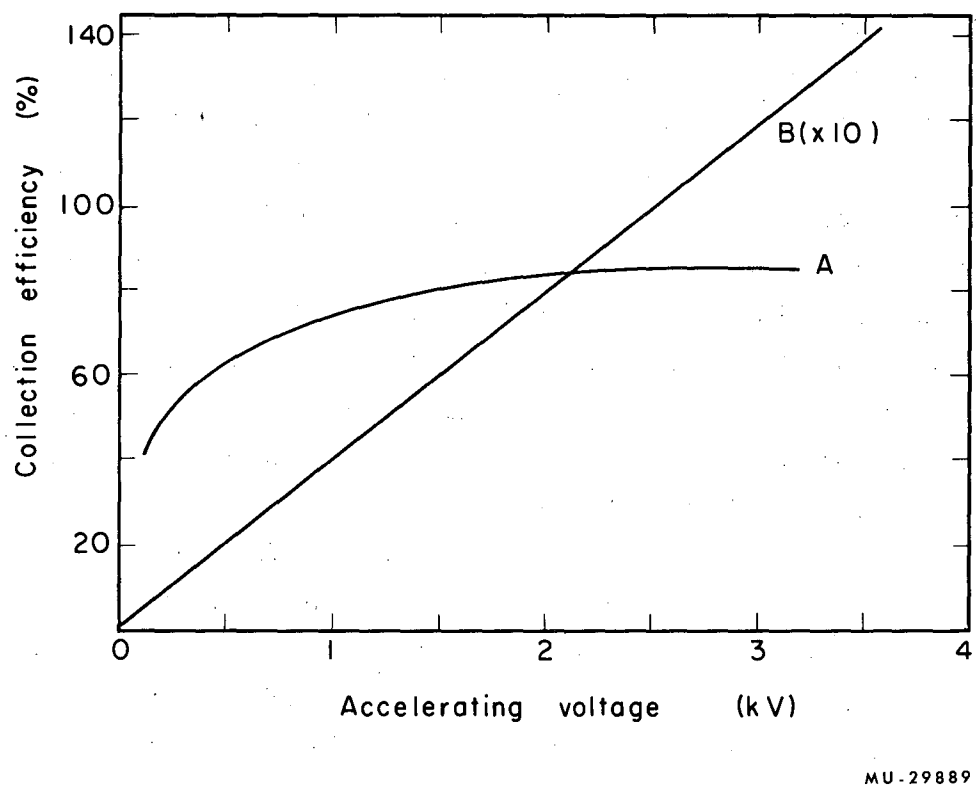

Fig. 24. Theoretical collection efficiencies, plotted as a function of the accelerating voltage, as calculated from Eq. 23. A: Thermal M/q=15 peak (from, e.g., methane); B: 2.27-eV excess-kinetic-energy M/q=15 peak (from, e.g., benzene).

A comparison of Figs. 7 and 24 shows that although the general shape of the curves and the qualitative relation between the two types of curves are duplicated by the calculated curves, the curvature of the experimental thermal-ion curve is much greater than that predicted by the theory. The only explanation for the discrepancy would seem to lie in the approximations made in making the theoretical calculation, namely, that the electric field is uniform and the effect of the magnetic field is negligible in the accelerating region. In the Consolidated instrument there are interposed in the accelerating region two electrodes, the focus electrodes, to which are applied potentials that serve to maximize the focus of the ions. Since the voltage applied to these electrodes is always greater than the uniform field potential would be at that point, and since, moreover, slightly different potentials are applied to the two electrodes, the electric field in the accelerating region is certainly not uniform but is nonuniform in a way that promotes the focusing of thermal ions on the accelerating slit. In addition, the magnetic field is of course not quite negligible; in the accelerating region it perturbs somewhat the collection efficiency.

It should be noted that there are other perturbing effects operating in the ion source that may have a measurable effect on the collection efficiency. In the Consolidated instrument there can be four such effects, all of which act by causing the electric field to deviate somewhat from the ideal linear dependence on which is based the statement that the exit slit causes no discrimination. The most important of these is probably the nonuniformity in the repeller field resulting because there are two repellers, one on each side of the molecular leak into the source, which generally are operated at slightly different potentials to improve the focusing of the instrument. Since the two repellers generally are operated within a few percent of each other, the maximum perturbation from this cause is probably no greater than several percent. A second perturbing effect is the penetration through the exit slit of the accelerating field. This causes nonuniformity of a type that would be expected to focus more ions on the exit slit. Two other perturbing agents are the space-charge effects due to the electron beam, which have been considered by Brubaker,[46] and any contact potentials that may be built up, either uniformly or nonuniformly, on the surfaces of the ion sources. All these latter effects are estimated to be small.

One can also make use of Eq. (23) to calculate the collection efficiency of the mass spectrometer for ions of various kinetic energies at different accelerating voltages. In Fig. 25 the results of such calculations are plotted as a function of the parameter V/T_i , the ratio of accelerating voltage to initial kinetic energy of the ions.

Absolute Abundances

If one knows the excess-kinetic-energy peak height at some given accelerating voltage and the excess kinetic energy of the ions, one can use the plot in Fig. 25 to calculate the absolute abundance of the ion in question. Such absolute abundances, expressed both as peak heights and as percentage of total ions observed in the mass spectrometer, are given in Table XI. The higher the collection efficiency, the less error should be involved in the application of Berry's equation; for this reason, the abundances given in the table are calculated from the peak heights measured at the maximum possible accelerating voltage. These peak heights were determined from total measured peak heights at the same accelerating voltage by the method outlined in the data section.

In Fig. 26, the abundance of excess-kinetic-energy M/q=15 ions for straight-chain hydrocarbons, expressed as the percentage of total ions observed, is plotted against number of carbon atoms. In this figure there is also given an estimated curve for the M/q=29 excess-kinetic-energy ions. This curve was constructed from peak heights measured at MV = 6000, as given in the tables in Appendix II. The general shape of the M/q=29 curve is accurate, but extrapolation of peak heights from the very low collection efficiency of the mass spectrometer at MV = 6000 to 100% collection efficiency is probably not very accurate.

Fragmentation Patterns

It is quite clear from a comparison of Tables VII and XI that if one wishes to measure a true fragmentation pattern in a mass spectrometer, one must operate at very high accelerating voltages. This is particularly true for excess-kinetic-energy ions for which, in fact, the Consolidated 21-103 mass spectrometer cannot be operated at high enough accelerating

Table XI. Calculated absolute abundances of excess-kinetic-energy ions.

Compound	M/q	Measured peak height acc. V=3700[a]	Calculated collection efficiency acc. V=3700[b]	Calculated peak height @100% coll. efficiency	Total peak height, all fragment ions[c]	% of total peak height that excess KE ion represents
ethane	15	550	0.1355	4060	46100	8.8
propane	15	1143	0.1265	9040	64950	13.9
n-butane	15	1622	0.1342	12100	80740	15.0
isobutane	15	1977	0.1260	15680	79700	19.7
n-pentane	15	1462	0.1490	9820	88100	11.1
neopentane	15	3146	0.1230	25600	99810	25.6
n-heptane	15	966	0.177	5460	120430	4.5
2,4-dimethyl pentane	15	2481	0.1605	15380	116480	13.2
n-decane	15	670	0.1595[d]	4200	156390	2.7
benzene	15	576	0.1475	3900	75020	5.2
p-xylene	15	1552	0.140[d]	11100	94960	11.7
ethyl benzene	15	1958	0.1480	17350	104330	16.6
isopropyl chloride	15	995	0.1130	8710	65220	13.4

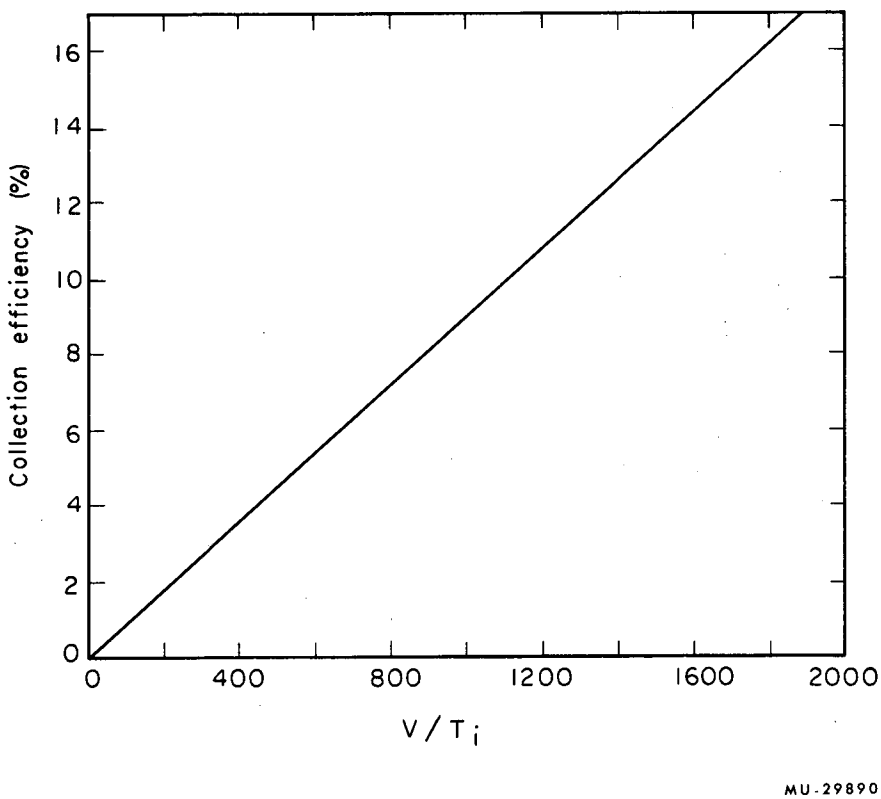

Fig. 25. Theoretical collection efficiencies, calculated from Eq. 23 and plotted as a function of the parameter V/T_i, the ratio of accelerating voltage to initial kinetic energy of the ions.

Table XI. (Cont.)

Compound	M/q	Measured peak height acc. V=3700[a]	Calculated collection efficiency acc. V=3700[b]	Calculated peak height @ 100% coll. efficiency	Total peak height, all fragment ions[c]	% of total peak height that excess KE ion represents
isopropyl alcohol	15	1513	0.1180	12800	65630	19.5
n-heptane	29	2455[e]	0.1605[d]	15300	120430	12.7

[a]All peak heights corrected to source pressure of 50 μ at high amplifier sensitivity. Peak height of M/q=58 peak of n-butane equals 2590 divisions under these conditions.

[b]Obtained from the curve given in Fig. 24.

[c]Obtained by summation of peak heights under normal operating conditions with a correction added for the extra contribution of excess-kinetic-energy peaks.

[d]Estimated.

[e]Measured at accelerating voltage of 3560 V.

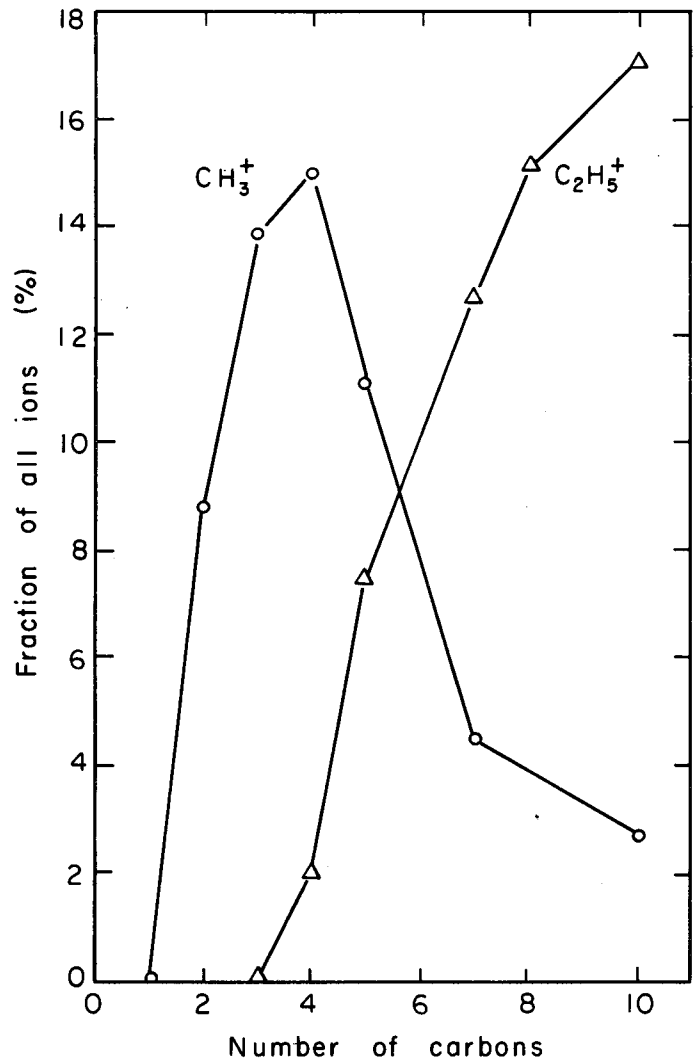

MU-29891

Fig. 26. Absolute abundances of excess-kinetic-energy ions as a function of the number of carbon atoms in the hydrocarbon molecule. CH_3^+ figures are from Table XI; $C_2H_5^+$ figures are estimated, by use of Fig. 25, from peak heights tabulated in Appendix II.

voltages to get a true fragmentation pattern. It is also true, however, for fragment ions of near-thermal energy. Note, for example, the variation of peak height with accelerating voltage for the methyl ion from methyl chloride, shown in Fig. 9. For this ion, which possesses 0.25 eV excess kinetic energy, the mass spectrometer must be operated at 1800-V accelerating voltage before 90% efficiency is attained, and 100% efficiency is not attained until an accelerating voltage of 3500 V is reached. It is concluded that the fragmentation patterns determined under normal conditions, where the magnetic field is held constant and the accelerating voltage varied to focus various M/q ions, underestimate the proportion of higher-mass fragments, since these fragments are collected at lower voltages. Optimal determination of fragmentation patterns should be carried out by magnetic scanning at the maximum available accelerating voltage, in order to minimize kinetic-energy discrimination effects.

A comparison of the mass spectral patterns tabulated by the API[47] for compounds whose patterns have been measured both at constant accelerating voltage and at constant magnetic field shows that discrimination effects are important. For M/q ratios shown to possess excess-kinetic-energy components, the patterns fluctuate widely. Observed fragmentation patterns therefore must be used with caution. Pattern factors when expressed relative to the parent ion peak would if anything be too low, since the parent peak, composed of thermal ions only, is collected with maximum efficiency. When expressed as percentage of total ions observed, however, the pattern factors for thermal ions would be too high and those for excess-kinetic-energy ions would be too low.

Implications for the Quasi-Equilibrium Theory of Mass Spectra

The quasi-equilibrium (Q-E) theory of mass spectra, first proposed by Rosenstock, Wallenstein, Wahrhaftig, and Eyring, represents one of the very few serious attempts to develop a theory that can explain the various phenomena observed in mass spectra.[48] The theory attempts to describe fragmentation processes induced by electron impact as essentially

statistical in nature, which permits the rather powerful methods of statistical mechanics to be applied to the problem of calculating rates of decomposition and fragmentation patterns. In order for a statistical treatment to be valid, it is necessary that the energy transferred to the molecule by the initial excitation process be randomized before decomposition occurs; this has been assumed to be the case by Q-E-theory workers, with the proposed mechanism for such randomization being radiationless transitions between different electronic-vibrational (vibronic) states of the molecule. It is asserted that such radiationless transitions are extremely frequent in polyatomic molecules, since there is a very large number of energy levels of such molecules. For molecules as large as propane, for example, the spacing between energy levels in the energy region above the ionization threshold is on the average 1 mV; it is therefore expected that interlevel crossings will be frequent.

The original formulation of the Q-E theory was immediately subjected to close scrutiny by many of the investigators in the mass-spectroscopy field. Although it apparently predicted adequately some of the observed behavior of mass spectra, other experimental data were definitely at variance with the predictions of the theory. Recently, modification of the rate expression appearing in the theory has permitted Vestal, Wahrhaftig, and Johnston to eliminate many of these discrepancies.[49] The basic assumption of this improved form of the theory still remains the same, however.

This basic assumption of rapid randomization of excitation energy among the vibrational modes of the molecule has been questioned by several experimenters. Chupka has pointed out that data of Hurzeler, Inghram, and Morrison[50] indicate that the energy-level spacing between the ground state and the first excited state of some ketone and amine ions is of the order of a volt, much greater than the 1-mV average spacing cited to justify the assumption of frequent radiationless transitions.[27] In this case, Chupka notes, there is evidence of intramolecular energy transfer, perhaps by a purely vibrational mechanism, which might serve to make the randomization hypothesis valid. However, Chupka also discusses the implications of the observations of upward breaks in the ionization-probability curves for the parent ions of propylene and benzene, for both

of which one observes breaks at energies greater than the energies required to instigate dissociative processes. He concludes that the breaks constitute excellent evidence that the excited states whose excitation is indicated by the upward breaks do not readily make transitions to the lower-lying electronic states that give rise to dissociation.

Further evidence that the density of electronic states in the threshold region is not sufficient to justify the assumption of rapid randomization of excitation energy was found by Steiner, Giese, and Inghram in a study of the photoionization of alkanes.[51] These investigators studied the shapes of photoefficiency curves and found that departures from linearity, expected in the presence of many electronic states, were absent. They concluded from this that there is only a limited number of electronic states near the ionization threshold for the compounds studied.

The observations made in this work indicate that in the energy region from 15 to 20 V above threshold there is also a lack of randomization of the excitation energy. The existence of a class of ions possessing a discrete amount of excess kinetic energy requires that dissociation leading to such ions take place before randomization occurs. In the presence of randomization it is expected that the molecule ion reaches a given mode of dissociation possessing just enough, or at most slightly more than enough, energy present in the bond to break it. The excess-kinetic-energy fragment ion results from the parent ion's reaching the mode of dissociation with considerably more energy residing in the bond in question. Moreover, there is a sharp distribution of kinetic energies about the most probable value; this is consistent with excitation to a dissociative portion of a potential-energy curve followed directly by such dissociation, but is not consistent with processes involving randomization of energy. One might obtain such a distribution of kinetic energies from a mechanism involving an intersystem crossing, such as that shown in Fig. 27. However, it is hard to see how such a process could exhibit a second-power dependence of the ionization efficiency curve on electron energy. Moreover, even if the process illustrated by Fig. 27 represents a correct mechanism for excess-kinetic-energy ion formation, the fact remains that complete randomization

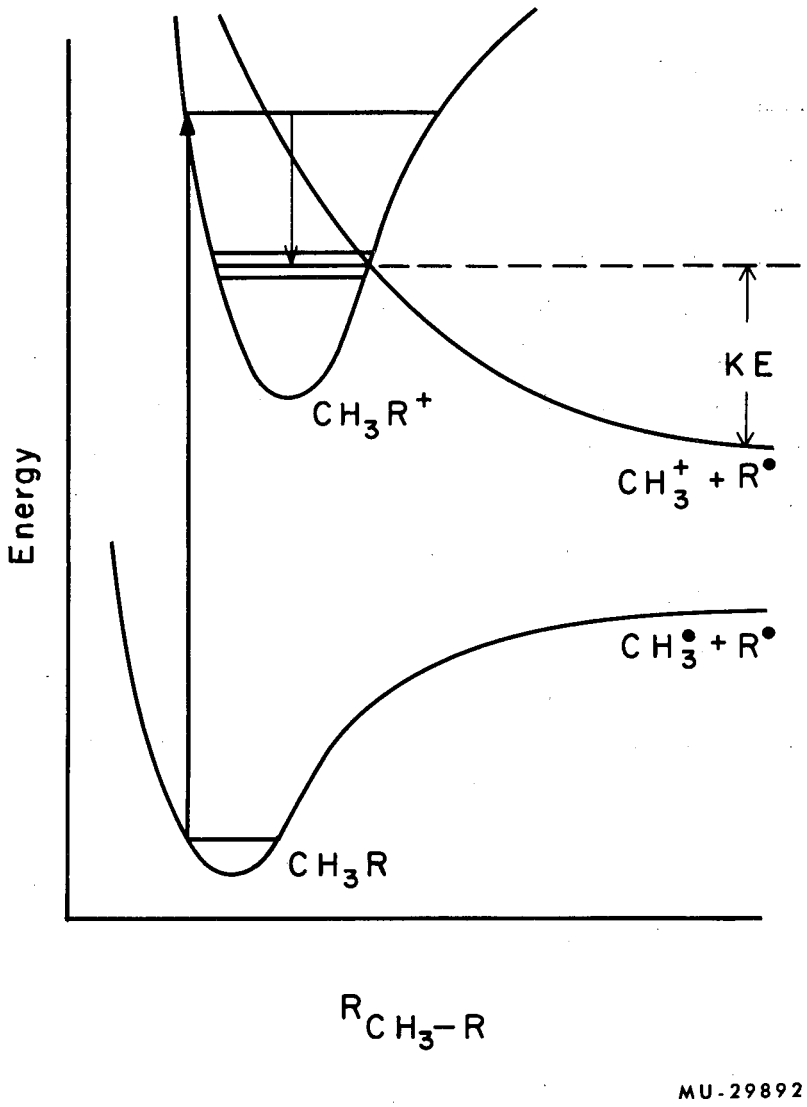

Fig. 27. Potential-energy curves for the CH_3R molecule and a pair of its possible ionic states illustrating a transition process involving both a radiationless transition and the appearance of excess-kinetic-energy ions (after Chupka).[27]

of energy does not occur in the time required for the molecule to dissociate after it has undergone the interlevel crossing.

Thus, there is definitely a breakdown of the basic assumption of the Q-E theory, not only in the region near threshold as was previously shown, but also in the region well above threshold where the closest approach to randomization might be expected. Interlevel crossings are apparently not nearly as frequent as Rosenstock et al. initially supposed. This may be due in large part to the operation of selection rules for radiationless transitions, which have been formulated by Sponer and Teller.[52] The symmetry and angular-momentum-dictated selection rules are probably not of importance for polyatomic molecules with many atoms, but the selection rule requiring that the multiplicity be maintained in the transition indicates that there are probably at least two relatively independent systems of potential-energy surfaces corresponding to doublet and quadruplet states of the molecule ion.

It might be argued that, although the assumption of randomization of energy is not entirely valid, the fragment ions resulting from processes that do not involve randomization make up such a small part of the mass spectra that they can effectively be ignored. That this is not the case is indicated by the information given in Fig. 26, whence it is seen that for propane, for which most of the calculations of the Q-E theory have been made, excess-kinetic-energy M/q=15 ions alone are estimated to constitute 14% of the mass spectrum at an ionizing voltage of 70V. This can hardly be termed an insignificant part of the total fragmentation pattern.

This also illustrates an experimental feature of mass spectra that must be taken into account in any comparison of theoretical with experimental fragmentation patterns. Since the mass spectrometer discriminates strongly against excess-kinetic-energy ions, the experimental mass spectra must be corrected considerably to give true fragmentation patterns. For propane, for example, the experimental mass spectrum as measured on the Consolidated 21-103 instrument under normal conditions shows only 2% of the spectrum to be made up of M/q=15 ions, both thermal and excess energy, whereas this research indicates that, in reality, more than 10% of the spectrum is constituted of such ions. This leads to another indication that the Q-E theory is in error, namely that it

seems to be incapable of predicting the existence of any M/q=15 ions in the propane mass spectrum, let alone 10% of all ions.

An alternative theory of mass spectra within whose framework the phenomena observed in this research could more easily be explained is one of a type suggested by Steiner, Giese, and Inghram.[51] Such a theory would treat dissociation as a phenomenon that could be explained by making assumptions similar to those of Slater's theory of unimolecular reactions.[53] Slater's theory itself is not applicable, since he did not consider zero-pressure dissociations, and unfortunately no detailed formulation of such a theory has resulted yet from the suggestions of Steiner, Giese, and Inghram.

In conclusion, it may be said that the one fact becoming quite clear from work undertaken in the field of electron impact studies is that very few of the pehnomena observed are really understood. One is forced to conclude that more as well as more precise data are required before the excitation processes and the dissociation mechanisms can be adequately characterized.

APPENDIX I

Excess Kinetic Energies

In Tables A-I through A-VII are listed semiquantitative values for the excess kinetic energies of a large number of various M/q ions from many organic compounds. In the experiments in which these values were determined the mass-spectrometer operating conditions were as follows: MV = 6000, repellers at 0 V, metastable suppressor voltage set at 103% of the accelerating voltage (Conditions A). This metastable suppressor setting prevents many thermal ions from reaching the collector and in so doing shifts the kinetic-energy distribution of thermal ions reaching the collector in the direction of higher kinetic energies. For this reason, the energy difference measured under the above conditions is always less than the actual energy difference. In addition, in these experiments no attempt was made to measure the excess kinetic energies associated with the thermal peaks. As a result of these factors, the values listed in Tables A-I through A-VII are all considerably smaller than the true excess kinetic energies of the peaks in question. Table A-VIII shows the excess kinetic energies measured under conditions A compared with the actual excess kinetic energies tabulated in Table IV for those compounds and M/q values for which the actual excess kinetic energies are available. It can be seen that virtually all these values are low by 0.5 ± 0.15 eV.

Table A-I. Energy differences of thermal and high-energy peaks for various M/q ions in paraffins

Compound	ΔE for ion of M/q[a]				Others					
	14	15	16	29	M/q	ΔE	M/q	ΔE	M/q	ΔE
ethane	2.0	2.1	2.5	N[b]						
propane	2.1	2.3	2.5	N						
n-butane	1.8	2.0	2.1	1.8						
isobutane	2.3	2.2	2.4	N	13	2.0				
n-pentane	1.8	1.7	1.9	1.8						
isopentane	2.3	2.0	2.2	1.8						
neopentane	2.1	2.1	2.6	N						
n-hexane	1.5	1.5	1.5	1.5						
isohexane	1.7	1.6	1.8	1.9						
3-methyl pentane	1.5	2.0	2.2	1.7	26	1.7	27	1.8	28	1.8
neohexane	2.1	2.0	2.2	1.7	26	1.7	27	1.8	28	1.9
di-isopropyl	1.9	2.0	2.2	N						
n-heptane	--[c]	1.5	--	1.5						
3-methyl hexane	--	1.6	1.9	1.7	26	1.7	28	1.7		
2,3-dimethyl pentane	--	1.8	--	2.0						
2,4-dimethyl pentane	1.3	1.5	1.7	--	41	1.6	42	1.3	43	1.9
n-octane	--	1.3	--	1.2						
2,5-dimethyl hexane	1.7	1.4	1.7	--	41	1.6	42	1.4	43	1.5
2,2,4-trimethyl pentane	-	1.5	--	--						
2,2,5-trimethyl hexane	--	1.6	--	--	43	1.4				
n-decane	--	1.6	--	1.2	26	1.3				
n-undecane	--	1.5	--	--						

[a] All energy differences measured under conditions A: MV = 6000, repellers at 0 V, metastable suppressor voltage 103% of accelerating voltage.

[b] An N indicates that no excess kinetic energy peak was observed at that M/q for that compound.

[c] A blank indicates that the peak resolution was insufficient to permit measurement of excess kinetic energy.

Table A-II. Energy differences of thermal and high-energy peaks for various M/q ions in olefins

Compound	ΔE for ion of M/q					
	14	15	26	27	28	29
butene-1	2.0	2.1	1.6	1.9	--	--
cis-butene-2	2.0	2.1	1.6	1.7	1.8	--
trans-butene-2	2.1	2.2	1.6	--	--	--
pentene-1	1.7	1.9	--	1.8	--	1.9
3-methyl butene-1	2.2	2.1	--	--	--	--
hexene-1	--	1.6	--	--	--	1.7
hexene-2	--	1.8	--	--	--	1.8
1,5-hexadiene	--	1.8	1.7	1.8	--	--

Table A-III. Energy differences of thermal and high-energy peaks for various M/q ions in alcohols.

Compound	ΔE for ion of M/q	
	15	31
ethanol	2.5	--
n-propanol	2.2	1.7
isopropanol	2.6	--
n-butanol	1.8	1.8
isobutanol	2.4	1.9
t-butyl alcohol	2.5	N
n-amyl alcohol	1.8	1.6
n-hexyl alcohol	1.7	1.3
n-heptyl alcohol	1.7	1.2
n-octyl alcohol	--	1.4

Table A-IV. Energy differences of thermal and high-energy peaks for various M/q ions in halides

Compound	ΔE for ion of M/q						
	14	15	26	27	29	35	36
methyl chloride	3.1	3.6	N	N	N	0.8	--
ethyl chloride	2.2	2.5	1.9	1.6	--	1.2	1.3
vinyl chloride	2.7	2.7	1.8	1.9	N	1.2	1.1
n-butyl chloride	--	1.9	--	--	2.1	--	--
n-amyl chloride	--	1.8	--	--	1.6	--	--
n-hexyl chloride	--	1.6	--	--	1.5	--	--
n-heptyl chloride	--	1.2	--	--	1.4	--	--
1,1-dichlorobutane	--	2.1	--	--	2.2	--	--
ethyl bromide	--	2.7	--	2.7	--	N	N
n-butyl bromide	--	1.9	--	--	2.0	N	N
n-butyl iodide	--	1.8	--	--	2.2	N	N

Table A-V. Energy differences of thermal and high-energy peaks for various M/q ions in nitrogen compounds

Compound	ΔE for ion of M/q						
	15	16	17	28	29	30	46
nitroethane	2.7	--	N	--	--	--	--
1-nitropropane	2.0	--	N	--	--	1.6	1.5
2-nitropropane	2.4	--	N	--	--	1.6	1.6
dimethyl amine	2.7	2.5	--	1.6	1.6	N	N
ethyl amine	2.5	2.4	2.8	--	--	N	N
di-n-propyl amine	1.8	--	--	--	1.8	N	N

Table A-VI. Energy differences of thermal and high-energy peaks for various M/q ions in aromatic and cyclic compounds

Compound	ΔE for ion of M/q				Others					
	15	26	27	28	M/q	ΔE	M/q	ΔE	M/q	ΔE
benzene	1.8	1.9	1.6	--	37	1.9	38	1.6	38	1.6
toluene	1.8	1.7	1.9	1.9						
ethyl benzene	1.7	1.7	1.9	2.1	29	2.0				
n-propyl benzene	--	1.7	1.7	1.8	29	1.8				
isopropyl benzene	--	1.7	1.9	1.9	39	1.6				
aniline	1.8	1.7	1.7	--						
benzaldehyde	--	1.8	--	--	29	2.0	37	1.7	38	1.6
benzonitrile	--	1.8	1.7	--						
chlorobenzene	1.8	1.8	1.9	--	35	1.3	37	1.8	38	1.5
nitrobenzene	--	--	--	--	30	2.0	[illegible]	[illegible]		
m-chlorotoluene	--	1.6	1.8	--						
p-chlorotoluene	--	1.5	1.7	--						
o-chlorotoluene	--	1.6	1.8	--						
m-xylene	1.8	1.5	2.0	1.9						
o-xylene	1.9	1.5	1.9	1.7						
p-xylene	1.9	1.7	1.9	1.8						
phenol	2.2	--	--	--	29	1.9				
methyl cyclopropane	2.2	--	--	--	14	2.1				
cyclopentane	2.1	--	--	2.2						
methyl cyclopentane	1.8	--	--	2.1						
cyclohexane	1.8	--	--	2.1						
methyl cyclohexane	1.8	--	--	1.9						
ethyl cyclohexane	1.7	--	--	--	29	1.8				

Table A-VII. Energy differences of thermal and high-energy peaks for various M/q ions in miscellaneous compounds

Compound	M/q	ΔE	M/q	ΔE	M/q	ΔE	M/q	ΔE
acetic acid	15	3.2	17	2.4				
propionaldehyde	15	2.6						
n-butyraldehyde	15	1.9	29	1.8				
isobutyraldehyde	15	2.4	29	1.9				
di-n-propyl ether	15	1.9	29	1.4				
di-n-propyl ketone	15	1.3	29	1.8				
diborane	11	2.7	13	1.9	14	2.0	15	2.4
deuteroethylene[a]	2	2.7						
deuteromethane[a]	2	2.1						

[a] Measured at MV = 1200.

Table A-VIII. Comparison of M/q = 15 energies measured under conditions A with actual kinetic energies

Compound	ΔE, conditions A	ΔE, Table IV	Difference between column 3 and column 2
ethane	2.12	2.45	0.33
propane	2.28	2.65	0.37
n-butane	1.98	2.48	0.50
isobutane	2.20	2.66	0.46
n-pentane	1.66	2.24	0.58
neopentane	2.15	2.71	0.56
n-hexane	1.47	1.95	0.58
di-isopropyl	2.01	2.50	0.49
n-heptane	1.48	1.73	0.25
2,4-dimethyl pentane	1.45	2.08	0.63
2,5-dimethyl hexane	1.43	2.06	0.63

APPENDIX II

Excess-Kinetic-Energy Ion Peak Heights

In Tables A-IX through A-XV, Parts A, the excess-kinetic-energy peak heights measured under conditions A (MV = 6000, repellers at 0 V, metastable-suppressor voltage 103% of accelerating voltage) are given for a wide variety of organic compounds. In Parts B of the same tables are listed the peak heights for the same M/q values for the same compounds, measured under normal operating conditions of the mass spectrometer. Since under normal conditions the thermal and excess-kinetic-energy peaks are not resolved, the peak heights given in Parts B represent the sums of contributions of thermal and excess-kinetic-energy components. Since the collection efficiencies for excess-kinetic-energy ions are grossly different under conditions A from those under normal conditions, the difference in collection efficiencies between these two sets of conditions must be estimated before comparison of peak heights can be attempted. Such an estimate can be made by utilizing the abundance figures tabulated in the text (Table VII) for several compounds. The peak heights of excess-kinetic-energy ions under conditions A and under normal conditions are given in Table A-XVI, wherein the ratios of these peak heights are also given. It is seen that, in general, multiplication of the conditions-A peak height by about 17 gives the normal-conditions peak height for excess-kinetic-energy ions. Hence, one can estimate the thermal-ion and excess-kinetic-energy-ion components of a peak height measured under normal conditions by multiplying the conditions-A excess-kinetic-energy peak height by 17 to obtain the excess-kinetic-energy component, and by subtracting that peak height from the total measured peak height under normal conditions to obtain the thermal-energy component. This has been done for several example compounds, and the results are shown in Table A-XVII. From the variation in the ratios given in Table A-XVI, it is evident that this process gives only a very crude approximation to the correct normal-conditions peak-height breakdowns.

Table A-IX. Paraffin peak heights

Compound	13	14	15	16	26	27	28	29	M/q	peak hgt.	M/q	peak hgt.	M/q	peak hgt.
A. Excess-energy peak heights at MV = 6000														
ethane	2.6	12.0	28.1	1.0	--	--	--	--						
propane	2.5	11.8	56.2	1.2	--	--	--	--	12	0.5				
n-butane	2.8	8.7	83.2	1.6	11.9	29.6	6.9	5.8	12	0.8				
isobutane	2.6	12.9	102.0	3.7	3.2	3.4	--	--	12	1.0				
n-pentane	--	6.2	54.2	1.6	9.6	37.8	--	23.2						
isopentane	1.4	8.1	98.7	4.3	6.5	20.3	4.7	11.9						
neopentane	1.3	13.5	135.6	5.0	1.8	4.0	--	--						
n-hexane	--	4.0	44.2	3.0	9.2	59.8	6.7	46.3						
isohexane	--	5.5	74.1	6.6	5.1	33.3	11.8	22.3						
3-methyl pentane	--	4.8	53.1	1.9	7.9	39.8	6.1	41.9						
neohexane	--	8.0	106.2	7.4	5.6	22.2	5.2	22.7						
di-isopropyl	1.2	5.3	108.6	6.4	--	--	--	--	39	14.7	41	11.9		
n-heptane	--	3.1	30.7	1.1	8.7	65.8	9.4	76.6	30	1.7				
3-methyl hexane	0.5	3.6	40.6	1.4	7.0	55.4	8.4	60.9						
2,3-dimethyl pentane	--	4.0	57.4	2.3	4.6	37.9	4.6	34.8						
2,4-dimethyl pentane	--	5.1	93.9	9.3	2.7	--	6.1	--	39	22.6	41	27.6	42	14.1
n-octane	--	1.9	21.4	--	7.8	--	11.1	105.3	30	2.2				

Table A-IX. (cont.)

Compound	13	14	15	16	26	27	28	29	M/q	peak hgt.	M/q	peak hgt.	M/q	peak hgt.
2,5-dimethyl hexane	--	3.2	60.3	2.4	2.2	---	5.5	--	41	40.6	42	6.4	43	25.1
2,2,4-trimethyl pentane	-	4.4	99.0	7.4	1.8	--	7.8	--						
2,2,5-trimethyl hexane	--	2.9	58.8	1.4	--	--	--	--	43	19.9				
n-decane[b]	--	1.4	11.3	--	6.4	--	--	156.4	30	2.3				
n-undecane[b]	--	1.2	10.0	--	--	--	--	--						
n-dodecane[b]	--	--	9.1	--	--	--	--	--						
B. Peak heights under normal conditions														
ethane	328	823	1140	15	--	--	--	--						
propane	210	589	1730	47	--	--	--	--						
n-butane	108	364	1980	44	1760	8920	6780	8860						
isobutane	144	486	2490	85	745	6920	--	--						
n-pentane	66	84	1660	50	1100	9090	2180	5580						
isopentane	101	350	2340	97	938	7120	1200	6520						
neopentane	119	494	3180	116	554	4880	787	10050						
n-hexane	--	181	1290	47	907	7960	2160	8980						
isohexane	--	241	2185	120	676	7595	1060	4590						
3-methyl pentane	--	200	1500	53	807	7440	1465	11590						
neohexane	--	367	2850	148	739	6363	1010	7452						

Table A-IX (cont.)

Compound	13	14	15	16	26	27	28	29	M/q	peak hgt.	M/q	peak hgt.	M/q	peak hgt.
di-isopropyl	79	312	2840	145	--	--	--	--	39	5040	41	8820		
n-heptane	--	153	1260	40	865	8970	1850	9480						
3-methyl hexane	34	156	1365	46	723	7995	1285	9190						
2,3-dimethyl pentane	38	180	1730	70	630	7385	1345	8115						
2,4-dimethyl pentane	--	265	2650	177	422	6660	837	4850	39	5457	40	980		
n-octane	--	106	1015	33	729	9425	2075	10510	30	253				
2,5-dimethyl hexane	--	193	1970	120	450	7210	1236	5210	42	8230	43	24160		
2,2,5-trimethyl hexane	--	144	1860	59	314	6065	1210	8075	43	8855				

[a] Absences of a value for a peak height in these tables does not necessarily indicate that that peak is not present in the spectrum, but only that it was not measured in this research.

[b] No reliable normal conditions patterns available for these compounds.

Table A-X. Olefin peak heights

Compound	13	14	15	16	26	27	28	29
A. Excess-energy peak heights at MV = 6000								
butene-1	3.8	14.8	54.0	1.0	13.6	20.0	3.1	--
cis-butene-2	2.0	8.1	50.9	0.9	18.0	19.4	5.7	--
trans-butene-2	1.6	9.9	45.2	1.0	15.4	16.9	5.0	--
pentene-1	--	9.3	53.7	1.3	12.9	31.8	5.2	8.2
3-methyl butene-1	2.8	14.9	92.0	4.0	8.5	14.1	2.0	--
hexene-1	--	6.4	37.1	1.7	11.6	42.0	6.5	22.2
hexene-2	--	5.7	61.2	2.3	12.2	38.6	8.0	21.3
1,5-hexadiene	2.4	9.3	20.1	0.8	14.4	29.9	3.4	--
B. Peak heights under normal conditions								
butene-1	208	519	1330	28	2220	5880	4990	2240
cis-butene-2	134	282	1145	22	2540	5910	4950	2350
trans-butene-2	124	280	1155	21	2495	6000	5025	3015
pentene-1	116	360	1575	36	1430	6800	1080	4770
3-methyl butene-1	150	487	2180	83	1310	7180	1205	5420
hexene-1	73	224	1070	36	994	8200	1600	3290
hexene-2	63	207	1380	73	1120	7290	1450	5060
1,5-hexadiene	133	336	1020	18	1340	5840	1320	1120

Table A-XI. Alcohol peak heights

Compound	14	15	16	17	26	27	28	29	30	31
A. Excess-energy peak heights at MV = 6000										
methanol	3.5	3.7	--	5.5	--	--	--	--	--	--
ethanol	8.6	24.1	1.0	4.9	--	--	--	--	--	4.5
n-propyl alcohol	5.3	24.2	1.0	2.2	7.5	17.8	5.4	11.0	2.8	12.9
isopropyl alcohol	9.6	51.5	1.5	3.4	--	--	--	10.3	2.0	26.0
n-butyl alcohol	4.5	36.9	0.8	0.9	6.6	19.1	11.5	12.5	1.8	25.5
isobutyl alcohol	6.8	40.1	1.7	1.0	--	--	--	10.3	2.0	26.0
t-butyl alcohol	12.8	83.2	2.8	2.7	--	--	--	--	--	--
n-amyl alcohol	3.6	23.5	1.0	0.6	6.0	24.2	--	18.5	1.8	39.7
n-hexyl alcohol	2.7	17.3	--	--	--	--	--	28.3	--	57.7
n-heptyl alcohol	1.8	12.9	--	--	5.8	--	--	30.5	--	82.5
n-octyl alcohol[b]	1.1	8.7	--	--	--	--	--	40.9	--	101.1
B. Peak heights under normal conditions										
methanol	805	3630	111	222	--	--	--	--	--	--
ethanol	954	1560	99	147	--	--	--	--	--	14530
n-propyl alcohol	483	1280	55	88	1470	4525	1540	4195	654	24060
isopropyl alcohol	1045	3240	140	134	769	4025	342	2800	237	13650

Table A-XI (cont.)

Compound	14	15	16	17	26	27	28	29	30	31
n-butyl alcohol	351	1370	52	43	1015	6470	2150	3960	294	11020
isobutyl alcohol	453	1740	67	71	842	6290	1120	3570	293	8490
t-butyl alcohol	739	3525	119	112	600	2550	608	3185	112	8435
n-amyl alcohol	316	1410	58	44	1100	6560	2480	8920	376	9320
n-hexyl alcohol	177	1070	--	--	690	--	--	6280	--	6830
n-heptyl alcohol	148	898	--	--	558	--	--	6330	--	6065

[b] No reliable normal conditions patterns available for these compounds.

Table A-XII. Halide peak heights

Compound	14	15	16	27	29	35	36	M/q	Peak hgt.	M/q	Peak hgt.
A. Excess-energy peak heights at MV = 6000											
methyl chloride	8.5	14.0	--	--	--	15.8	--				
ethyl chloride	7.6	23.0	0.3	14.9	--	11.9	4.4				
vinyl chloride	10.8	10.5	--	7.3	--	13.7	2.5	13	7.5	26	9.3
n-propyl chloride	9.2	38.0	0.7	--	2.0	6.6	5.0				
isopropyl chloride	8.1	47.9	1.1	--	--	7.5	7.2				
n-butyl chloride	8.0	46.1	1.1	20.9	5.9	3.0	3.6	26	10.1		
isobutyl chloride	12.7	81.8	3.2	--	--	3.0	3.5				
t-butyl chloride	12.3	82.4	1.8	--	--	5.3	6.6				
n-amyl chloride	6.3	46.4	1.6	46.0	17.9	1.4	1.8	26	10.4	28	7.6
isoamyl chloride	8.7	72.9	4.0	--	--	1.4	2.4				
n-hexyl chloride	4.5	34.9	1.3	--	38.5	--	--	26	10.8		
n-heptyl chloride	2.9	23.5	--	--	56.7	--	--	26	8.9		
n-octyl chloride	1.9	17.7	--	--	72.5	--	--	26	8.5		
1,1-dichloroethane	5.1	21.6	0.5	--	--	22.4	6.5				
1,1-dichloropropane	8.5	46.0	0.9	12.7	3.5	13.8	7.8	26	7.4	28	2.3
1,2-dichloropropane	9.0	31.0	0.7	--	1.8	11.7	10.5				
1,1-dichlorobutane	7.4	54.0	1.1	--	9.8	6.6	5.5	28	6.6		
2,3-dichlorobutane	7.4	65.8	1.3	--	--	5.8	7.7				
1,1,1-trichloroethane	5.5	18.7	--	--	--	37.3	6.6				

Table A-XII (cont.)

Compound	14	15	16	27	29	35	36	M/q	Peak hgt.	M/q	Peak hgt.
1,1,1,2-tetrachloropropane	5.5	31.9	0.7	7.9	1.4	29.9	12.0	26	3.1	28	7.7
ethyl bromide	5.2	13.0	--	13.2	2.7	--	--	26	7.0	28	3.2
n-propyl bromide	8.1	43.2	0.7	--	--	--	--				
2-bromopropane	6.1	29.1	0.4	--	--	--	--				
n-butyl bromide	6.9	38.1	0.9	--	10.0	--	--				
isobutyl bromide	9.8	80.7	1.8	--	--	--	--				
t-butyl bromide	8.2	50.2	--	--	--	--	--				
1,1-dibromoethane	3.1	8.5	--	--	--	--	--				
1,2-dibromopropane	7.3	12.1	0.3	--	1.9	--	--				
methyl iodide	9.9	30.2	--	--	--	--	--	13	8.8		
n-butyl iodide	5.0	22.2	0.6	--	17.3	--	--				
isobutyl iodide	12.0	47.5	1.5	--	--	--	--				
carbon tetrafluoride	--	--	--	--	--	--	--	19	10.8		
B. Peak heights under normal conditions											
methyl chloride	1320	12000	--	--	--	1190	--				
ethyl chloride	632	704	12	9180	--	743	302				
vinyl chloride	450	169	--	14400	--	1120	386				
n-propyl chloride	579	1575	34	9075	7390	349	432				
isopropyl chloride	474	1575	36	9150	40	360	500				

Table A-XII (cont.)

Compound	14	15	16	27	29	35	36	M/q	Peak hgt.	M/q	Peak hgt.
n-butyl chloride	418	1510	35	9670	4450	205	250				
isobutyl chloride	414	2030	45	8475	6140	211	332				
t-butyl chloride	630	2430	52	3450	4730	326	669				
n-amyl chloride	319	1570	44	8730	6400	114	176	26	1460		
isoamyl chloride	405	2110	94	8430	4340	120	215				
n-hexyl chloride	228	1270	36	--	6390	--	--	26	1220		
n-heptyl chloride	137	975	30	--	7370	--	--	26	870		
n-octyl chloride	99	819	26	--	8320	--	--	26	742		
1,1-dichloroethane	335	563	14	--	--	1690	577				
1,1-dichloropropane	446	1460	32	5410	7280	735	587	26	1710		
1,2-dichloropropane	487	1110	22	7840	18	594	618				
1,1-dichlorobutane	331	1430	32	10130	3450	459	460	28	1303		
2,3-dichlorobutane	278	1385	26	--	--	323	529				
1,1,1-trichloroethane	281	497	--	--	--	2445	752				
1,1,1,2-tetrachloropropane	247	826	16	5975	19	1615	1075	26	1045	28	278
ethyl bromide	554	507	--	11410	12310	--	--	26	4160	28	2640
n-propyl bromide	592	1740	36	--	--	--	--				
isopropyl bromide	315	939	26	--	--	--	--				
n-butyl bromide	345	1180	30	--	9800	--	--				
isobutyl bromide	543	2300	70	--	--	--	--				

Table A-XII (cont.)

Compound	14	15	16	27	29	35	36	M/q	Peak hgt.	M/q	Peak hgt.
t-butyl bromide	413	1495	26	--	--	--	--				
1,1-dibromoethane	229	230	--	--	--	--	--				
1,2-dibromopropane	470	944	18	4540	48	--	--				
methyl iodide	955	7560	85	--	--	--	--	13	588		
n-butyl iodide	270	914	28	--	16580	--	--				
isobutyl iodide	432	1685	51	--	--	--	--				
carbon tetrafluoride	--	--	--	--	--	--	--	19	741		

Table A- XIII. Aromatic and cyclic compound peak heights

Compound	13	14	15	16	25	26	27	28	29	37	38	39	M/q	Peak hgt.	M/q	Peak hgt.
A. Excess-energy peak heights at MV = 6000																
benzene	2.1	2.2	33.1	--	2.8	21.1	9.7	--	--	18.1	17.0	13.2				
toluene	1.2	4.4	6.2	--	1.0	18.6	26.0	2.6	--	3.1	8.1	13.1				
ethyl benzene	1.8	7.6	97.8	1.5	--	14.7	30.6	5.6	2.7	1.4	4.5	9.2				
n-propyl benzene	0.8	4.6	47.0	1.6	--	15.4	62.4	10.7	41.3	--	--	--				
isopropyl benzene	--	8.7	116.1	4.8	--	10.0	33.0	7.2	2.1	--	--	13.0				
m-xylene	0.9	4.5	73.7	1.0	--	13.2	29.0	3.9	--	1.9	6.0	14.6				
o-xylene	0.9	4.0	74.1	1.1	--	14.8	31.0	4.2	--	1.7	5.7	14.2				
p-xylene	0.8	4.3	74.1	0.9	--	15.8	31.5	4.2	--	1.4	4.5	12.2				
chlorobenzene	1.9	1.6	11.5	--	2.7	13.8	5.0	--	--	22.9	15.8	7.7	35	5.9	36	3.1
m-chlorotoluene	--	4.6	20.2	--	1.4	17.7	28.8	1.6	--	--	--	--	35	2.8	36	1.5
o-chlorotoluene	--	4.7	17.7	--	1.2	17.9	29.0	1.7	--	--	--	--	35	2.1	36	2.4
p-chlorotoluene	--	4.5	20.4	--	1.2	18.1	28.3	1.6	--	--	--	--	35	2.6	36	1.3
aniline	1.0	1.5	10.5	3.7	1.4	12.7	17.4	12.4	2.8	--	--	--	30	0.9		
benzaldehyde	1.3	1.0	2.6	--	1.4	8.1	2.6	--	63.9	7.3	10.9	3.1				
benzonitrile	1.5	3.5	4.6	--	2.5	16.7	9.6	9.7	--	--	--	--				
nitrobenzene	0.4	0.6	0.6	4.1	--	4.0	--	--	--	--	--	--	30	36.2	46	14.8
phenol	1.1	1.3	7.6	--	--	11.3	5.5	--	16.7	5.2	7.0	7.0				
methyl cyclopropane	4.0	13.7	48.8	1.3	--	16.9	18.7	7.9	--	--	--	--				

Table A-XIII (cont.)

Compound	13	14	15	16	25	26	27	28	29	37	38	39	M/q	Peak hgt.	M/q	Peak hgt.
cyclopentane	1.1	5.7	33.7	0.8	--	13.8	23.1	27.3	1.0	--	--	--				
methyl cyclopentane	0.8	4.6	63.1	2.6	--	9.7	21.9	22.6	1.3	--	--	--				
cyclohexane	0.2	2.4	50.2	1.0	--	10.1	24.2	28.5	1.9	--	--	--				
methyl cyclohexane	--	2.5	56.1	2.1	--	7.7	27.8	28.4	6.8	--	--	--				
ethyl cyclohexane	0.5	1.9	31.1	0.7	--	7.3	47.9	14.0	66.2	--	--	--	30	1.5		
B. Peak heights under normal conditions																
benzene	113	66	464	--	211	1265	932	89	--	1370	1730	3880				
toluene	82	142	572	--	91	784	1500	96	--	763	1475	5010				
ethyl benzene	81	243	1775	33	48	672	2230	225	154	349	810	3400				
n-propyl benzene	39	146	928	31	36	627	2785	329	923	--	--	--				
isopropyl benzene	87	309	2365	105	28	460	2735	277	162	218	587	72				
m-xylene	46	138	1265	23	32	533	2435	212	91	405	1025	4585				
o-xylene	45	129	1220	24	38	626	2600	251	92	368	901	4210				
p-xylene	45	136	1255	22	39	654	2745	220	90	334	811	3910				
chlorobenzene	123	53	189	--	240	749	664	34	--	1810	2600	883	35	421	36	581
m-chlorotoluene	--	145	412	--	125	671	1010	106	--	--	--	--	35	206	36	167
o-chlorotoluene	--	156	371	--	121	706	984	88	--	--	--	--	35	168	36	197
p-chlorotoluene	--	144	412	--	115	663	994	101	--	--	--	--	35	193	36	164
aniline	119	176	351	122	177	781	990	2130	130	--	--	--	30	201		

Table A-XIII (cont.)

Compound	13	14	15	16	25	26	27	28	29	37	38	39	M/q	Peak hgt.	M/q	Peak hgt.
benzaldehyde	82	40	39	33	142	564	984	256	1450	955	1040	1380				
benzonitrile[c]	113	170	--	--	293	2305	1570	383	--	--	--	--				
nitrobenzene	88	77	32	297	153	504	1122	385	68	1010	1180	1820	30	2890	46	392
phenol	122	211	183	24	190	703	964	228	669	1210	2080	5630				
methyl cyclopropane	239	640	1165	26	--	2620	5940	5300	2335	--	--	--				
cyclopentane	98	292	1185	29	--	1315	4560	1460	1160	--	--	--				
methyl cyclopentane	47	183	1540	55	--	907	5245	2240	2135	--	--	--				
cyclohexane	29	115	1265	27	--	1045	5810	2695	2095	--	--	--				
methyl cyclohexane	19	89	285	38	--	538	5075	3485	2910	--	--	--				
ethyl cyclohexane	24	124	1185	30	--	711	6920	1485	5155	--	--	--	30	108		

[c] Obtained from API mass-spectral data.

Table A-XIV. Nitrogen compound peak heights

Compound	14	15	16	26	27	28	29	30	46	M/q	Peak hgt.	M/q	Peak hgt.
A. Excess-energy peak heights at MV = 6000													
nitroethane	3.9	8.5	4.1	6.1	11.0	3.6	1.2	14.1	5.6				
1-nitropropane	4.6	17.3	2.6	--	--	--	--	17.9	9.5				
2-nitropropane	3.7	19.6	2.0	--	--	--	--	19.1	8.1				
dimethyl amine	11.1	37.2	0.9	--	--	27.5	4.7	--	--	13	2.9		
ethyl amine	12.1	28.0	8.0	--	--	--	--	--	--	13	2.0	17	2.6
di-n-propyl amine	4.0	43.7	1.1	7.5	52.8	--	40.0	--	--				
B. Peak heights under normal conditions													
nitroethane	679	1040	357	2300	14960	2120	16940	4000	699				
1-nitropropane	493	1175	234	--	--	--	--	2505	586				
2-nitropropane	441	1515	152	--	--	--	--	2280	424				
dimethyl amine	1160	3130	106	104	1060	9115	567	--	--				
ethyl amine	68	1785	313	891	2500	4875	--	--	--				
di-n-propyl amine	236	1860	49	659	6125	--	2065	--	--				

Table A-XV. Miscellaneous compound peak heights

Compound	14	15	16	17	M/q	Peak hgt.	M/q	Peak hgt.	M/q	Peak hgt.	M/q	Peak hgt.
A. Excess-kinetic-energy peak heights at MV = 6000												
acetic acid	6.8	10.0	1.5	6.7	45	6.0						
propionic acid	5.0	15.5	1.0	5.0	26	6.7	27	10.5	28	3.6		
n-butyric acid	5.7	30.4	1.0	--	27	13.8	29	6.0	45	13.3		
n-valeric acid	4.2	31.2	1.2	1.1	26	6.4	27	20.2	29	13.9		
propionaldehyde	6.1	13.1	1.0	0.8	26	8.3	27	13.4	28	4.8	29	21.4
n-butyraldehyde	6.0	23.6	1.0	--	29	29.0						
isobutyraldehyde	7.6	33.9	1.5	--	29	29.2						
propyl propionate	4.5	24.1	1.0	--	29	16.8						
di-n-propyl ether	4.3	26.2	1.0	0.5	27	61.0	29	18.4				
di-n-propyl ketone	3.7	33.0	1.1	--	26	8.0	27	44.2	28	18.3	29	18.4
di-n-butyl ketone	2.2	18.0	0.7	--	26	6.5	29	83.4				
diborane	2.7	0.5	--	--	11	8.9	12	22.9	13	33.9		
deuteroethylene[d]	--	--	1.2	--	2	29.9	4	1.7				
deuteromethane[d]	--	--	--	--	2	23.7	4	0.6				

Table A-XV (cont.)

Compound	14	15	16	17	M/q	Peak hgt.	M/q	Peak hgt.	M/q	Peak hgt.	M/q	Peak hgt.
B. Peak heights under normal conditions												
acetic acid	2015	5010	731	395	45	8585						
propionic acid	710	837	111	358	26	2870	27	7090	28	9315		
n-butyric acid	626	1485	130	--	27	6720	29	3325	45	3425		
n-valeric acid	419	1250	96	97	26	1365	27	7000	29	5430		
propionaldehyde	850	1455	90	23	26	3190	27	8465	28	10070	29	14390
n-butyraldehyde	650	1780	93	--	29	7535						
isobutyraldehyde	529	1670	82	--	29	6730						
propyl propionate	650	1780	93	--	29	7535						
di-n-propyl ether	206	1310	64	--	27	8045	29	2755				
di-n-propyl ketone	350	1860	59	--	26	954	27	10340	28	1570	29	1890
di-n-butyl ketone	168	1080	44	--	26	819	29	14120				
diborane[c]	94	13	--	--	11	3730	12	2375	13	3202		
deuteroethylene	--	--	1430	--	2	959	4	89				
deuteromethane	--	--	--	--	2	930	4	65				

[c] Obtained from API mass spectral data.

[d] Measurements for these compounds were made at MV = 1200.

Table A-XVI. Comparison of excess-kinetic-energy ion abundances under normal conditions with abundances under conditions A

Compound	M/q	Peak height under normal conditions[a]	Peak height under conditions A[b]	Ratio
ethane	15	468	28.1	16.6
propane	15	986	56.2	17.5
n-butane	15	1333	83.2	16.0
isobutane	15	1652	102.0	16.2
n-pentane	15	1217	54.2	22.5
neopentane	15	2613	135.6	19.3
n-heptane	15	805	30.7	26.2
2,4-dimethyl pentane	15	2087	93.9	22.2
n-decane	15	564	11.3	49.9
benzene	15	485	33.1	14.6
p-xylene	15	1232	74.1	16.6
ethyl benzene	15	1620	97.8	16.6
isopropyl chloride	15	820	47.9	17.2
isopropyl alcohol	15	1254	51.5	24.4
n-heptane	29	1077	76.6	14.2

[a] Taken from Table VII.

[b] Taken from Tables A-IX through A-XV.

Table A-XVII. Computed peak-height breakdowns under normal conditions into thermal and excess-kinetic-energy components for selected compounds

A. n-octane

M/q	14	15	26	28	29	30
Normal conds. pk. ht.[a]	106	1015	729	2075	10510	253
Excess K.E. component[b]	32	364	133	189	1790	37
Thermal component[c]	74	651	596	1886	8720	216

B. n-amyl alcohol

M/q	14	15	16	17	26	27	29	30	31
Normal conds. pk. ht.	316	1410	58	44	1100	6560	8920	376	9320
Excess K.E. component	61	400	17	10	102	411	315	31	675
Thermal component	255	1010	41	34	998	6149	8605	345	8645

C. n-amyl chloride

M/q	14	15	16	26	27	29	35	36
Normal conds. pk. ht.	319	1570	44	1460	8730	6400	114	176
Excess K.E. component	107	790	27	177	781	304	24	31
Thermal component	212	780	17	1283	7949	6096	90	145

[a] Entries from Table A-IX-B.

[b] Obtained by multiplying entries in Table A-IX-A by 17.

[c] Obtained by subtraction of previous two rows.

ACKNOWLEDGMENTS

The author gratefully acknowledges the guidance of Dr. Amos S. Newton and Professor Kenneth Street, under whose direction this research was done. Dr. Maynard C. Michel, Professor Dudley R. Herschbach, and Professor Gilbert J. Mains contributed answers to questions on physical chemical topics pertinent to the research. Special thanks are given to Mr. Aldo F. Sciamanna, who assisted in obtaining much of the mass-spectral data, and to Mrs. Mary C. Pong, who helped prepare the data. The assistance of Mr. Frederick Vogelsberg and Mr. Milton Firth of the electronics staff of the Lawrence Radiation Laboratory is also acknowledged. The contributions of Paul D. Croft, Charles F. Smith, Dr. M. Lee Hyder, and John D. Mahony, all of whom assisted in peripheral aspects of the research, and of the author's daughter Jennifer, who provided the impetus for completion of the work, cannot adequately be assessed.

The author is indebted to the National Science Foundation for a fellowship provided during one portion of the tenure of this research.

This work was done under the auspices of the U. S. Atomic Energy Commission.

REFERENCES

1. W. Bleakney, Phys. Rev. 35, 1180 (1930).
2. W. W. Lozier, Phys. Rev. 36, 1285 (1930).
3. W. W. Lozier, Phys. Rev. 43, 776 (1933).
4. W. W. Lozier, Phys. Rev. 44, 575 (1933).
5. W. W. Lozier, Phys. Rev. 46, 268 (1934).
6. J. T. Tate and W. W. Lozier, Phys. Rev. 39, 254 (1932).
7. E. E. Hanson, Phys. Rev. 51, 86 (1937).
8. H. D. Hagstrum and J. T. Tate, Phys. Rev. 59, 354 (1941).
9. H. D. Hagstrum, Rev. Mod. Phys. 23, 185 (1951).
10. A. Hustrulid, P. Kusch, and J. T. Tate, Phys. Rev. 54, 1037 (1938).
11. J. A. Hipple, R. E. Fox, and E. U. Condon, Phys. Rev. 69, 347 (1946).
12. F. L. Mohler, V. H. Dibeler, and R. M. Reese, J. Chem. Phys. 22, 394 (1954).
13. H. E. Stanton, J. Chem. Phys. 30, 1116 (1959).
14. T. Tsuchiya, J. Chem. Phys. 36, 568 (1962).
15. T. Tsuchiya, Bull. Chem. Soc. Japan 35, 1221 (1962).
16. R. M. S. Hall, Nature 187, 683 (1960).
17. R. J. Kandel, J. Chem. Phys. 22, 1496 (1954).
18. R. J. Kandel, J. Chem. Phys. 23, 84 (1955).
19. N. D. Coggeshall, J. Chem. Phys. 12, 19 (1944).
20. H. W. Washburn and C. E. Berry, Phys. Rev. 70, 559 (1946).
21. C. E. Berry, Phys. Rev. 78, 597 (1950).
22. N. D. Coggeshall, J. Chem. Phys. 36, 1640 (1962).
23. A. J. Dempster, Phys. Rev. 11, 316 (1918).
24. A. S. Newton and H. X. DiGrazia, The Use of a Bismuth Wire Flux-Meter for Metering the Magnetic Field of the Consolidated Mass Spectrometer Model 21-103, UCRL-2994, May 1955.
25. J. D. Morrison, J. Chem. Phys. 19, 1305 (1951).

26. D. P. Stevenson and D. O. Schissler, Mass Spectrometry and Radiation Chemistry, in The Chemical and Biological Action of Radiations, M. Haissinsky, Ed. (Academic Press, Inc., London, 1961), Chapter III.

27. W. A. Chupka, J. Chem. Phys. 30, 191 (1959).

28. R. Taubert, Kinetic Energy of Fragment Ions, in Advances in Mass Spectrometry, J. D. Waldron, Ed. (Permagon Press, New York, 1959), p.489.

29. J. E. Monahan and H. E. Stanton, J. Chem. Phys. 37, 2654 (1962).

30. J. O. Hirschfelder, C. F. Curtiss, and R. B. Bird, Molecular Theory of Gases and Liquids (John Wiley and Sons, Inc., New York, 1954), p.1060.

31. D. R. Bates, K. Ledsham, and A. L. Stewart, Phil. Trans. Roy. Soc. London, A246, 215 (1953).

32. A. S. Coolidge, H. M. James, and R. D. Present, J. Chem. Phys. 4, 193 (1936).

33. D. P. Stevenson, J. Am. Chem. Soc. 82, 5961 (1960).

34. J. D. Morrison, J. Appl. Phys. 28, 1409 (1957).

35. A. O. Hurley and V. W. Maslen, J. Chem. Phys. 34, 1919 (1961).

36. R. I. Reed, Ion Production by Electron Impact (Academic Press, New York, 1962), Chapters I and II.

37. F. H. Field and J. L. Franklin, Electron Impact Phenomena (Academic Press, Inc., New York, 1957), Appendix.

38. J. Franck, H. Sponer, and E. Teller, Z. Physik. Chem. B18, 88 (1932).

39. E. P. Wigner, Phys. Rev. 73, 1002 (1948).

40. G. H. Wannier, Phys. Rev. 90, 817 (1953).

41. G. H. Wannier, Phys. Rev. 100, 1180 (1955).

42. M. B. Koffel and R. A. Lad, J. Chem. Phys. 16, 420 (1948).

43. O. Osberghaus and R. Taubert, Z. Physik. Chem. (Frankfurt) 4, 264 (1955).

44. N. D. Coggeshall, Phys. Rev. 70, 270 (1946).

45. Tables of the Error Function and Its First Twenty Derivatives, H. H. Aiken, Ed. (Harvard Univ. Press, Cambridge, Mass., 1952).

46. W. M. Brubaker, J. Appl. Phys. 26, 1007 (1955).

47. Mass Spectral Data, American Petroleum Institute Research Project 44, B. J. Zwolinski, Director (Agricultural and Mechanical College of Texas, College Station, Texas).

48. H. M. Rosenstock, M. B. Wallenstein, A. L. Wahrhaftig, and H. Eyring, Proc. Nat. Acad. Sci. 38, 667 (1952).

49. M. Vestal, A. L. Wahrhaftig, and W. H. Johnston, Theoretical Studies in Basic Radiation Chemistry, ARL-62-426, Sept. 1962; See also J. Chem. Phys. 37, 1276 (1962).

50. H. Hurzeler, M. G. Inghram, and J. D. Morrison, J. Chem. Phys. 28, 76 (1958).

51. B. Steiner, C. F. Giese, and M. G. Inghram, J. Chem. Phys. 34, 189 (1961).

52. H. Sponer and E. Teller, Rev. Mod. Phys. 13, 75 (1941).

53. N. B. Slater, Theory of Unimolecular Reactions (Cornell Univ. Press, Ithaca, New York, 1959).

This report was prepared as an account of Government sponsored work. Neither the United States, nor the Commission, nor any person acting on behalf of the Commission:

A. Makes any warranty or representation, expressed or implied, with respect to the accuracy, completeness, or usefulness of the information contained in this report, or that the use of any information, apparatus, method, or process disclosed in this report may not infringe privately owned rights; or

B. Assumes any liabilities with respect to the use of, or for damages resulting from the use of any information, apparatus, method, or process disclosed in this report.

As used in the above, "person acting on behalf of the Commission" includes any employee or contractor of the Commission, or employee of such contractor, to the extent that such employee or contractor of the Commission, or employee of such contractor prepares, disseminates, or provides access to, any information pursuant to his employment or contract with the Commission, or his employment with such contractor.